THE

LONDON, EDINBURGH, AND DUBLIN

PHILOSOPHICAL MAGAZINE

AND

JOURNAL OF SCIENCE.

[SEVENTH SERIES.]

FEBRUARY 1933.

XXI. *Electromagnetic Shielding at Radio Frequencies.*

By LOUIS V. KING, *F.R.S., Macdonald Professor of Physics, McGill University, Montreal* *.

Section 1.—*Introduction.*

IT is often necessary in the design of radio receiving apparatus to protect some part of the circuit from the disturbing effect of the electromagnetic radiation field in its neighbourhood. This is done by enclosing the part to be protected in a metallic container. In order to determine the dimensions of the container and the thickness of metal of which it is made the following investigation was undertaken, as there does not seem to be an adequate treatment of the subject in such literature as the writer has examined, with the exception of an investigation by Larmor †, whose results, however, only apply to low frequencies. In the following sections we consider the shielding effect of containers of such extreme shapes as are represented by a spherical shell and an infinite cylindrical shell. It is supposed that the wave-length of the radiation field is large compared to the linear dimensions of the shielding containers, so that the problem is reduced to determining the ratio of the internal

* Communicated by the Author.

† Larmor, J., Phil. Mag. p. 4, Jan. 1884; 'Mathematical and Physical Papers,' i. p. 18 (Cambridge University Press, 1929). Barfield, J. I. E. E. lxii. p. 249 (1924), deals with practical problems of screening by wire cages.

magnetic field to the external field considered as uniform over the region of space occupied by the conductor, except for the disturbance caused by the induced currents.

Section 2.—*Shielding Ratio for a Conducting Spherical Shell of Finite Thickness.*

If we take the external magnetic field at a great distance from the sphere to be H_0 along the axis of z, the electric field E arising from the time-variation of H_0 will be symmetrical with respect to the axis of z. If we express the Maxwell–Faraday laws in polar coordinates and write $\mu = \cos\theta$, we have *, in an obvious notation,

$$H_r = -\frac{c}{r^2}\frac{\partial \psi}{\partial \mu}, \quad H_\theta = -\frac{c}{r\sin\theta}\frac{\partial \psi}{\partial r}, \quad E = \frac{\psi}{r\sin\theta}, \quad (1)$$

and in addition

$$\frac{1}{r}\left\{\frac{\partial}{\partial r}(rH_\theta) - \frac{\partial H_r}{\partial \theta}\right\} = -\frac{1}{c}\frac{\partial E}{\partial t} - \frac{4\pi E}{\rho}, \quad . \quad . \quad (2)$$

where ρ is the specific resistance of the conductor, c being the ratio of the electrostatic to the electromagnetic measure of magnetic field intensity. From (1) and (2) we obtain the propagation equation for the *electrical work-function* ψ,

$$\frac{\partial^2 \psi}{\partial r^2} + \frac{1-\mu^2}{r^2}\frac{\partial^2 \psi}{\partial \mu^2} = \frac{1}{c^2}\frac{\partial^2 \psi}{\partial t^2} + \frac{4\pi}{\rho}\frac{\partial \psi}{\partial t}. \quad . \quad . \quad (3)$$

If we denote by κ the operational symbol

$$\kappa = \left\{\frac{1}{c^2}\frac{\partial^2}{\partial t^2} + \frac{4\pi}{\rho}\frac{\partial}{\partial t}\right\}^{1/2} \quad . \quad . \quad . \quad . \quad (4)$$

or, in the case of waves of frequency f,

$$\kappa = \left\{\frac{\omega^2}{c^2} + \frac{4\pi i\omega}{\rho}\right\}^{1/2}, \quad . \quad . \quad . \quad . \quad . \quad (5)$$

where $2\pi f = \omega$, the propagation equation takes the form

$$\frac{\partial^2 \psi}{\partial r^2} + \frac{1-\mu^2}{r^2}\frac{\partial^2 \psi}{\partial \mu^2} = \kappa^2 \psi, \quad . \quad . \quad . \quad . \quad (6)$$

* Livens, G. H., 'The Theory of Electricity,' §§ 451–453, pp. 398–400 (Cambridge University Press, 1918). In this paper electrical fields are measured in e.s. units, magnetic fields in e.m. units.

of which a general type of solution of the product is easily proved to be

$$\psi = \left[A\int^{\mu} P_{n-1}(\mu)\,d\mu + B\int^{\mu} Q_{n-1}(\mu)\,d\mu\right]$$
$$[C\sqrt{\kappa r}I_{-n+\frac{1}{2}}(\kappa r) + D\sqrt{\kappa r}K_{-n+\frac{1}{2}}(\kappa r)]\,f(t), \quad (7)$$

where $P_{n-1}(\mu)$ and $Q_{n-1}(\mu)$ are the two solutions of Legendre's equation, and $I_{-n+\frac{1}{2}}(\kappa r)$ and $K_{-n+\frac{1}{2}}(\kappa r)$ are the two solutions of Bessel's equations. In general n is unrestricted and the second factor represents a symbolic operation on the arbitrary function $f(t)$, useful in studying the penetration of transient electromagnetic waves into conducting media. The functions $Q_{n-1}(\mu)$ and $P_{n-1}(\mu)$ have, in general, singularities at the poles $\mu = \pm 1$, unless n is integral, in which case $Q_{n-1}(\mu)$ has a logarithmic singularity at the poles $\mu = \pm 1$.

It is convenient to designate by C the combination of variables given by

$$C^2 = \frac{\rho}{4\pi\omega} = \frac{\rho}{8\pi^2 f}. \quad . \quad . \quad . \quad . \quad . \quad (8)$$

Obviously C has the dimensions of a length and may conveniently be called the "induction constant" of the medium. If ρ is expressed in ohms/cm./cm.^{2} then

$$C(\text{cm.}) = \left\{\frac{\rho(\text{ohms}) \times 10^9}{8\pi^2 f}\right\}^{1/2}. \quad . \quad . \quad . \quad (9)$$

For a radiation field of wave-length λ, equation (5) may be written

$$\kappa = \left\{\left(\frac{2\pi}{\lambda}\right)^2 + \frac{i}{C^2}\right\}^{1/2}, \quad . \quad . \quad . \quad . \quad (10)$$

from which it may be seen that when λ is very much greater than C we may neglect propagation effects and write, approximately, $\kappa^2 \sim i/C^2$, or

$$\kappa \sim \sqrt{i}/C = \sqrt{\tfrac{1}{2}}(1+i)/C. \quad . \quad . \quad . \quad . \quad (11)$$

When $\rho \to \infty$ or $\kappa \to 0$ it is easily seen that the general solution of the propagation equation corresponding to (7) is

$$\kappa \to 0, \quad \psi = \left[A\int^{\mu} P_{n-1}(\mu)\,d\mu + B\int^{\mu} Q_{n-1}(\mu)\,d\mu\right]$$
$$\left[Cr_n + \frac{D}{r^{n-1}}\right]. \quad (12)$$

It follows from (1) that the value of ψ corresponding to a uniform periodic field H_0 is expressed by

$$\psi = -\tfrac{1}{2}H_0 r^2(1-\mu^2),$$

so that the appropriate solutions for the field arising from currents induced in a spherical shell correspond to $n=2$ in the general solutions (7) and (12). If a is the outer radius of the shell and b the inner radius, we have to adjust the constants $\dot{A}$, $\dot{B}$, $\dot{C}$ of the three solutions :

$$\left.\begin{aligned} &\infty > r > a, \quad \psi_0 = -\tfrac{1}{2}\dot{H}_0 r^2 \sin^2\theta + \tfrac{1}{2}\dot{A}\sin^2\theta/r, \\ &a > r > b, \quad \psi = \tfrac{1}{2}\{\dot{B}\sqrt{\kappa r}\,I_{-\frac{3}{2}}(\kappa r) + \dot{C}\sqrt{\kappa r}\,K_{-\frac{3}{2}}(\kappa r)\}\sin^2\theta, \\ &b > r > 0, \quad \psi_i = -\tfrac{1}{2}\dot{H}_i r^2 \sin^2\theta, \end{aligned}\right\} \quad . \quad . \quad . \quad (13)$$

to satisfy the boundary conditions expressing the continuity of the magnetic fields (1) at $r=a$ and $r=b$,

$$\left.\begin{aligned} &\psi_0 = \psi, \qquad \partial\psi/\partial r = \partial\psi_0/\partial r \quad \text{at } r=a \\ \text{and} \quad &\psi = \psi_i, \qquad \partial\psi/\partial r = \partial\psi_i/\partial r \quad \text{at } r=b. \end{aligned}\right\} \quad . \quad (14)$$

We find without difficulty, after making some reductions and utilizing the well-known formulæ

$$\left.\begin{aligned} &\frac{d}{dt}(t^n I_n) = t^n I_{n-1}, \qquad \frac{d}{dt}(t^n K_n) = -t^n K_{n-1}, \\ &K_n I_n' - K_n' I_n = 1/t, \qquad K_{n+1} I_n + K_n I_{n+1} = 1/t, \end{aligned}\right\} \quad (15)$$

that

$$\frac{H_i}{H_0} = \frac{3(\kappa a)^{1/2}}{(\kappa b)^{5/2}\left[I_{-\frac{1}{2}}(\kappa a)K_{-\frac{5}{2}}(\kappa b) - K_{-\frac{1}{2}}(\kappa a)I_{-\frac{5}{2}}(\kappa b)\right]}. \quad (16)$$

Section 3.—*Thin Spherical Shell. Approximate Formula for Low Frequencies.*

Most shielding containers in practice consist of sheet metal of thickness d, small compared with the linear dimensions of the container. We write

$$a - b = d. \quad . \quad . \quad . \quad . \quad . \quad . \quad (17)$$

Denoting by t the variable $t=\kappa b$ and making use of Taylor's theorem for the I- and K-functions of $\kappa a = t + \kappa d$

which appear in the denominator of (16), we find after some reductions * that

$$[I_{-\frac{1}{2}}(\kappa a)K_{-\frac{5}{2}}(\kappa b)-K_{-\frac{1}{2}}(\kappa a)I_{-\frac{5}{2}}(\kappa b)]\sim\frac{3}{t^2}+\kappa d\left(\frac{1}{t}+\frac{3}{2t^2}\right)+\ldots,$$

which enables us to write

$$\frac{H_i}{H_0}\sim\frac{(1+\kappa d/t)^{1/2}}{(1+\frac{1}{2}\kappa d+\frac{1}{3}\kappa dt)}. \quad . \quad . \quad . \quad . \quad (18)$$

Restoring $t\sim\kappa a$, where a may now be taken to be the mean radius of the thin spherical shell, and remembering that in terms of the induction constant C we have

$$\kappa^2=i/C^2, \quad . \quad . \quad . \quad . \quad . \quad . \quad (19)$$

formula (18) gives, finally, for the shielding ratio,

$$\frac{H_i}{H_0}\sim\frac{1}{1+\frac{1}{3}iad/C^2}. \quad . \quad . \quad . \quad . \quad (20)$$

It is convenient for purposes of calculation to introduce the auxiliary angle α given by

$$\tan\alpha=\frac{1}{3}\frac{ad}{C^2}, \quad . \quad . \quad . \quad . \quad . \quad (21)$$

which enables us to write the shielding ratio in the convenient form

$$|H_i|/|H_0|=\cos\alpha. \quad . \quad . \quad . \quad . \quad . \quad (22)$$

It is a simple matter to verify this result by an independent calculation, following the lines of Larmor's treatment already referred to.

Section 4.—*Thin Spherical Shell. Asymptotic Formula for Radio Frequencies.*

The exact expressions for the I- and K-functions which appear in the denominator of (16) are most easily written down from the asymptotic formulæ for these functions, which terminate when the order of the functions is half an odd integer †. In terms of the variable t we have

* Details of similar reductions are given in Section 7.

† Gray, Mathews, and MacRobert, 'Treatise on Bessel Functions,' § 3, p. 58 (Macmillan & Co., 1922). Watson, 'Theory of Bessel Functions,' § 7.23, p. 202 (Cambridge University Press, 1922).

$$\left.\begin{aligned} I_{-\frac{1}{2}}(t) &= \sqrt{\frac{2}{\pi t}}\cosh t, \\ I_{-\frac{5}{2}}(t) &= \sqrt{\frac{2}{\pi t}}\left\{\cosh t - \frac{3}{t}\sinh t + \frac{3}{t^2}\cosh t\right\}, \\ K_{-\frac{1}{2}}(t) &= \sqrt{\frac{\pi}{2t}}e^{-t}, \\ K_{-\frac{5}{2}}(t) &= \sqrt{\frac{\pi}{2t}}e^{-t}\left\{1+\frac{3}{t}+\frac{3}{t^2}\right\}. \end{aligned}\right\} \quad (23)$$

We now make use of these formulæ with $t=\kappa a$ and $t=\kappa b$ to obtain an asymptotic expression for the denominator of (16) under the conditions that the thickness d is small compared with the mean radius of the shell. The wave-length is still very great compared with C, so that (11) is valid, *i. e.* $\kappa \sim \sqrt{i}/C$. For radio frequencies and for shielding containers of practical dimensions, $\kappa a \sim \sqrt{i}a/C$ is so large that terms in $1(\kappa a)^2$ and $1/(\kappa b)^2$ in (23) are neglected, and $\cosh \kappa a \sim \sinh \kappa a \sim \frac{1}{2}e^{\kappa a}$, while $\cosh \kappa b \sim \sinh \kappa b \sim \frac{1}{2}e^{\kappa b}$.

In these circumstances we easily find in terms of the mean radius a and thickness d,

$$\left[I_{-\frac{1}{2}}(\kappa a)K_{-\frac{5}{2}}(\kappa b) - K_{-\frac{1}{2}}(\kappa a)I_{-\frac{5}{2}}(\kappa b)\right] \sim \frac{1}{\kappa a}\left\{\sinh(\kappa d) + \frac{3}{\kappa a}\cosh(\kappa d)\right\}. \quad (24)$$

We thus obtain the asymptotic formula

$$\frac{H_i}{H_0} \sim \frac{1}{\cosh \kappa d + \frac{1}{3}\kappa a \sinh \kappa d}, \quad . \quad . \quad . \quad (25)$$

from which it is a simple matter to derive the shielding ratio $|H_i|/|H_0|$, making use of tables of hyperbolic functions of complex argument.

The above formula is valid over a wide range of frequencies, since for κd small it reduces to (20). At high frequencies, when the first term in (25) is negligible compared to the second, we have the approximate formula

$$\frac{|H_i|}{|H_0|} \sim \frac{3C}{a}\frac{1}{\left|\sinh(1+i)\frac{d}{C\sqrt{2}}\right|} = \frac{3C}{a}\frac{1}{\left\{\sinh^2\frac{d}{C\sqrt{2}} + \sin^2\frac{d}{C\sqrt{2}}\right\}^{1/2}} \quad . \quad . \quad . \quad (26)$$

Section 5.—*Shielding Ratio for a Cylindrical Shell of Finite Thickness in Longitudinal Magnetic Field.*

In cylindrical coordinates (r, z) it is easily found that the electrical work function ψ satisfies the differential equation

$$r\frac{\partial}{\partial r}\left(\frac{1}{r}\frac{\partial \psi}{\partial r}\right)+\frac{\partial^2\psi}{\partial z^2}=\frac{1}{c^2}\frac{\partial^2\psi}{\partial t^2}+\frac{4\pi}{\rho}\frac{\partial \psi}{\partial t}, \quad . \quad (27)$$

while the field components are given by

$$\dot{H}_r=\frac{c}{r}\frac{\partial \psi}{\partial z}, \qquad \dot{H}_z=-\frac{c}{r}\frac{\partial \psi}{\partial r}, \qquad E=\psi/r. \quad (28)$$

For an alternating field along the direction of the z-axis we require a solution of (27) independent of z. Under the same conditions as in Section 3, neglecting propagation effects, it is easily seen that the required solution applicable to a cylinder of external radius a, internal radius b, is of the form

$$\left.\begin{aligned} &\infty > r > a, && \psi_0=-\tfrac{1}{2}\dot{H}_0 r^2+\dot{A}, \\ &a > r > b, && \psi=\tfrac{1}{2}\{\dot{B}\kappa r I_1(\kappa r)+\dot{C}\kappa r K_1(\kappa r)\}, \\ &b > r > 0, && \psi_i=-\tfrac{1}{2}\dot{H}_i r^2, \end{aligned}\right\} \quad (29)$$

subject to the boundary conditions

$$\left.\begin{aligned} &\psi_0=\psi, && \partial\psi/\partial r=\partial\psi_0/\partial r \quad \text{at } r=a, \\ &\psi=\psi_i, && \partial\psi/\partial r=\partial\psi_i/\partial r \quad \text{at } r=b, \end{aligned}\right\}$$

expressing the continuity of the magnetic fields given by (28) at $r=a$ and $r=b$. We find, after some reductions, making use of the formulæ of the type (15), that

$$\frac{H_i}{H_0}=\frac{2}{(\kappa b)^2}\cdot\frac{1}{[I_0(\kappa a)K_2(\kappa b)-K_0(\kappa a)I_2(\kappa b)]}. \quad . \quad (30)$$

From this result the shielding ratio may be obtained in terms of the functions $ber(x)$, $bei(x)$, $ker(x)$, $kei(x_1)$ and their derivatives, which are tabulated. The final formula is, however, very cumbersome *.

* There is need in problems of this kind for nomograms of the functions $J_0(x+iy)$, $K_0(x+iy)$, etc., of the same type as Kennelly's well-known charts of the hyperbolic functions of complex argument used in line-transmission work (Harvard University Press, 1925).

Section 6.—*Shielding Ratio for a Cylindrical Shell of Finite Thickness in a Transverse Magnetic Field.*

As in the preceding section we take the axis of z along that of the cylindrical shell of radii a and b $(a>b)$. Let the external magnetic field be uniform and in the direction of the x-axis. In the conductor of which the shell is made, the induced current w will be in the direction of the z-axis, while the magnetic field at (r, ϕ) is independent of z and has radial and tangential components H_r and H_ϕ. If E_z is the electric field along the z-axis the Maxwell–Faraday laws in cylindrical coordinates (r, ϕ) give

$$-\frac{1}{c}\dot{H}_r=\frac{1}{r}\frac{\partial E_z}{\partial \phi}, \qquad \frac{1}{c}\dot{H}_\phi=\frac{\partial E_z}{\partial r}, \qquad cE_z=w\rho, \quad (31)$$

$$\frac{1}{r}\left\{\frac{\partial}{\partial r}(rH_\phi)-\frac{\partial H_r}{\partial \phi}\right\}=-\frac{1}{c}\frac{\partial E_z}{\partial t}-4\pi w, \quad . \quad (32)$$

where ρ is the specific resistance in electromagnetic units.

From these we find that the differential equation for w is

$$\frac{1}{r}\frac{\partial}{\partial r}\left(r\frac{\partial w}{\partial r}\right)+\frac{1}{r^2}\frac{\partial^2 w}{\partial \phi^2}=\frac{1}{c^2}\frac{\partial^2 w}{\partial t^2}+\frac{4\pi}{\rho}\frac{\partial w}{\partial t}. \quad . \quad (33)$$

It follows from (31) that, in terms of w, the field-components are given by

$$\dot{H}_r=-\frac{\rho}{r}\frac{\partial w}{\partial \phi}, \qquad \dot{H}_\phi=\rho\frac{\partial w}{\partial r}, \qquad E_z=\frac{w\rho}{c}. \quad . \quad (34)$$

In the regions external to the conducting medium of the shell we may consider $\rho\to\infty$, so that the right-hand side of (32) vanishes. This is the condition that H_r and H_ϕ are derivable from a potential Ω, giving

$$H_r=\frac{\partial \Omega}{\partial r}, \qquad H_\phi=\frac{1}{r}\frac{\partial \Omega}{\partial \phi}. \quad . \quad . \quad . \quad (35)$$

The appropriate solutions of Laplace's equation, corresponding to a periodic field H_0, uniform along the x-axis at great distances from the cylinder, are

$$\left.\begin{aligned} a<r<\infty, \qquad & \Omega_0=H_0 r\cos\phi+C\cos\phi/r, \\ 0<r<b, \qquad & \Omega_i=H_i r\cos\phi. \end{aligned}\right\} \quad . \quad (36)$$

The continuity of H_r and H_ϕ at the boundaries $r=a$ and $r=b$ requires us, according to (34) and (35), to make use of a solution of (33) of the form $w=R\sin\phi$, where R is a

function of r only. We find, without difficulty, that the required form of solution is

$$w = \{\dot{A}I_1(\kappa r) + \dot{B}K_1(\kappa r)\}\sin\phi \quad . \quad . \quad . \quad (37)$$

in the standard notation of Bessel functions.

The four boundary conditions at $r=a$ and $r=b$ enable us to eliminate the constants A, B, C occurring in (36) and (37). After some reductions which involve the use of fundamental formulæ of the type (15), we find

$$2H_0 = (\kappa b)^2 H_i[I_0(\kappa a)K_2(\kappa b) - K_0(\kappa a)I_2(\kappa b)], \quad (38)$$

which is exactly the same as (30), corresponding to a longitudinal external field. By a superposition of these two solutions we conclude that (30) holds when the external field makes any angle with the axis of the cylindrical shell.

Section 7.—*Thin Cylindrical Shell. Approximate Formula for Low Frequencies.*

As in Section 3, we write $a=b+d$, where d is the thickness of the shell, small compared to a or b. According to Taylor's theorem we have

$$I_0(\kappa a) = I_0(\kappa b) + \kappa d I_1(\kappa b) + \ldots,$$
$$K_0(\kappa a) = K_0(\kappa b) - \kappa d K_1(\kappa b) + \ldots;$$

thus

$$[I_0(\kappa a)K_2(\kappa b) - K_0(\kappa a)I_2(\kappa b)] \sim (I_0K_2 - K_0I_2) + \kappa d(I_1K_2 + K_1I_2) + \ldots,$$

where the argument on the right-hand side is $t=\kappa b$. From the relations

$$K_2 = K_0 + (2/t)K_1, \qquad I_2 = I_0 - (2/t)I_1,$$

we have, on multiplying the first by I_0, the second by K_0, subtracting, and remembering that

$$I_0K_1 + I_1K_0 = 1/t, \qquad I_1K_2 + K_1I_2 = 1/t,$$

the result

$$[I_0(\kappa a)K_2(\kappa b) - K_0(\kappa a)I_2(\kappa b)] \sim \frac{2}{t^2} + \frac{\kappa d}{t} + \ldots.$$

We thus have the approximate formula for the ratio H_i/H_0 given by (30),

$$\frac{H_i}{H_0} \sim \frac{2}{t^2(2/t^2 + \kappa d/t)} = \frac{1}{1 + \frac{1}{2}\imath ad/C^2}, \quad . \quad . \quad (39)$$

where we have written $t=\kappa b$, or approximately $t\sim\kappa a$ and $\kappa^2\sim i/C^2$, propagation effects being negligible and C being the induction constant given by (9). Writing

$$\tan\beta = \tfrac{1}{2}ad/C^2, \quad . \quad . \quad . \quad . \quad . \quad (40)$$

we finally obtain for a thin cylindrical shell the convenient expression for the shielding ratio in the form

$$|H_i|/|H_0| = \cos\beta, \quad . \quad . \quad . \quad . \quad . \quad (41)$$

valid for all angles between the external field H_0 and the axis of the cylinder.

It is a simple matter to derive this result directly for low frequencies when the thickness d is so small that the current density throughout is sensibly constant.

Section 8.—*Thin Cylindrical Shell. Asymptotic Formula for Radio Frequencies.*

At sufficiently high frequencies the arguments $|\kappa a| = a/C$, $|\kappa b| = b/C$ are so large that to a sufficient order of accuracy we may replace the I- and K-functions in (30) and (38) by one or two terms of their asymptotic expansion. In general we have *, when $0<am(t)<\pi$,

$$I_\kappa(t) = \frac{1}{\sqrt{(2\pi t)}}e^t\left\{1-\frac{4\kappa^2-1^2}{1!\,8t}+\ldots\right\} + \frac{e^{i(\kappa+\frac{1}{2})\pi}}{\sqrt{(2\pi t)}}e^{-t}\left\{1+\frac{4\kappa^2-1^2}{1!\,8t}+\ldots\right\}$$

and

$$K_\kappa(t) = \sqrt{\frac{\pi}{2t}}e^{-t}\left\{1+\frac{4\kappa^2-1^2}{1!\,8t}+\ldots\right\}. \quad (42)$$

We find, after some reductions, that for a thin cylindrical shell, for which $a=b+d$, that

$$[I_0(\kappa a)K_2(\kappa b)-K_0(\kappa a)I_2(\kappa b)] \sim \frac{1}{\kappa a}\left\{\sinh(\kappa d)+\frac{2}{\kappa a}\cosh(\kappa d)\right\}, \quad (43)$$

and for the shielding ratio,

$$\frac{H_i}{H_0}\sim\frac{1}{\cosh(\kappa a)+\frac{1}{2}\kappa a\sinh\kappa d}. \quad . \quad . \quad . \quad (44)$$

This formula is valid over a wide range of frequencies, since for κa small it reduces to (39). When the frequency

* Gray and Mathews, 'Bessel Functions,' p. 58.

is sufficiently high, so that the first term is negligible in comparison with the second, we have for the shielding ratio the formula

$$\frac{|H_i|}{|H_0|} \sim \frac{2C}{a} \frac{1}{\left|\sinh(1+i)\frac{d}{C\sqrt{2}}\right|} = \frac{2C}{a} \cdot \frac{1}{\left\{\sinh^2 \frac{d}{C\sqrt{2}} + \sin^2 \frac{d}{C\sqrt{2}}\right\}^{\cdot}} \quad . \quad . \quad . \quad (45)$$

Section 9.—*Effect of Magnetic Permeability on Shielding Ratio of Thin Spherical Shell.*

The introduction of magnetic permeability μ_m as a new property of the material forming the shell requires us to modify the preceding analysis in two ways.

(1) In the Maxwell–Faraday relations of Section 1, equations (1) are replaced by

$$\mu_m \dot{H}_r = \frac{c}{r^2} \frac{\partial \psi}{\partial \mu} \quad \text{and} \quad \mu_m \dot{H}_\theta = -\frac{c}{r \sin\theta} \frac{\partial \psi}{\partial r}, \quad (46)$$

while (2) remains unaltered. As a result, κ in the propagation equation (6) is replaced by κ_m, where $\kappa_m = \kappa\sqrt{\mu}$, or, according to (11) the induction constant C is replaced by

$$C_m = C/\sqrt{\mu_m}. \quad . \quad . \quad . \quad . \quad . \quad (47)$$

(2) At the boundaries $r=a$ and $r=b$ the tangential components of the fields are continuous. If H_r is the normal field component, $\mu_m H_r$ is continuous across the boundaries.

Reference to (46) gives the boundary conditions

$$\left.\begin{aligned} &\psi = \psi_0, \quad \frac{1}{\mu_m}\frac{\partial \psi}{\partial r} = \frac{\partial \psi_0}{\partial r} \quad \text{at } r=a \\ \text{and} \quad &\psi = \psi_i, \quad \frac{1}{\mu_m}\frac{\partial \psi}{\partial r} = \frac{\partial \psi_i}{\partial r} \quad \text{at } r=b, \end{aligned}\right\} \quad . \quad . \quad (48)$$

where we now have, as in equations (13),

$$\left.\begin{aligned} a<r<\infty, \quad &\psi_0 = -\tfrac{1}{2}\dot{H}_0 r^2 \sin^2\theta + \tfrac{1}{2}\dot{A}\sin^2\theta/r, \\ b<r<a, \quad &\psi = \tfrac{1}{2}\dot{R}\sin^2\theta, \\ 0<r<b, \quad &\psi_i = -\tfrac{1}{2}\dot{H}_i \sin^2\theta, \end{aligned}\right\} \quad (49)$$

R being a function of r only.

On substituting in the propagation equation (6) it is easily seen that ψ satisfies the differential equation

$$\frac{d^2\mathrm{R}}{dr^2} - \frac{2\mathrm{R}}{r^2} = \kappa_m{}^2\mathrm{R}. \quad . \quad . \quad . \quad . \quad . \quad (50)$$

While it is possible to derive a solution for a shell of finite thickness of permeability μ, the results as expressed in terms of I- and K-functions are extremely complicated and difficult to interpret numerically. In dealing with thin shells, however, it is possible to proceed directly to a solution by making use of the differential equation (50).

The boundary conditions (48) at $r=a$ now give

$$\left.\begin{aligned} -\mathrm{H}_0a^2 + \mathrm{A}/a &= \mathrm{R}(\kappa a), \\ -\mathrm{H}_0a^2 - \tfrac{1}{2}\mathrm{A}/a &= \tfrac{1}{2}(\kappa a/\mu)\mathrm{R}'(\kappa a), \end{aligned}\right\}$$

where for convenience the suffix in κ_m has been dropped until the final formula is obtained.

Eliminating A we have

$$-3\mathrm{H}_0a^2 = \mathrm{R} + (\kappa a/\mu)\mathrm{R}', \quad . \quad . \quad . \quad (51)$$

while the boundary conditions at $r=b$ give

$$\left.\begin{aligned} -\mathrm{H}_0b^2 &= \mathrm{R}(\kappa b), \\ -\mathrm{H}_ib^2 &= \tfrac{1}{2}(\kappa b/\mu)\mathrm{R}'(\kappa b). \end{aligned}\right\} \quad . \quad . \quad . \quad (52)$$

Shielding Ratio for Low Frequencies.

For a thin shell we write $a=b+d$ in (51) and expand the right-hand side by Taylor's Theorem. Making use of (52) to express

$$\mathrm{R}(\kappa b) + (\kappa b/\mu)\mathrm{R}'(\kappa b) = -3\mathrm{H}_ib^2,$$

we have

$$-3\mathrm{H}_0a^2\mu = -3\mathrm{H}_ib^2\mu + \kappa d\{(\mu+1)\mathrm{R}'(\kappa b) + \kappa b\mathrm{R}''(\kappa b)\} + \text{terms in } (\kappa d)^2, \text{ etc.},$$

an expansion which is convergent if $|\kappa d|$ is sufficiently small, *i. e.*, if the frequency is so low that d/C is small compared to unity.

In the above equation we express $\mathrm{R}''(\kappa b)$ in terms of $\mathrm{R}(\kappa b)$ from the differential equation (50), and finally eliminate $\mathrm{R}(\kappa b)$ and $\mathrm{R}'(\kappa b)$ by making use of equations (52). In this way we obtain the result

$$3\mathrm{H}_0a^2 \sim 3\mathrm{H}_ib^2[1 + \tfrac{2}{3}(d/b)\{(\mu+1) + 1/\mu\} + \tfrac{1}{3}\kappa^2bd/\mu].$$

If we now write $b^2/a^2 \sim 1-2d/b+\ldots$ and replace κ by κ_m, remembering that $\kappa_m{}^2/\mu = \kappa^2 = i/C^2$, we finally obtain for the shielding ratio of a *thin magnetic shell* the result

$$\frac{H_i}{H_0} \sim \frac{1}{\left\{1+\frac{2}{3}\frac{(\mu-1)^2}{\mu}\frac{d}{b}+\frac{1}{3}\frac{i}{}\frac{bd}{C^2}\right\}}, \quad \ldots \quad (53)$$

where $C^2 = \rho/(8\pi^2 f)$.

It is a simple problem to derive directly the magnetostatic shielding formula

$$\frac{H_i}{H_0} = \frac{9\mu}{(2+\mu)(2\mu+1)-2(b^3/a^3)(\mu-1)^2}, \qquad (f=0). \quad (54)$$

If we write $a=b+d$ we obtain for a thin shell the approximate formula

$$\frac{H_i}{H_0} \sim \frac{1}{1+\frac{2}{3}\frac{(\mu-1)^2}{\mu}\frac{d}{b}}, \qquad (f=0),$$

to which (53) reduced when $f\to 0$, *i. e.*, $C\to\infty$.

Shielding Ratio at High Frequencies.

At radio frequencies, $\kappa_m r$ is so large that we may employ the approximate solution of (50) in the form

$$R(\kappa r) \sim Ae^{\kappa r} + Be^{-\kappa r},$$

where we write κ for κ_m.

At $r=b$ the boundary conditions give rise to two linear equations in A and B, which when solved give

$$2\kappa b A e^{\kappa b} = -H_i b^2(\kappa b+2\mu), \quad 2\kappa b B e^{\kappa b} = -H_i b^2(\kappa b-2\mu), \quad (55)$$

while at $r=a$, (51) gives

$$-3H_0 a^2\mu = (\kappa a+\mu)Ae^{\kappa a} - (\kappa a-\mu)Be^{-\kappa a}.$$

On substituting for A and B from (55) we obtain the result

$$6H_0 a^2\mu = \{(\kappa a+\mu)(\kappa b+2\mu)e^{\kappa(a-b)} - (\kappa a-\mu)(\kappa b-2\mu)e^{-\kappa(a-b)}\}H_i(b/\kappa). \quad (56)$$

Writing $a-b=d$ we may write for a *thin* shell, when $a\sim b$, except in the exponentials,

$$6H_0\frac{\mu}{\kappa a} \sim H_i\left[\left\{1+\frac{3\mu}{\kappa a}+2\left(\frac{\mu}{\kappa a}\right)^2\right\}e^{\kappa d} - \left\{1-\frac{3\mu}{\kappa a}+2\left(\frac{\mu}{\kappa a}\right)^2\right\}e^{-\kappa d}\right]. \quad (57)$$

The general formula (56) holds over a very wide range of frequencies; in fact, if the exponentials are expanded and $(a-b)$ replaced by d, this formula reduces to (53).

We may write (57) in the form

$$\frac{H_i}{H_0}=\frac{1}{\cosh\kappa d+\frac{1}{3}\frac{\kappa a}{\mu}\left\{1+2\left(\frac{\mu}{\kappa a}\right)^2\right\}\sinh\kappa d}. \quad (58)$$

(where instead of κ_m we have written $\kappa=\sqrt{\mu}/C$), from which the shielding ratio may be computed from nomograms giving the real and imaginary parts of hyperbolic functions of complex variables. At sufficiently high frequencies, when $\mu C_m/a$ is small compared to unity, the following approximate formula is easily derived:

$$\left|\frac{H_i}{H_0}\right|\sim\frac{3\mu C_m}{a}\cdot\frac{1}{\left|\sinh(1+i)\frac{d}{C_m\sqrt{2}}\right|}$$

$$=\frac{3\mu C_m}{a}\cdot\frac{1}{\left\{\sinh^2\frac{d}{C_m\sqrt{2}}+\sin^2\frac{d}{C_m\sqrt{2}}\right\}}, \quad (59)$$

where

$$C_m=C/\sqrt{\mu} \quad \text{and} \quad C^2=\rho/(8\pi^2 f),$$

which agrees with (26) when $\mu=1$. Graphs are most easily drawn by the use of Kennelly's charts, giving

$$\sinh(u+iv)=re^{i\theta}.$$

Section 10.—*Effect of Magnetic Permeability on the Shielding Ratio of Thin Cylindrical Shells.*

(i.) *Longitudinal field. Low-frequency formula.*

Making use of the electrical work-function ψ, as in Section 5, the appropriate solutions may be written:

$$\left.\begin{aligned} a<r<\infty, &\quad \psi_0=-\tfrac{1}{2}\dot{H}_0 r^2+\dot{A},\\ b<r<a, &\quad \psi=\tfrac{1}{2}\dot{R},\\ 0<r<b, &\quad \psi_i=-\tfrac{1}{2}\dot{H}_i r^2, \end{aligned}\right\} \quad (60)$$

where R is independent of z, and satisfies (27). Neglecting propagation, the equation for R is

$$r\frac{d}{dr}\left(\frac{1}{r}\frac{dR}{dr}\right)=\kappa_m^2 R \quad \text{or} \quad R''(\kappa r)-\frac{1}{r\kappa}R'(\kappa r)=R, \quad (61)$$

when, in the second equation, it is understood that κ stands for κ_m.

The boundary conditions are, at $r=b$,

$$\psi=\psi_i \quad \text{and} \quad \frac{1}{\mu}\frac{\partial\psi}{\partial r}=\frac{\partial\psi_i}{\partial r},$$

giving

$$-\mathrm{H}_i b^2=\mathrm{R}(\kappa b)$$

and

$$-\mathrm{H}_i b^2=\tfrac{1}{2}(\kappa b)/\mu\,.\,\mathrm{R}'(\kappa b). \quad . \quad . \quad . \quad . \quad (62)$$

At $r=a$ we only make use of the condition

$$\frac{1}{\mu}\frac{\partial\psi}{\partial r}=\frac{\partial\psi_0}{\partial r},$$

giving

$$-\mathrm{H}_0 a=\tfrac{1}{2}(\kappa/\mu)\mathrm{R}'(\kappa a).$$

Writing $a=b+d$ and expanding by Taylor's theorem, we have, when κd is small,

$$-\mathrm{H}_0 a=\tfrac{1}{2}(\kappa/\mu)[\mathrm{R}'(\kappa b)+\kappa d\mathrm{R}''(\kappa b)+\ \ldots\ ].$$

Substituting for $\mathrm{R}''(\kappa b)$ from the differential equation (61), we express the above equation in terms of $\mathrm{R}(\kappa b)$ and $\mathrm{R}'(\kappa b)$, which in turn may be expressed in terms of H_i by (62). We finally obtain, replacing κ by κ_m,

$$(a/b)\mathrm{H}_0/\mathrm{H}_i=(1+d/b)+\tfrac{1}{2}\kappa_m{}^2 bd/\mu,$$

or, for a thin shell, neglecting d/b, and remembering that

$$\kappa_m{}^2/\mu=\kappa^2=i/\mathrm{C}^2,$$

we have the shielding formula

$$\frac{\mathrm{H}_i}{\mathrm{H}_0}=\frac{1}{1+\frac{1}{2}i\frac{ad}{\mathrm{C}^2}}, \quad . \quad . \quad . \quad . \quad . \quad (63)$$

which, on comparison with (39), shows that for low frequencies the magnetic permeability plays no part in shielding.

(ii.) *Longitudinal field. High-frequency formula.*

Instead of (60) we make use of the solutions

$$\left.\begin{array}{ll} a<r<\infty, & \psi_0=-\tfrac{1}{2}\dot{\mathrm{H}}_0 r^2+\dot{\mathrm{A}}, \\ b<r<a, & \psi\sim-\tfrac{1}{2}\dot{\mathrm{B}}\sqrt{\kappa r}e^{\kappa r}+\tfrac{1}{2}\dot{\mathrm{C}}\sqrt{\kappa r}\,e^{-\kappa r}, \\ 0<r<b, & \psi_i=-\tfrac{1}{2}\dot{\mathrm{H}}_i r^2, \end{array}\right\} . \quad (64)$$

where the asymptotic solution of (61) for ψ is employed. The boundary conditions at $r=b$,

$$\psi=\psi_i \quad \text{and} \quad \frac{1}{\mu}\frac{\partial\psi}{\partial r}=\frac{\partial\psi_i}{\partial r},$$

give, neglecting $1/|\kappa b|$ compared to unity,

$$\left.\begin{aligned} -\mathrm{H}_i b^2 &\sim \sqrt{\kappa b}\{\mathrm{B}e^{\kappa b}+\mathrm{C}e^{-\kappa b}\},\\ -\mathrm{H}_i b &\sim \tfrac{1}{2}(\kappa/\mu)\sqrt{\kappa b}\{\mathrm{B}e^{\kappa b}-\mathrm{C}e^{-\kappa b}\},\end{aligned}\right\}$$

which enables B and C to be calculated.

At $r=a$ the condition

$$\frac{1}{\mu}\frac{\partial\psi}{\partial r}=\frac{\partial\psi_0}{\partial r}$$

gives

$$-\mathrm{H}_0 a \sim \tfrac{1}{2}(\kappa/\mu)\sqrt{\kappa a}\{\mathrm{B}e^{\kappa a}-\mathrm{C}e^{-\kappa a}\}.$$

Substituting for B and C, we obtain finally, writing $a=b+d$,

$$\frac{\mathrm{H}_0}{\mathrm{H}_i}\sim\sqrt{\frac{b}{a}}\left(\cosh\kappa d+\frac{1}{2}\frac{b\kappa}{\mu}\sinh\kappa d\right),$$

or for a thin shell we have, remembering that κ stands for κ_m,

$$\frac{\mathrm{H}_i}{\mathrm{H}_0}\sim\frac{1}{\cosh\kappa_m d+\frac{1}{2}(\kappa_m a/\mu)\sinh\kappa_m d}, \quad \ldots \quad (65)$$

a formula which holds for a wide range of frequencies, since for $\kappa_m d$ small it reduces, on expanding the denominator in powers of $\kappa_m d$, to (63).

For high frequencies, when the first term is negligible compared to the second,

$$\frac{|\mathrm{H}_i|}{|\mathrm{H}_0|}\sim 2\mu\frac{\mathrm{C}_m}{a}\frac{1}{\left|\sinh(1+i)\dfrac{d}{\mathrm{C}_m\sqrt{2}}\right|}$$

$$=2\mu\frac{\mathrm{C}_m}{a}\frac{1}{\left\{\sinh^2\dfrac{d}{\mathrm{C}_m\sqrt{2}}+\sin^2\dfrac{d}{\mathrm{C}_m\sqrt{2}}\right\}^{1/2}}, \quad (66)$$

where

$$\mathrm{C}_m=\mathrm{C}/\sqrt{\mu} \quad \text{and} \quad \mathrm{C}^2=\rho/(8\pi^2 f).$$

The formulæ (65) and (66) agree with (44) and (45) when $\mu=1$.

(iii.) *Transverse field. Low-frequency formula.*

Referring to Section 6 we write, instead of (37),

$$w = \mathrm{R}(\kappa r)\sin\phi,$$

where $\mathrm{R}(\kappa r)$ is a solution of the differential equation

$$\frac{d^2\mathrm{R}}{dr^2} + \frac{1}{r}\frac{d\mathrm{R}}{dr} - \left(\kappa_m^2 + \frac{1}{r^2}\right)\mathrm{R} = 0; \quad . \quad . \quad (67)$$

and κ now has the meaning κ_m appropriate to a cylindrical shell of magnetic material.

In the material of the shell the magnetic field components are, according to (34),

$$\mathrm{H}_r = -\frac{\rho}{r}\mathrm{R}(\kappa r)\cos\phi, \qquad \mathrm{H}_\phi = \rho\kappa\mathrm{R}'(\kappa r)\sin\phi. \quad (68)$$

Within the shell and in the space outside, the magnetic field is expressible by the exponentials

$$a < r < \infty, \qquad \Omega_0 = \mathrm{H}_0 r\cos\phi + \mathrm{C}\cos\phi/r$$

and

$$0 < r < b, \qquad \Omega_i = \mathrm{H}_i r\cos\phi.$$

At the boundaries $r=a$, $r=b$, the the tangential components H_φ of the magnetic field are continuous, while $\mu\mathrm{H}_r$ is also continuous at each boundary. We thus have, at $r=a$,

$$\left.\begin{aligned} -a\mathrm{H}_0 + \mathrm{C}/a &= \mu\rho\mathrm{R}(\kappa a), \\ -a\mathrm{H}_0 - \mathrm{C}/a &= \rho\kappa a\mathrm{R}'(\kappa a), \end{aligned}\right\}$$

giving

$$-2a\mathrm{H}_0/\rho = \mu\mathrm{R}(\kappa a) + \kappa a\mathrm{R}'(\kappa a). \quad . \quad . \quad (69)$$

At $r=b$ the boundary conditions give

$$-b\mathrm{H}_i = \mu\rho\mathrm{R}(\kappa b) \quad \text{and} \quad -b\mathrm{H}_i = \rho\kappa b\mathrm{R}'(\kappa b). \quad (70)$$

If we now write $a=b+d$ in (69) and expand by Taylor's Theorem, we may eliminate $\mathrm{R}''(\kappa b)$ from the differential equation (67) and finally express $\mathrm{R}(\kappa b)$ and $\mathrm{R}'(\kappa b)$ in terms of H_i by (70). We finally obtain

$$a\mathrm{H}_0 = b\mathrm{H}_i\{1 + \tfrac{1}{2}(\mu + 1/\mu)d/b + \tfrac{1}{2}\kappa^2 bd/\mu\},$$

or writing $b/a \sim 1 - d/b$ and replacing κ by κ_m we find, remembering that $\kappa_m^2/\mu = \kappa^2 = i/\mathrm{C}^2$,

$$\frac{\mathrm{H}_i}{\mathrm{H}_0} \sim \frac{1}{\left\{1 + \frac{1}{2}\frac{(\mu-1)^2}{\mu}\frac{d}{a} + \frac{1}{2}\frac{ad}{i\mathrm{C}^2}\right\}}, \quad . \quad . \quad (71)$$

a result which reduces to (39) when $\mu=1$.

We note, in passing, the magnetostatic shielding formula

$$\frac{H_i}{H_0}=\frac{4\mu}{(\mu+1)^2-(b^2/a^2)(\mu-1)^2}, \qquad (f=0). \qquad (72)$$

When $a=b+d$ this gives for a thin shell the appropriate formula

$$\frac{H_i}{H_0}\sim\frac{1}{1+\frac{1}{2}\frac{(\mu-1)^2}{\mu}\frac{d}{a}}, \qquad (f=0), \quad . \quad . \quad (73)$$

to which (71) reduces when $f\to 0$ or $C\to\infty$.

(iv.) *Transverse field. High-frequency formula.*

When κr is large for $b<r<a$ we make use of the asymptotic solution

$$w=R(\kappa r)\sin\phi\sim\frac{1}{\sqrt{\kappa r}}(Ae^{\kappa r}+Be^{-\kappa r})\sin\phi. \quad . \quad (74)$$

At $r=b$ the boundary conditions (70) give approximately, neglecting $1/|\kappa b|$ compared to unity,

$$\left.\begin{aligned}\frac{1}{\sqrt{(\kappa b)}}(Ae^{\kappa b}+Be^{-\kappa b})&=-bH_i/(\mu\rho),\\ \frac{1}{\sqrt{(\kappa b)}}(Ae^{\kappa b}-Be^{-\kappa b})&=-bH_i/(\rho\kappa b).\end{aligned}\right\}$$

At $r=a$ the boundary conditions lead to (69), which results in

$$-\frac{2aH_0}{\rho}\sim\frac{1}{\sqrt{(\kappa a)}}\{(\mu+\kappa a)Ae^{\kappa a}+(\mu-\kappa a)Be^{-\kappa a}\}.$$

Eliminating A and B between the last three equations we finally obtain for a thin shell, for which $a=b+d$ and d/b is small, the result

$$4\mu\kappa aH_0\sim H_i[(\mu+\kappa a)^2e^{\kappa d}-(\mu-\kappa a)^2e^{-\kappa d}]$$

or

$$\frac{H_i}{H_0}=\frac{1}{\cosh\kappa d+\frac{1}{2}\frac{\kappa a}{\mu}\left\{1+\left(\frac{\mu}{\kappa a}\right)^2\right\}\sinh\kappa d}. \quad . \quad (75)$$

When $\mu/|\kappa a|$ is negligible compared to unity we have, replacing κ by κ_m,

$$\frac{H_i}{H_0} \sim \frac{1}{\cosh \kappa_m d + \frac{1}{2}\frac{\kappa_m a}{\mu}\sinh \kappa_m d}, \quad . \quad . \quad (76)$$

and at sufficiently high frequencies, when the first term in the denominator of (76) is negligible compared to the second,

$$\frac{|H_i|}{|H_0|} \sim 2\mu \frac{C_m}{a} \frac{1}{\left|\sinh (1+i)\frac{d}{C_m\sqrt{2}}\right|}$$

$$= \frac{2\mu C_m}{a} \frac{1}{\left\{\sinh^2 \frac{d}{C_m\sqrt{2}} + \sin^2 \frac{d}{C_m\sqrt{2}}\right\}^{1/2}}, \quad (77)$$

showing, on comparison with (65) and (66), that at high frequencies the shielding ratio is the same for longitudinal and transverse fields, and it may be inferred that this result holds when the field makes any angle with the axis of the cylindrical shell. For low frequencies, however, the transverse and longitudinal shielding ratios are not the same when the cylindrical shell is magnetic.

Section 11.—*Numerical Examples.*

An estimate of shielding ratios may be made from the following table calculated for a thin cylindrical shell of

TABLE I.

f.	C(cm.).	$\frac{C}{a}$.	$\frac{d}{(C\sqrt{2})}$.	$\frac{\lvert H_i \rvert}{\lvert H_0 \rvert}$ (formula (39)).	$\frac{\lvert H_i \rvert}{\lvert H_0 \rvert}$ (formula (45)).
10^2	$6{\cdot}1\times10^{-1}$	$2{\cdot}4\times10^{-1}$	·030	·98	.....
10^3	$1{\cdot}9\times10^{-1}$	$7{\cdot}6\times10^{-2}$	·094	·75	.....
10^4	$6{\cdot}1\times10^{-2}$	$2{\cdot}4\times10^{-2}$	·30	·112	$1{\cdot}12\times10^{-1}$
10^5	$1{\cdot}9\times10^{-2}$	$7{\cdot}6\times10^{-3}$	·94	·0115	$1{\cdot}14\times10^{-2}$
10^6	$6{\cdot}1\times10^{-3}$	$2{\cdot}4\times10^{-3}$	3·0	...	$4{\cdot}9\times10^{-4}$
10^7	$1{\cdot}9\times10^{-3}$	$7{\cdot}6\times10^{-4}$	9·4	...	$5{\cdot}6\times10^{-7}$
10^8	$6{\cdot}1\times10^{-4}$	$2{\cdot}4\times10^{-4}$	30	...	$4{\cdot}4\times10^{-10}$

aluminium of radius $a=2{\cdot}54$ cm., wall thickness $d=2{\cdot}54 \times 10^{-2}$ cm., and specific resistance $\rho=3\times10^{-6}$ ohm–cms. or $\rho=3\times10^{3}$ absolute ohm–cms. Magnetic permeability $\mu=1$.

It will be noticed that over a considerable range of frequencies the low-frequency formula (39) gives results in rough agreement with the high-frequency formula (45).

In order to estimate the relative advantages of shielding by a magnetic cylinder, a corresponding table is calculated for a cylindrical shell of soft iron, radius $a=2{\cdot}54$ cm., wall thickness $d=2{\cdot}54\times10^{-2}$ cm., and specific resistance $\rho=10\times10^{-6}$ ohm-cms. or $\rho=10^{4}$ absolute ohm-cms. The magnetic permeability is taken as $\mu=1000$.

It will be noticed that for frequencies greater than 10^4 the magnetic permeability plays an enormous part in improving the efficiency of shielding. It must be remembered that there is little to justify the value $\mu=1000$ at these high frequencies, and the writer has been unable to find satisfactory experimental data as to the effective permeability of iron at radio frequencies. In fact, the use of the theory of the present paper offers a means of determining experimentally the effect of very high frequencies on the permeability of magnetic materials.

The figures of Table II. show, apparently, a very great advantage in the use of soft iron in the construction of shielding containers. The writer is informed by Mr. Lyons that when it is used for shielding radio transformers the stray fields from the latter set up induction currents from the inside which, owing to hysteresis effects, add very greatly to the transformer losses.

The theoretical formulæ we have derived indicate two possible methods of overcoming this difficulty. First, if space is available, by increasing the mean radius a of the container better shielding from outside disturbances is obtained in the ratio $\mu C_m/a$, and at the same time the interaction of the stray transformer fields with the container walls is greatly diminished. Secondly, by using a double or composite container, the inner one of highly conducting non-magnetic metal, affecting transformer fields by phase changes with little induced current losses, the outer iron container may be protected from interior fields. At the same time the interior container—and with it the transformers—may be protected from outside disturbances by the greatly enhanced shielding effect of the iron outer container. By making use of the methods of this paper there is no difficulty in estimating the most suitable dimensions of such a composite container.

TABLE II.

f.	C_m(cm.).	$\frac{C_m}{a}$.	$\frac{d}{(C_m\sqrt{2})}$.	$\frac{\lvert H_i \rvert}{\lvert H_0 \rvert}$ (formula (63)).	$\frac{\lvert H_i \rvert}{\lvert H_0 \rvert}$ (formulæ (66), (77)).	$\frac{\lvert H_i \rvert}{\lvert H_0 \rvert}$ (formula (71)).
10^2	$3{\cdot}6 \times 10^{-2}$	$1{\cdot}4 \times 10^{-2}$	·50	1·00	...	·17
10^3	$1{\cdot}13 \times 10^{-2}$	$4{\cdot}5 \times 10^{-3}$	1·60	·95	...	·17
10^4	$3{\cdot}6 \times 10^{-3}$	$1{\cdot}4 \times 10^{-3}$	5·0	...	$3{\cdot}1 \times 10^{-2}$	...
10^5	$1{\cdot}13 \times 10^{-3}$	$4{\cdot}5 \times 10^{-4}$	16·0	...	$2{\cdot}2 \times 10^{-7}$	...
10^6	$3{\cdot}6 \times 10^{-4}$	$1{\cdot}4 \times 10^{-4}$	50	...	$1{\cdot}8 \times 10^{-23}$	...
10^7	$1{\cdot}13 \times 10^{-4}$	$4{\cdot}5 \times 10^{-5}$	160	...	$6{\cdot}4 \times 10^{-72}$	...
10^8	$3{\cdot}6 \times 10^{-5}$	$1{\cdot}4 \times 10^{-5}$	500	...	$5{\cdot}6 \times 10^{-227}$	...

In the last column of Table II. is given the shielding ratio for a magnetic field at right angles to the axis of the cylindrical shell. At low frequencies the magnetic permeability greatly improves the shielding. For frequencies above 1000 the shielding ratio becomes the same for longitudinal and transverse fields.

For non-magnetic shells the theory of the present paper has been satisfactorily verified by a series of experiments carried out at McGill University by Mr. W. Lyons, M.Sc., for frequencies ranging from 1000 to 30,000 cycles. Among these results it is shown that in longitudinal fields the shielding ratios for cylinders of finite length rapidly approach the calculated values for infinite cylinders when the length is of the order of the diameter. It is hoped that these experiments will be continued to higher frequencies and to include measurements on magnetic shielding containers for which theory indicates a decided advantage.

Section 12.—*Summary and Conclusions.*

1. It is possible to calculate the alternating field inside a closed conducting spherical shell of uniform thickness placed in a uniform alternating magnetic field such as that due to plane electromagnetic waves of wave-length large compared to the linear dimensions of the shell in question.

2. Corresponding formulæ may also be obtained for cylindrical shells of uniform thickness.

3. In the case of *thin* shells formulæ suitable for numerical calculation are obtained, valid over the entire range of frequencies from a few cycles per second to radio frequencies.

4. A method of calculating the shielding ratio for thin shells is developed which makes direct use of the differential equation for current distribution in the shell, and of its asymptotic solutions. This method makes it possible to extend the calculations and take into account the effect of magnetic permeability on the shielding ratio. The method also makes it possible to calculate the shielding ratio for other shapes than thin cylindrical or spherical shells, as, for instance, ellipsoidal shells and others defined by appropriate curvilinear coordinates.

5. Numerical calculations indicate marked advantages in the use of shielding containers of iron. To finally substantiate this conclusion experimental data on the effective magnetic permeability of iron at radio frequencies are required.

6. At radio frequencies the shielding ratio is approximately given by the formula

$$\frac{|H_i|}{|H_0|} \sim s\sqrt{\mu} \cdot \frac{C}{a} e^{-\frac{d\sqrt{\mu}}{C\sqrt{2}}}, \quad . \quad . \quad . \quad . \quad (78)$$

where C is the induction constant given by $C^2 = \rho/(8\pi^2 f)$, while ρ is the specific resistance in C.G.S. units and f is the frequency. The factor $s=4$ for a cylindrical, and $s=6$ for a spherical shell of mean radius a and wall thickness d, the magnetic permeability being μ. We conclude, in general, that the shielding ratio of a closed conductor of wall thickness d of *any shape* may be roughly estimated from (78) by taking a to represent some average linear dimension corresponding to the radius of a sphere, while s is a *shape factor*, a pure numeric between 4 and 6.

XXII. *Some Observations on Residual Charge in Dielectrics.* *By* D. K. McCleery, *M.Sc.*, *A.M.I.E.E.* (*Woolwich Polytechnic*)*.

Introduction.

THE phenomenon of residual charge in dielectrics is well known. This is also referred to as "absorption," a term which, though descriptive, is not to be taken too literally. When a potential difference is applied to a dielectric the resulting current is generally considered to consist of three components: (*a*) the so-called geometric charging current, which is practically instantaneous; (*b*) the absorption current, sometimes known as the anomalous charging current; (*c*) the true conduction current. The present observations are concerned with the second component.

The absorption current should diminish with time; this property is, in fact, the criterion of a good dielectric. Often there is a slow decrease for days or even months. The true conduction current in a dielectric, if it exists at all, must be very difficult to determine owing to this persistence of the absorption current; for this reason the expression "dielectric resistance" is applied to the

* Communicated by the Author.

apparent resistance after an arbitrary period of time, usually one minute.

Maxwell's Theory [1].

Maxwell based his theory of dielectric absorption on an assumption of heterogeneity of the material. He imagined first a stratified dielectric in which the layers had different values of the product of dielectric constant by specific resistance, assuming that the individual layers were quite free from the absorptive effect. Taking a simple case of two layers, this is represented in fig. 1 by an arrangement of pure capacities and resistances.

The problem of determining the transient current in such a network, set up by the sudden application

Fig. 1.

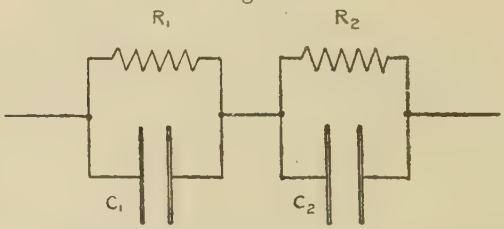

of a potential V_0, may be solved by Heaviside's expansion theorem [2]. The operational impedance is written

$$f(p) = \frac{R_1}{1+pC_1R_1} + \frac{R_2}{1+pC_2R_2}, \quad . \quad . \quad . \quad (1)$$

and, equating this to zero, we have

$$p = -\frac{R_1+R_2}{R_1R_2(C_1+C_2)} = -\frac{1}{T}, \quad . \quad . \quad . \quad . \quad (2)$$

$$f(p) = \frac{pTR+R}{(1+pC_1R_1)(1+pC_2R_2)}, \quad . \quad . \quad . \quad . \quad (3)$$

where $$R = R_1+R_2. \quad . \quad . \quad . \quad . \quad . \quad . \quad . \quad . \quad . \quad (4)$$

Differentiating (3),

$$f'(p) = \frac{TR}{(1+pC_1R_1)(1+pC_2R_2)},$$

$$1/[p\,f'(p)] = \frac{1/p+C_1R_1+C_2R_2+pC_1C_2R_1R_2}{TR} \quad . \quad . \quad (5)$$

Let

$$C = \frac{C_1 C_2}{C_1 + C_2}, \quad \ldots \ldots \quad (6)$$

and

$$k = \frac{(C_1 R_1 - C_2 R_2)^2}{C_1 C_2 (R_1 + R_2)^2}; \quad \ldots \ldots \quad (7)$$

then, combining (5), (6), and (7),

$$1/[p f'(p)] = \frac{CR(1+k) - CR}{TR} = Ck/T. \quad \ldots \quad (8)$$

Hence, by the expansion theorem

$$i_t = V_0 \left\{ \frac{1}{R} + \frac{Ck}{T} e^{-\frac{t}{T}} \right\}. \quad \ldots \ldots \quad (9)$$

This shows that in a simple Maxwellian dielectric of two layers the absorption current is exponential with regard to time.

Fig. 2.

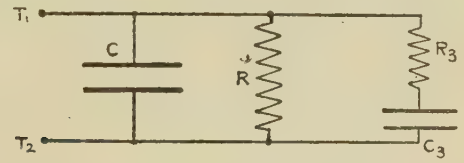

The addition of more meshes to the circuit in fig. 1 makes the calculation increasingly laborious. A useful simplification is shown in fig. 2. The current into this system at any time after applying a potential V_0 across the condenser C is easily seen to be

$$i_t = V_0 \left\{ \frac{1}{R} + \frac{1}{R_3} e^{-\frac{t}{R_3 C_3}} \right\}. \quad \ldots \ldots \quad (10)$$

This does not include the charging current into the condenser C, which is instantaneous, since we are considering pure capacities and resistances. Now the expression (10) is of the same form as (9), and it will be seen that the two circuits are exactly equivalent if

$$R = R_1 + R_2, \quad \ldots \ldots \quad (11)$$

$$C = \frac{C_1 C_2}{C_1 + C_2}, \quad \ldots \ldots \quad (12)$$

$$R_3 = \frac{R_1 R_2}{R_1 + R_2} . m^2, \quad . \quad . \quad . \quad . \quad . \quad . \quad . \quad . \quad . \quad (13)$$

$$C_3 = (C_1 + C_2)/m^2, \quad . \quad . \quad . \quad . \quad . \quad . \quad . \quad . \quad . \quad (14)$$

where

$$m = \frac{(C_1 + C_2)(R_1 + R_2)}{(C_1 R_1 - C_2 R_2)} . \quad . \quad . \quad . \quad . \quad . \quad . \quad (15)$$

The addition of a third and further layers is imitated by placing further resistance-capacity elements in parallel with the first; each of these will supply its own particular time constant $R_n C_n$, and produce a fresh exponential term in the expression for the absorption current. It is a fact that, although a single term function is a poor imitation of the absorption currents met with in practice, yet when many such terms are taken the representation becomes tolerably accurate.

The strata can hardly be imagined to exist in reality, and Maxwell wrote [3] :—

"An investigation of the cases in which the materials are arranged otherwise than in strata would lead to similar results, though the calculations would be more complicated, so that we may conclude that the phenomenon of electric absorption may be expected in the case of substances composed of parts of different kinds even though these parts should be microscopically small."

Recently Kouenhoven [4] announced that he was attempting to obtain two or more "perfect dielectrics having no absorption but different conductivities and dielectric constants," and that he proposed to make a mixture of these materials, expecting to find absorption "if Maxwell's theory is correct." It is difficult to see what useful purpose could be served by such an experiment in working backwards. Maxwell's theory is susceptible of rigorous mathematical proof, and there can be no doubt that a mixture such as proposed by Kouenhoven would exhibit absorption in virtue of its inhomogeneity. Even if the so-called perfect dielectrics could be found the experiment would not be proof that inhomogeneity was the sole cause of absorption, but only that it was one of the causes. It is exceedingly probable that all solid insulators show the property of absorption whether homogeneous or not.

The Superposition Principle.

Hopkinson applied Boltzmann's treatment of the after-effect of mechanical strain ("elastische Nachwirkung") to the residual charge of a dielectric, and postulated that the effects of successively applied potentials could be superposed [5]. This means that, supposing an absorption current i is flowing in a dielectric under an e.m.f. V applied at time $t = 0$, and the e.m.f. is suddenly changed by an amount ΔV at time $t = t_1$, the resulting current will be the sum of two components, the first equal to i flowing as if nothing had happened, and the second, i_1, which is equal to the current which would be produced by an e.m.f. of magnitude ΔV acting on the uncharged dielectric at time t_1.

It is generally assumed that the absorption current in a dielectric is proportional to the potential V. Hence it may be written.

$$i = \mathrm{V}\,\psi(t),$$

where $\psi(t)$ is a decreasing function of the time. If now the potential is changed to V+ΔV at time $t = t_1$, the current becomes, by the superposition principle,

$$i' = \mathrm{V}\,\psi(t) + \Delta\mathrm{V}\,\psi(t-t_1). \quad . \quad . \quad . \quad . \quad (16)$$

The simplest case is that in which the potential is reduced to zero after charging for a time t_1, *i. e.*, ΔV is equal to $-$V. We have then

$$i' = \mathrm{V}\,\{\psi(t) - \psi(t-t_1)\}, \quad . \quad . \quad . \quad . \quad . \quad (17)$$

where the zero of time is taken to be the moment of application of the e.m.f. V. This is the expression for the discharge current produced by the absorption effect on short-circuiting the electrodes.

In general let the dielectric be subjected to an e.m.f. applied in steps Δ_0V, Δ_1V, Δ_2V, and so on, acting at times $t = 0$, t_1, t_2, etc. The expression for the absorption current derived from the superposition principle is

$$i = \{\Delta_0\mathrm{V}\,\psi(t) + \Delta_1\,\psi(t-t_1) + \Delta_2\mathrm{V}\,\psi(t-t_2) + \ldots\}\,. \quad (18)$$

It may be remarked that the superposition principle is independent of any explanation of the property of absorption, though such explanation must take account of it, as it has experimental support.

Observations of the Residual Charge.

The tests of gutta-percha, about to be described, were taken on a piece of submarine telegraph-cable 11·51 nautical miles in length, this being a very convenient form of specimen.

A quadrant electrometer E, connected idiostatically, was used to measure the potential of the residual charge (see fig. 3). With the switch S_1 in the left-hand position the cable was charged to the potential of the battery V_0. After a time t_1 the switch S_1 was moved to the right, S_2 being closed. The cable having been to earth for a suitable period, S_2 was opened at time t_2 and the accumulation of the residual potential was observed. The results are shown in figs. 4 and 5. In the former

Fig. 3.

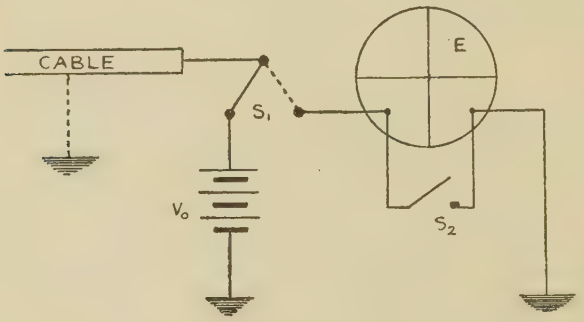

the effect of varying the time of charge is seen, the earthing interval (t_2-t_1) being constant, 5 seconds; in the latter the charging period was constant, 5 minutes, and various earthing intervals were taken.

It is interesting to see how Maxwell's theory predicts the course of the returning charge. Referring back to fig. 2, the operational conductance between terminals T_1 and T_2 is

$$pC+\frac{1}{R}+\frac{pC_3}{1+pC_3R_3} \quad . \quad . \quad . \quad . \quad . \quad . \quad (19)$$

The relation between the potential across T_1, T_2, and the current into the system is therefore

$$i=V_0\frac{p^2CRC_3R_3+p(C_3R_3+CR+C_3R)+1}{R(1+pC_3R_3)} \quad . \quad . \quad (20)$$

The current produced by a potential V_0 applied at time $t=0$ we have already seen to be

$$i_t = V_0 \left\{ \frac{1}{R} + \frac{1}{R_3} e^{-\frac{t}{C_3 R_3}} \right\}. \quad . \quad (10 \text{ above})$$

Fig. 4.

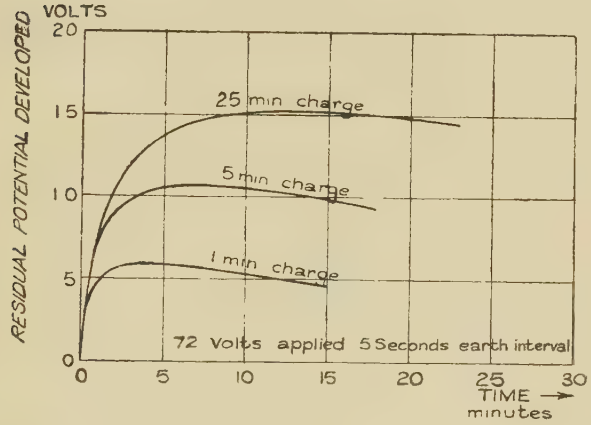

Fig. 5.

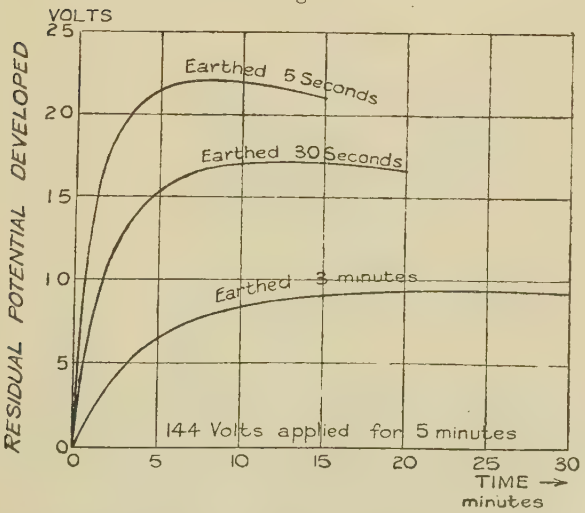

If the potential is reduced to zero after time $t=t_1$ then, using Hopkinson's principle, the current is

$$i' = \frac{V_0}{R_3} \cdot e^{-\frac{t}{C_3 R_3}} (1 - e^{\frac{t_1}{C_3 R_3}}). \quad . \quad . \quad . \quad . \quad (21)$$

The short-circuit across T_1, T_2 is removed at time $t=t_2$ and the system left to itself. The problem is to find V_t the potential across the condenser C at any time $(t-t_2)$ after freeing. The removal of the short-circuit is equivalent to impressing suddenly upon the circuit an equal and opposite current, and the resulting potential difference is given in operational form from (20). This may be written

$$V_t = -i'/F(p), \quad . \quad . \quad . \quad . \quad . \quad . \quad . \quad . \quad . \quad . \quad (22)$$

where

$$F(p) = \frac{p^2CRC_3R_3 + p(C_3R_3 + CR + C_3R) + 1}{R(1 + pC_3R_3)} \quad . \quad . \quad . \quad (23)$$

Let $a = 1/C_3R_3$, $b = 1/CR$, and $c = 1/C_3R$, (24)

$$F(p) = \frac{p^2 + p(a+b+c) + ab}{Rb(a+p)} \quad . \quad . \quad . \quad . \quad . \quad . \quad . \quad (25)$$

Equating this to zero, we find two roots for p. Let these be

$$p = \alpha \pm \beta, \quad . \quad . \quad . \quad . \quad . \quad . \quad . \quad (26)$$

where $$\alpha = -\tfrac{1}{2}(a+b+c), \quad . \quad (27)$$

and $$\beta^2 = \alpha^2 - ab. \quad . \quad . \quad . \quad . \quad . \quad (28)$$

Now (28) is essentially positive, hence the values of p cannot be complex.

Differentiating $F(p)$ with respect to p :—

$$F'(p) = \frac{2p - 2\alpha}{Rb(a+p)}, \quad . \quad . \quad . \quad . \quad . \quad . \quad (29)$$

$$1/[p.F'(p)] = \frac{R(ab/p + b)}{\pm 2\beta}$$

$$= \pm \frac{R}{2\beta}\left[\frac{\alpha^2 - \beta^2}{\alpha \pm \beta} + b\right]$$

$$= \frac{R}{2}\left[-1 \pm \frac{\alpha + b}{\beta}\right]. \quad . \quad . \quad . \quad . \quad (30)$$

Putting $p = 0$ in (23) we have $1/F(0) = R$.
Hence, substituting n the expansion formula,

$$V_t = -i'R\left[1 - e^{\alpha(t-t_2)}\left\{\cosh\beta(t-t_2) - \frac{\alpha+b}{\beta}\sinh\beta(t-t_2)\right\}\right]. \quad . \quad . \quad . \quad (31)$$

Substituting for i' from (21),

$$V_t = V_0 \frac{R}{R_3}(e^{at_1}-1)e^{-at}\left[1-e^{a(t-t_2)}.\left\{\cosh\beta(t-t_2) - \frac{\alpha+b}{\beta}\sinh\beta(t-t_2)\right\}\right]. \quad . \quad . \quad . \quad (32)$$

Example.—Taking

$$R = 10^7\Omega, \quad C = 50\mu F,$$
$$R_3 = 10^8\Omega, \quad C_3 = 20\mu F,$$

Fig. 6.

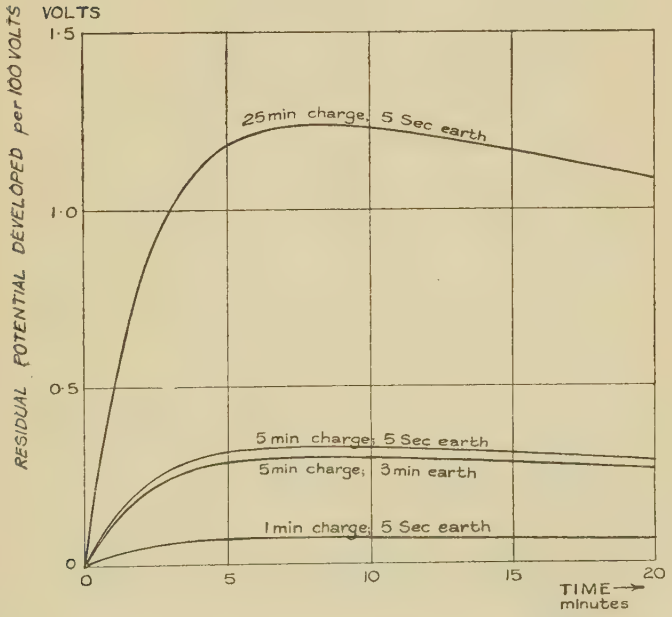

the residual potentials which would be developed for various times of charging per 100 volts have been calculated from (32). The results are shown in fig. 6.

The values of resistance and capacity taken in this particular case were quite at random, and the results can only be compared qualitatively with those shown in figs. 4 and 5. It is demonstrated, however, that a model of a two-layer Maxwell dielectric exhibits the phenomenon of residual charge. The most notable feature of divergence between the observed and calculated curves

is that in the latter the maxima all occur at the same time after freeing, while the experimental results show displaced maxima according to the conditions of charging and earthing. This is due to the fact that the model has but a single exponential term, while the actual dielectric has several. The longer time constants may

Fig. 7.

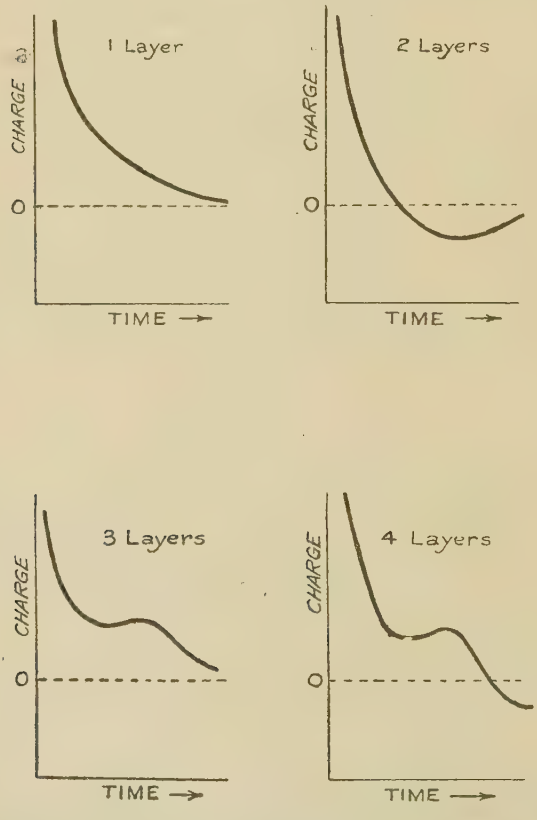

be expected to show up more for the longer charging periods, the residual charge will contain more long period terms, and the maximum will therefore occur later. On the other hand, for a fixed period of charge the shorter time constants will tend to disappear for the longer earthing interval, leaving a preponderance of long period terms and causing the maximum to be smaller but to be attained at a later time.

The Charge Layer Effect.

Hopkinson was led to believe that if a dielectric was subjected to reversals of potential then the current on discharge would change polarity as though the absorbed charges formed distinct layers [6].

"Suppose a condenser be charged positively for a long time, the polarization of all the substances will be fully developed; let the charge be next negative

Fig. 8.

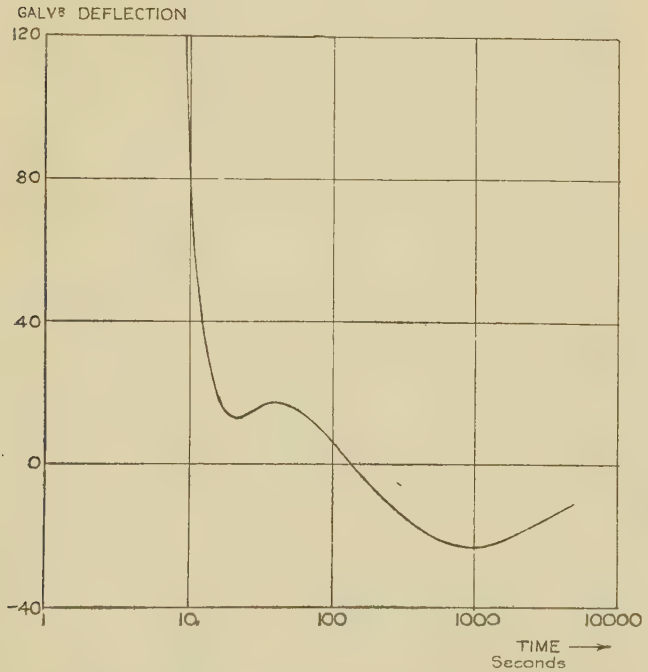

for a shorter time, the rapidly changing polarities will change their sign, but the time is insufficient to reverse those which are more sluggish. Let the condenser be then discharged and insulated, the rapid polarization will decay, first liberating a negative charge; but after a time the effect of the slow terms will make itself felt and the residual charge becomes positive, rises to a maximum, and then decays by conduction."

This hypothesis was verified for glass, and it is, in fact, a necessary condition of the superposition principle, as will

be shown below. The dielectric may be said to "remember" the various charges administered to it. The forms of discharge curves to be expected for various layers up to four are shown in fig. 7.

Fig. 9.

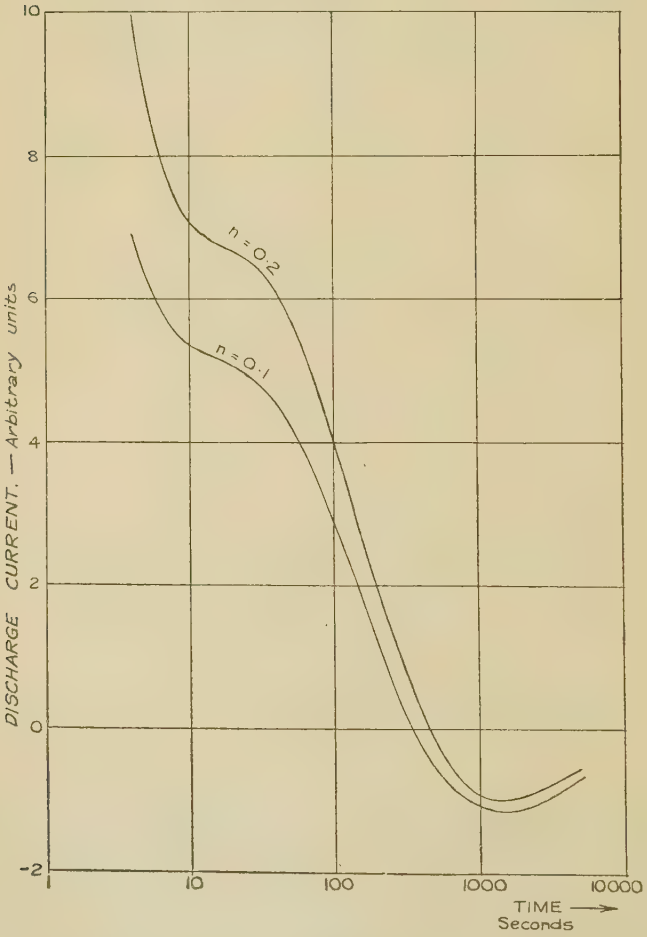

An attempt to obtain a discharge curve of the fourth type was made on a 22·5 mile length of gutta-insulated cable (a different type from the one previously used). The following sequence was carried out :—

Charged 30 minutes with negative polarity.

Earthed 5 minutes.

Charged 10 minutes with positive polarity.

,, 30 seconds ,, negative ,,

,, 5 ,, ,, positve ,,

The cable was then put to earth through a galvanometer and its discharge characteristic observed. This is shown in fig. 8, the current being considered positive when produced by a positive potential on the conductor of the cable.

In order to apply the superposition principle to the above case it is necessary to know the form of the discharge current function $\psi(t)$. The single term exponential is very far from the truth, and the formula usually employed is

$$\psi(t) = At^{-n}, \qquad (n<1 \text{ and } A = \text{constant.})$$

This has been obtained experimentally by many workers. It has also been shown by Wagner [7] to follow from an assumption of many time constants grouped about a certain most probable value according to the Gaussian error law. The validity of the expression is, however, limited to small ranges of t. If we insert this function in equation (18) and use the same time intervals as in the above experimental case we obtain as the discharge current

$$i = V_0 A \{t^{-n} - (t-1800)^{-n} - (t-2100)^{-n} + 2(t-2700)^{-n} - 2(t-2730)^{-n} + (t-2735)^{-n}\},$$

beginning at time $t = 2735$ seconds. A positive sign indicates a positive charge on the conductor of the cable. Curves are shown in fig. 9 for $n = 0{\cdot}1$ and $0{\cdot}2$, when AV_0 is made arbitrarily equal to 100. The similarity between these curves and that experimentally obtained (fig. 8) is not, admittedly, very striking. We have, however, assumed in the theoretical case that n is constant over the whole range of time, while in practice it changes considerably. The divergence is therefore to be expected, but the layer effect is unmistakable in both cases.

Summary.

1. Observations have been made of the residual charge in a dielectric and compared with the effect anticipated from a two-layer model according to Maxwell.

2. The charge layer effect has been investigated experimentally, and the behaviour predicted by Hopkinson's superposition principle has been verified.

References.

(1) ' Treatise on Electricity and Magnetism,' vol. i. p. 374 (1873).
(2) ' Electromagnetic Theory,' vol. ii. p. 127.
(3) ' Treatise,' vol. i. p. 381.
(4) Trans. A. I. E. E. vol. xlvi. p. 269 (1927).
(5) Phil. Trans. vol. clxvii. II. p. 599 (1877).
(6) Phil. Trans. vol. clxvi. II. p. 489 (1876)
(7) *Annalen der Physik*, vol. xl. p. 433 (1913).

XXIII. *A Mechanical Theory of Wave Mechanics and Quantum Mechanics.* *By* Arthur Korn (*Berlin, Charlottenburg*)*.

WAVE MECHANICS, which have given a new foundation to quantum mechanics (not easily accessible to ordinary mechanical theories), have taken their origin in De Broglie's investigations about the waves bearing his name and demonstrated by recent experimental researches. It has been experimentally proved that, together with the electrons emitted with enormous speed from the cathodes of a vacuum tube, a certain kind of waves is travelling, and that the reciprocal value of their wave-length is proportional to the velocity of the electrons. The existence of these waves has been experimentally demonstrated by photographic and electrometrical experiments. Nearly all the theoretical physicists occupied with this matter give a certain mystical feature to the phenomenon by leaving in full darkness the question what is really propagated in the form of waves. If we wish to find a mechanically satisfactory theory we have to explain in which manner mechanical vibrations are propagated, together with the ordinary velocities of the particles, and we want an exact theory of those vibrations.

There can be no doubt that the electron matter must be compressible : I shall not dwell here on the mechanical

* Communicated by A. W. Conway, M.A., D.Sc., F.R.S.

pulsation theory of electrons, I mention this here only to show the usefulness of the idea that the electron matter has to be considered compressible. So we shall start from the hydrodynamical equations for this matter:

$$\mu \frac{du}{dt} = -\frac{\partial p}{\partial x}, \quad \ldots \quad (1)$$

where p represents the pressure, μ the density, and u, v, w the velocities of a point (x, y, z) at the time t. There must be added a supplementary equation between p and μ given by the classical theory of gases (in a first approximation) in the form of the Mariotte-Gay Lussac law:

$$p = \mathrm{RT}.\mu, \quad \ldots \quad (1')$$

T being the absolute temperature and R the gas constant. In the classical theory the absolute temperature is proportional to the mean energy of the irregular motion of the gas-particles in small volumes. To the velocities u, v, w there must be added, indeed, the velocities of an irregular motion the mean values of which are zero. All this is well known, but it is important to lay stress upon the fact that the supplementary equation (1′) becomes intuitive by the aid of the classical theory only under the conditions that the ordinary velocities of the particles are relatively small in comparison to the mean absolute irregular velocities, and that u, v, w do not contain vibrations of very high frequency. It is easy to understand that in the case of vibrations with high frequency the constant c in the supplementary equation

$$p = c.\mu \quad \ldots \quad (2)$$

can become dependent on the frequency ν. I shall return to this point later on, and for the moment consider the supplementary equation in the general form (2), and I shall consider the simplest case, in which the velocities have a velocity-function

$$u = \frac{\partial \phi}{\partial x}, \quad v = \frac{\partial \phi}{\partial y}, \quad w = \frac{\partial \phi}{\partial z}, \quad \ldots \quad (3)$$

and finally that the forces

$$\mathrm{X}.\mu\, d\tau, \quad \mathrm{Y}.\mu\, d\tau, \quad \mathrm{Z}.\mu\, d\tau,$$

acting on the particles, $\mu\, d\tau$, can be derived from a function ϕ:

$$\mathrm{X} = -\frac{\partial \phi}{\partial x}, \quad \mathrm{Y} = -\frac{\partial \phi}{\partial y}, \quad \mathrm{Z} = -\frac{\partial \phi}{\partial z},$$

ϕ being explicity free from t. In these cases the hydrodynamical equations are reduced to one equation,

$$\frac{\partial\phi}{\partial t}+\frac{1}{2}\left\{\left(\frac{\partial\phi}{\partial x}\right)^2+\left(\frac{\partial\phi}{\partial y}\right)^2+\left(\frac{\partial\phi}{\partial z}\right)^2\right\}=-\phi+c\int^t\Delta\phi\,dt, \quad (4)$$

where the arbitrary constant of the integral can be defined by the initial state of the matter.

The fundamental idea of my theory is that to the ordinary velocities

$$\frac{\partial\phi_0}{\partial x}, \quad \frac{\partial\phi_0}{\partial y}, \quad \frac{\partial\phi_0}{\partial z},$$

defined by Hamilton-Jacobi differential equation

$$\frac{1}{2}\left\{\left(\frac{\partial\phi_0}{\partial x}\right)^2+\left(\frac{\partial\phi_0}{\partial y}\right)^2+\left(\frac{\partial\phi_0}{\partial z}\right)^2\right\}=-\phi, \quad . \quad (5)$$

and by boundary and initial conditions, there must be added, in a new approximation, vibrational velocities in such a way that

$$\phi=\phi_0+\chi, \quad \chi=\Sigma f_j(x,y,z)\,e^{i\nu t}, \quad . \quad . \quad . \quad (6)$$

then we shall have for χ the linear equation

$$\frac{\partial\chi}{\partial t}+\frac{\partial\phi_0}{\partial x}\frac{\partial\chi}{\partial x}+\frac{\partial\phi_0}{\partial y}\frac{\partial\chi}{\partial y}+\frac{\partial\phi_0}{\partial z}\frac{\partial\chi}{\partial z}=c\int^t\Delta\chi\,dt, \quad . \quad (7)$$

under the condition that the vibrational velocities are small in comparison to the ordinary velocities

$$\frac{\partial\phi_0}{\partial x}, \quad \frac{\partial\phi_0}{\partial y}, \quad \frac{\partial\phi_0}{\partial z};$$

and if we define

$$f_j=e^{\frac{1}{2c}i\nu_j\phi_0}\phi_j(x,y,z), \quad . \quad . \quad . \quad . \quad . \quad (8)$$

we shall have for the functions ϕ_j the differential equation

$$\Delta\phi_j+\frac{\nu_j^2}{c}\phi_j-\frac{\nu_j^2}{4c^2}\phi\phi_j=0, \quad . \quad . \quad . \quad . \quad (9)$$

in which we recognize a likeness with the Schrödinger equation.

We shall consider one of the possible vibrations with the frequency ν_0, viz., the solution

$$\phi=\phi_0+e^{\frac{1}{2c}i\nu_0\phi_0}\phi_0 e^{i\nu_0 t}, \quad . \quad . \quad . \quad . \quad (10)$$

where ϕ_0 satisfies the differential equation

$$\Delta\phi_0+\frac{\nu_0^2}{c}\phi_0-\frac{\nu_0^2}{4c^2}\phi\phi_0=0. \quad . \quad . \quad . \quad (11)$$

If the constant c of the supplementary equation

$$p=c\mu \quad . \quad . \quad . \quad . \quad . \quad . \quad . \quad (12)$$

is proportional to ν_0,

$$c=\alpha\nu_0, \quad . \quad . \quad . \quad . \quad . \quad . \quad . \quad (13)$$

we shall have

$$\Delta\phi_0+\phi_0\left(\frac{\nu_0}{\alpha}-\frac{\phi}{4\alpha^2}\right)=0. \quad . \quad . \quad . \quad . \quad . \quad (14)$$

If the function ϕ is constant, then

$$\phi=-\tfrac{1}{2}v_0^2, \quad . \quad . \quad . \quad . \quad . \quad . \quad (15)$$

v_0 representing the initial velocity. In this case (case of the de Broglie waves) the wave-length

$$\lambda_0=\frac{\text{const.}}{v_0} \quad . \quad . \quad . \quad . \quad . \quad . \quad (16)$$

will be inversely proportional to the velocity v_0, in harmony with the experimental results.

In the general case we can find the possible frequencies ν_j and vibrations ϕ_j by the aid of the equation

$$\Delta\phi_j+\left(\frac{\nu}{\alpha}-\frac{\phi}{\alpha^2}\right)\phi_j=0 \quad . \quad . \quad . \quad . \quad (17)$$

in the same way, as in Schrödinger's theory. However, we have in our mechanical theory to pay attention to the following considerations:—

The function ϕ contains an arbitrary additional constant which can be defined by initial conditions, according to (5). Let us consider a particle with an initial velocity v_0; for different initial velocities v_0 we shall obtain different series of vibrations; the differences

$$\nu_j-\nu_k,$$

however, will form a well-defined set of numbers connected with the function ϕ. For a system of particles with irregularly distributed initial velocities the possible vibrations added to the ordinary velocities would cover the entire spectrum, and the combination vibrations corresponding to the differences of those frequencies would represent the real spectral vibrations.

Now the question is raised: How can we explain the differences of the frequencies? a question the solution of

which leads equally to the explanation of the Raman and the Compton effects. We should be helpless in front of this question if we had to do with linear differential equations; but if we consider in the equations of physics members of the second and higher degrees (as it has become necessary in different investigations of hydrodynamics) we shall always obtain, in the case of superposition of a plurality of vibrations, vibrations the frequencies of which correspond to the differences and the sums of the original vibrations. In the differences

$$\nu_j - \nu_k$$

we obtain the preference series necessary for the explanation of the spectra.

So we arrive at a mechanical explanation, intuitively and formally satisfactory, not only of the De Broglie waves and the phenomena described by the Schrödinger equation, but also an introduction into quantum mechanics, and an explanation of the Raman and Compton effects.

Anyhow, I must lay stress on the essential point in which we have parted a little from the classical methods of mechanics. This point is the hypothesis of a modification of the Mariotte-Gay Lussac law for the matter composing electrons. We consider this as a compressible matter satisfying the hydrodynamical equations with the supplementary equation

$$p = c\mu,$$

in which, for the case of vibrations with high frequencies ν, the equation

$$c = \mathrm{RT}$$

must be replaced by the formula

$$c = \alpha\nu,$$

that is to say, c becomes with growing ν proportional to the frequency ν; if there are several high frequencies the law will become a little more complicated.

A mechanical explanation of this modification of the Mariotte-Gay Lussac law can be given in the following way:—

Let us consider one of the particles of our matter bombarded from all sides by other particles; the pressure will be proportional to the density and to the mean absolute velocity of the bombarding particles and to the frequency of the collisions. In the kinetic theory of gases the frequency of the collisions is also proportional to the mean

absolute velocity of the irregular motion, but under the conditions that the ordinary velocities are relatively small in comparison to those mean absolute irregular velocities and that we have not to count with vibrations of very high frequency. In the case of such vibrations with a very high frequency ν the frequency of the collisions may obviously satisfy a more complicated law in such a way that it is not any more proportional to the mean absolute velocity of the irregular motion, but becomes with growing ν more and more proportional to ν. So we arrive at a supplementary equation

$$p = c\mu,$$

where

$$c = \text{const.}\,\nu\,.\,\sqrt{\mathrm{T}}$$

is proportional to ν and to the square root of the absolute temperature.

So we obtain a mechanical explanation of that very equation which proves so useful for our mechanical theory of wave mechanics and quantum mechanics.

It may also be noticed that this equation offers an explanation for photoelectric phenomena and Richardson's law concerning the flow of electrons from hot electrodes, and, in fact, that a great number of new phenomena can be explained by this mechanical theory.

XXIV. *Theories of Electrical Discharge in Gases at Normal Pressures and Temperatures.* *By* J. D. Stephenson, *B.Sc., Armstrong College, Newcastle-upon-Tyne* *.

Introduction.

In a previous paper [1] by the writer, in which an account was given of an experimental study of electrical discharges in gases at normal temperatures and pressures, it was shown that the equations giving the critical conditions for discharge for the three principal types of electrode shape and field distribution in common use, are as follows:—

(1) Uniform field spark discharge:

$$G_{mean} = G_0\rho + Z\sqrt{\frac{\rho}{S}}, \quad . \quad . \quad . \quad . \quad (1)$$

* Communicated by Prof. W. M. Thornton, D.Sc., D.Eng.

where G_{mean} is the mean constant gradient in kv./cm., G_0 the true breakdown strength of the gas, also in kv./cm., S the spacing, ρ the gas density, and Z is a constant which is very nearly independent of the nature of the gas.

(2) Sphere-gap spark discharge between equal spheres:

$$G_m = 1{\cdot}11\,G_0\rho + X\sqrt{\frac{\rho}{r}}, \quad . \quad . \quad . \quad . \quad (2)$$

where r is the radius of either sphere in cm., G_m the maximum surface gradient in kv./cm., and X is a constant that is independent of the gas.

(3) Corona discharge on co-axial cylinders:

$$G_m = 1{\cdot}25\,G_0\rho + Y\sqrt{\frac{\rho}{r}}, \quad . \quad . \quad . \quad . \quad (3)$$

where r is the radius of the inner cylinder in cm., G_m is the gradient at the surface of the inner cylinder, and Y is a constant that is independent of the gas.

In these three equations the value of the breakdown strength G_0 *has the same value for the same gas.*

The density ρ is referred for all gases to unit value when the gases are at a fixed temperature and pressure, and is therefore the number of molecules per unit volume, not the actual gas density as generally understood: this is important. If the density is referred to a value of unity at 0° C. and 760 mm. barometric pressure, the coefficients Z, X, Y above have numerical values respectively of 7·54, 17·5, 12·3.

For electrical discharge at normal pressures, therefore, we see that the critical gradient for any gas under all conditions can be determined from a knowledge of one constant only, the true breakdown strength of the gas. The numerical values of G_0 for the different gases are best determined from experiments on corona discharge, using equation (3), since the laws of corona formation are extremely accurate and well established; moreover, the discharge does not produce chemical decomposition as does spark discharge in certain gases, so that corona discharge can be examined in all gases, such as the paraffins, whereas spark discharge cannot always be investigated.

An experimental study of corona discharge by the writer resulted in the following values of the breakdown strength of the thirteen gases investigated (see Table I.).

The object of the present paper is to give an account of an analysis of theories which have been suggested to explain the phenomena of discharge in gases at normal pressures and temperatures, in the light of the fundamental experimental equations (1), (2), (3) above. A new theory is proposed by the writer which, whilst essentially empirical, is shown to conform to the experimental results, and shows a remarkable dependence of the breakdown strength solely upon the electron

TABLE I.

The Breakdown Strength for Gases, calculated from Corona Discharge. Results at 0° C., 76 cm.

Gas.	G_0 kv./cm.
Air	28·4
Ammonia	45·3
Nitrogen	30·4
Carbon monoxide	36·4
Nitrous oxide	44·2
Carbon dioxide	21·0
Methane	17·8
Hydrogen	12·4
Oxygen	23·3
Ethane	29·7
Propane	29·7
Butane	38·2
Pentane	50·4

mean-free-path in the gas, a dependence which at present is still incapable of satisfactory explanation.

PREVIOUS THEORIES OF ELECTRICAL DISCHARGE IN GASES AT NORMAL PRESSURES.

The principal theories which have been developed in the past to account for the phenomena of corona and spark discharge at normal pressures and temperatures are due to Peek, Kunz, Townsend, Schumann, Davis, and Sah. Peek's theory, however, is purely empirical, and assumptions are made to fit the experimental facts without specifying their nature or physical meaning. Moreover, the theory is concerned primarily with the discharge in air, and will therefore

be omitted in this paper. For a detailed account of the theory the reader is referred to Peek's book on 'Dielectric Phenomena in High Voltage Engineering'[2].

The Kunz Theory of Corona Discharge.

Kunz[3] has attempted to explain the "energy distance" term by assuming that energy must be stored in the gas before breakdown, similar to the electrostatic energy stored in a solid or liquid dielectric under electric stress. He derives an expression for corona discharge,

$$G_m = G_0\left[1+\frac{1}{\sqrt{r}}\sqrt{\frac{4E}{kcG_0^2}}\right],$$

where c is the energy distance, k a constant analogous to the dielectric constant of the gas in the electrostatic case, and E the energy necessary to start the discharge.

Assuming that the "polarization effect" G_0 is proportional to the density of the gas, then in order that the condition $G_0B=$constant should be satisfied, $\sqrt{\frac{4E}{kc\rho}}$ must be constant for all gases, and directly proportional to the square root of the density. Kunz, in his analysis, considers the thickness of corona as constant; it is more correct, however, to make the distance proportional to $\sqrt{\frac{r}{\rho}}$, in fact, identical with the term $B\sqrt{\frac{r}{\rho}}$, the energy distance in equation (5a). The actual thickness of corona, once the glow has begun, is affected by the conducting nature of the glow itself and the consequent alteration of the field stress due to it.

In order that $\sqrt{\frac{4E}{kc\rho}}$ should have the same value for all gases, the following conditions must be satisfied:—

(a) The "dielectric constant" k should be the same for all gases. This would be so if it were comparable in magnitude with the true dielectric constant of gases, very nearly equal to unity.

(b) The energy for discharge E must be equal in every gas to $XB\sqrt{r\rho}$, where X is a constant which is independent of the gas and B is the "energy distance" factor of the gas as found experimentally in corona discharge.

The writer has conducted experiments upon the effect of corona glow on the chemical properties of gases, in which it was found that the energy in the discharge producing chemical change in the gas is actually proportional to the square root of the radius of the wire and the gas density; this is in agreement with the Kunz theory. Apart from this, however, nothing further can be derived from an analysis of the theory.

The Theory of Townsend.

Townsend[4], in explaining the phenomena of corona, and more particularly the "energy distance" term, correlates sparking potentials in uniform fields with corona discharge. He assumes that ionization by collision takes place between the corona forming electrode and the place where the gradient is equal to the value of the breakdown strength of the gas, and that a local spark discharge occurs between them. His argument is as follows:—

For concentric cylinders, as in corona discharge,

$$G_m = \frac{V}{r \log_e R/r},$$

$$G_0 = \frac{V}{(r+c) \log_e R/r},$$

where G_m is the gradient at the surface of the inner cylinder, of radius r, and G_0 is the gradient at the energy distance c from the surface;

$$\therefore \qquad \frac{G_m - G_0}{G_0} = \frac{c}{r}. \qquad \ldots\ldots \quad (4)$$

Assuming that the sparking equation for uniform fields is

$$G_{mean} = G_0 + \frac{D}{S}, \qquad \ldots\ldots \quad (5)$$

where S is the spacing and D is constant, we have, from equations (4) and (5), an equation for corona discharge,

$$G_m = G_0\left(1 + \frac{1}{\sqrt{r}} \cdot \sqrt{\frac{2D}{G_0}}\right).$$

In comparing sparking with corona discharge we should expect the best agreement between them under conditions for

which the mean gradients $\left(\frac{G_m + G_0}{2}\right.$ and G_{mean} respectively$\Big)$ are equal. We are led to expect therefore that sparking should be analogous to corona for spacings of the order 0 to 2 or 3 mm. In Keil's[5] determinations of sparking potentials between spheres of 1 cm. radii the field is uniform for spacings up to about 2·5 mm., and over this range, if Townsend's theory is correct, the condition for discharge should be represented by equations of the type

$$V = G_{mean}S = G_0S + \frac{G_0B^2}{2} = G_0S + D.$$

Analyzing the results of Keil we find that the linear law is approximately obeyed for the gases air, oxygen, nitrogen,

TABLE II.

Gas.	Keil's experimental results	Calculated results from corona.
Air	V=34·0 S+1·40	V=32·5 S+1·51
Nitrogen	V=32·0 S+2·75	V=34·9 S+1·72
Oxygen	V=34·0 S+0·80	V=26·8 S+2·34
Methane	V=31·5 S+0·80	V=21·2 S+3·50
Carbon monoxide	V=39·5 S+2·50	V=42·7 S+1·66

methane, and carbon monoxide, but not for hydrogen and carbon dioxide. The results for the constants G_0 and D are given in Table II., together with the calculated values from the writer's experimental corona discharge results, assuming Townsend's theory. All the results are given for density conditions unity at 25° C. and 760 mm. pressure.

It is at once apparent that, so far as the energy distance term is concerned, there is no agreement between calculated and observed results; moreover, the comparison of the breakdown strength terms cannot be regarded as satisfactory. To obtain agreement with the corona law,

$$G_0B = \text{constant},$$

it follows also that for spark discharge

$$G_0D = \text{constant}.$$

There is no evidence of this in the experimental results for uniform field discharge. Further, in order to give agreement with the variation of corona discharge with gas density,

$$G_m = G_0\rho\left(1 + \frac{B}{\sqrt{r\rho}}\right), \quad . \quad . \quad . \quad . \quad (5a)$$

D must be independent of density in the sparking equation

$$V = G_0\rho S + D.$$

The experimentally observed variation of sparking potentials with gas density, however, is not of this form.

The Theory of Schumann.

Schumann [6] has proposed a theory of electrical discharge in gases at normal pressures, based upon a simplified form of Townsend's fundamental law of discharge,

$$\int_0^l \alpha\epsilon^{\int_0^x (\beta-\alpha)\,dx} = 1.$$

The modified formula is

$$\int_0^l \alpha\,dx = K, \quad . \quad . \quad . \quad . \quad . \quad . \quad (5b)$$

where α is the coefficient of ionization of the negative electrons, K is a constant, and the integration is performed over the path 0 to l.

For uniform field spark discharge the gradient is constant, so that α is also constant, and the equation reduces to

$$\alpha S = K. \quad . \quad . \quad . \quad . \quad . \quad . \quad . \quad (6)$$

Schumann has proposed various formulæ for the form of the function showing the dependence of α upon the field G, such as

$$\alpha = \frac{A'}{G^2}\epsilon^{-\frac{B'}{G^2}}, \quad . \quad . \quad . \quad . \quad . \quad . \quad (7)$$

$$\alpha = A''\epsilon^{-\frac{B''}{G^2}}, \quad . \quad . \quad . \quad . \quad . \quad . \quad (8)$$

$$\alpha = \frac{A'''}{G}\epsilon^{-\frac{B'''}{G^2}} \quad . \quad . \quad . \quad . \quad . \quad . \quad (9)$$

Using equation (6), the laws for sparking in uniform fields become

$$S = \frac{G^2}{a'} \epsilon^{\frac{B'}{G^2}},$$

$$S = \frac{1}{a''} \epsilon^{\frac{B''}{G^2}},$$

$$S = \frac{1}{a'''} \epsilon^{\frac{B'''}{G^2}}.$$

Good agreement with the results for air up to spacings of 10 cm. are obtained by Schumann, but the values of the constants a and B are empirical and differ widely in the various cases.

For corona and spark discharge between co-axial cylinders the equation

$$\int_0^l \alpha \, dx = K$$

has been worked out fully by Schumann for the three functions (7), (8), (9) of α, and result respectively in the following:—

(1) $$\alpha = \frac{A'}{G^2} \epsilon^{-\frac{B'}{G^2}},$$

$$K = \frac{A'}{B'} \frac{G_m}{\sqrt{B'}} r \frac{1}{2} \left\{ \frac{\sqrt{B'}}{G_m} \cdot \epsilon^{-\frac{B'}{2 G_m}} + \frac{\sqrt{\pi}}{2} \left(1 - \phi \left(\frac{\sqrt{B'}}{G_m} \right) \right) \right\}; \quad (10)$$

(2) $$\alpha = A'' \epsilon^{-\frac{B''}{G^2}},$$

$$K = A'' \frac{G_m r}{\sqrt{B''}} \frac{\sqrt{\pi}}{2} \left[1 - \phi \left(\frac{\sqrt{B''}}{G_m} \right) \right]; \quad . \quad . \quad . \quad (11)$$

(3) $$\alpha = \frac{A'''}{G} \cdot \epsilon^{-\frac{B'''}{G^2}},$$

$$K = \frac{1}{2} \frac{A'''}{B'''} r G_m \epsilon^{-\frac{B'''}{2 G_m}};$$

where $\frac{\sqrt{\pi}}{2} \phi(x)$ is the integral $\int_0^x \epsilon^{-x^2} dx$, and G_m is the gradient at the surface of the inner cylinder.

The above formulæ have been further reduced by Schumann to the simple experimentally observed equation

$$G_m = G_0\rho\left(1 + \frac{B}{\sqrt{r\rho}}\right),$$

provided values are selected for the constants A, B, K, which are obtained from the results for sparking potentials in uniform fields.

The above equations are far too complicated to analyse in the light of the writer's corona and sparking results, whilst there is not sufficient evidence available to enable the constants A, B, K to be calculated for any other gas than air.

The Theory of B. Davis.

According to Townsend the coefficient of ionization of the negative ions, α, is given by

$$\alpha = \frac{1}{p} f\left(\frac{X}{p}\right),$$

where p is the pressure of the gas and X the field strength. The form of the function f has been deduced by Davis[7] on the assumption that for ionization to occur by impact the normal component of the energy of the electron at impact is equal to or greater than a certain fixed value—defined by the term "ionization potential" of the gas. If l is the mean free path of an electron in the gas ($4\sqrt{2} \times$ mean free path of the molecules), v the ionization potential, and G the field strength, then

$$\alpha l = \epsilon^{-\frac{v}{Gl}} + \frac{v}{Gl}\,Ei\left(-\frac{v}{Gl}\right).$$

Substituting this function for α in the equation $(5b)$ the condition for discharge becomes

$$\int_0^x \left[\frac{1}{l}\epsilon^{-\frac{v}{Gl}} + \frac{v}{Gl^2}\,Ei\left(-\frac{v}{Gl}\right)\right] dx = K, \quad . \quad . \quad (12)$$

where G may be a function of x.

The formula in this shape has been applied with apparent success to corona discharge by Davis[7] and to sphere-gap spark discharge by P. Sah[8].

The equation (12) is not directly integrable with respect to x, since it contains the exponential integral $Ei\left(-\frac{v}{Gl}\right)$:

the latter is a series every term of which would have to be separately integrated for every case. Davis and Sah therefore proposed approximate integrable forms of the equation, respectively

$$\alpha l = 0{\cdot}0002 + 0{\cdot}294\left[\frac{Gl}{v} - 0{\cdot}140\right]^2, \quad . \quad (12a)$$

$$\alpha l = 0{\cdot}261\left[\frac{Gl}{v} - 0{\cdot}131\right]^2; \quad . \quad . \quad . \quad . \quad (12b)$$

or, if $\frac{bv}{l} = G_a$ and $\frac{al}{v^2} = M$, equations of the form

$$\alpha l = M(G - G_a)^2.$$

Case of Co-axial Cylinders (Davis).

If the radii of the cylinders are r and R, G_m the gradient at the surface of r, and G_x the gradient at any point x from the common axis of the cylinders, we have

$$\frac{G_m}{G_x} = \frac{x}{r} \quad \text{and} \quad \frac{G_m}{G_a} = \frac{c}{r}.$$

Equation (12) may be written

$$\int_r^c MG_a^2\left[\frac{c}{x} - 1\right]^2 dx = K.$$

Integrating and substituting $\frac{c}{r} = \frac{G_m}{G_0}$, this becomes

$$K = MG_a^2 r\left[\left(\frac{G_m}{G_a}\right)^2 - 1 - 2\left(\log_\epsilon \frac{G_m}{G_a}\right) \times \frac{G_m}{G_a}\right],$$

which, using an approximation

$$\log_\epsilon \frac{G_m}{G_a} = 0{\cdot}28\frac{G_m}{G_a} - 0{\cdot}82\frac{G_a}{G_m} + 0{\cdot}53,$$

reduces to

$$K = MG_a^2 r\left[0{\cdot}663\frac{G_m}{G_a} - 0{\cdot}80\right]^2,$$

whence

$$G_m = 1{\cdot}207\,G_a\left[1 + 1{\cdot}25\sqrt{\frac{K}{r}} \cdot \frac{1}{\sqrt{MG_a^2}}\right]. \quad (13)$$

Case of Sphere-gap Spark Discharge (Sah).

For spheres of equal radii r we may write to a first approximation

$$\frac{G_m}{G_a} = \frac{c^2}{r^2} \quad \text{and} \quad \frac{G_x}{G_a} = \frac{r^2}{x^2}; \quad . \quad . \quad . \quad (13a)$$

$$\therefore \quad \int_0^x \alpha \, dx = \int_r^c MG_a^2 \left(\frac{b^2}{x^2} - 1\right)^2 dx = K'.$$

Integrating and substituting $\frac{b^2}{r^2} = \frac{G_m}{G_a}$, this reduces to

$$K' = MG_a^2 r \left(\frac{8}{3}\sqrt{\frac{G_m}{G_a}} + \frac{1}{3}\left(\frac{G_m}{G_a}\right)^2 - 2\frac{G_m}{G_a} - 1\right),$$

whence, using an approximate relation

$$\sqrt{\frac{G_m}{G_a}} = -0{\cdot}071\left(\frac{G_m}{G_a}\right)^2 + 0{\cdot}630\frac{G_m}{G_a} + 0{\cdot}441,$$

we have

$$K' = MG_a^2 r \left[0{\cdot}38\frac{G_m}{G_a} - 0{\cdot}42\right]^2$$

or

$$G_m = 1{\cdot}105\, G_a \left[1 + 2{\cdot}63\sqrt{\frac{K'}{r}} \cdot \frac{1}{\sqrt{MG_a^2}}\right]. \quad (14)$$

The above formulæ ((13), (14)) both lead to the correct variation of critical discharge gradient G_m with density as suggested by the experimental equation

$$G_m = G_0\rho\left(1 + \frac{B}{\sqrt{r\rho}}\right),$$

for the term G_a contains the factor $\frac{v}{l}$, where l is inversely proportional to the density ρ, whilst the MG_a^2 term is also proportional to the density. Further, the ratio of the "breakdown strength" factors in the two cases of corona and sphere-gap spark discharge obtained from the above equations is in good agreement with that obtained experimentally by the writer, and are respectively 1·092 and 1·125.

In order that the corona discharge law,

$$G_0 B = \text{constant},$$

should be satisfied it further follows that the constants K, K'

must be proportional to $\frac{L}{v^2}$, where L is the mean free path of the electrons at normal temperature and pressure. For, from the equations (13) and (14), if

$$G_0 B = \text{constant},$$

then

$$G_a \cdot \sqrt{\frac{K'}{MG_a^2}} = \text{constant},$$

i. e., $K \propto \frac{L}{v^2}$, having regard to density variations.

There is at present no reason why K, a constant depending upon the density of ionization necessary for discharge, should be proportional to $\frac{L}{v^2}$ for all gases. An attempt was made by the writer to explain the fact by assuming that the total energy of the electrons at breakdown was constant for all gases, but without success.

Davis and Sah were concerned primarily with electrical discharge in air, and to obtain agreement with the experimental results they chose empirical values for the constant K, numerically equal to 6·0 for corona discharge and 4·9 for sphere-gap spark discharge. There appears to be no reason however why K should vary with the type of discharge in the same gas, since the passage from corona to spark discharge is not marked by any sudden change in the values of the critical gradients.

A New Theory of Electrical Discharge in Gases at Normal Pressures.

As a result of the preceding examination of theories of corona and spark discharge the writer suggests a new formula for discharge in gases at normal pressures and temperatures which obeys the fundamental experimental laws of discharge (1), (2), (3) given at the commencement of this paper. The condition for discharge is

$$\int_a^b \frac{1}{N} \cdot (G - G_0 N)^2 \, dx = K, \quad . \quad . \quad . \quad . \quad (15)$$

where N is the number of gas molecules per unit volume, G the field strength in kv./cm. at any point x on the path along which discharge occurs, G_0 is a definite constant for a given gas at unit density or when N is a fixed number, and

is called the true "breakdown strength" of the gas, and K is a constant which is independent of the nature of the gas, and may therefore be called a true electrical "discharge constant." The integration is performed over the path a to b along which the discharge occurs, but negative values of $(G-G_0N)$ do not of course count in the integration.

For convenience, if N is considered unity when the gases are at a fixed temperature and pressure, we may write $N=\rho$, where ρ is the density referred to a value unity at the said temperature and pressure, so that if G_0 is taken for the gas at unit density the equation (15) becomes

$$\int_a^b (G-G_0\rho)^2\,dx = K\rho. \quad . \quad . \quad . \quad . \quad (16)$$

If the equation (15) is compared with Schumann's equation for discharge,

$$\int_a^b \alpha\,dx = K,$$

where α is the coefficient of ionization of the electrons, it follows that

$$\alpha = \frac{1}{N}(G-G_0N)^2,$$

an extremely simple expression involving both the density and the field, but, unlike previous functions, introducing a definite constant, the breakdown strength of the gas. Thus, ionization appears to begin when the gradient reaches a definite minimum value G_0N, and ionization for values of the field below this is apparently negligible in its contribution to the causes of the discharge.

The formula (16) contrasts with those given by (12*a*) and (12*b*) Davis and Sah in that the form of the function (f) is independent of the nature of the field, and the same function is used for all types of discharge.

We shall now consider the application of the new formula to the derivation of the experimental laws of discharge given above, (1), (2), (3).

Case of Corona Discharge on Co-axial Cylinders.

The treatment in the cases of corona and sphere-gap spark discharge involve the same assumptions as to the distribution of the field which were used by Davis, Sah, and Schumann.

For the formation of corona on a wire or cylinder of

radius r co-axial with an outer cylinder the equation (16) reduces to

$$K\rho = (G_0\rho)^2 r \left\{ \left(\frac{G_m}{G_0\rho}\right)^2 - 1 - 2\frac{G_m}{G_0\rho} \cdot \log_\epsilon \left(\frac{G_m}{G_0\rho}\right) \right\} \quad (17).$$

The function within the brackets is best reduced to a quadratic form by means of a graphical method, as shown in fig. 1, and for a range of $\frac{G_m}{G_0\rho}$ from 1·4 to 2·6 it becomes

$$\left\{ 0{\cdot}667\frac{G_m}{G_0\rho} - 0{\cdot}843 \right\}^2, \quad . \quad . \quad . \quad . \quad (18)$$

Fig. 1.

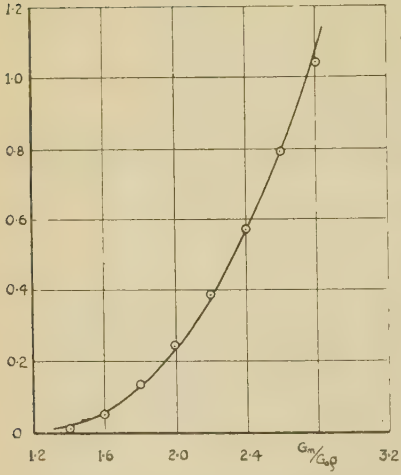

Fig. 2.

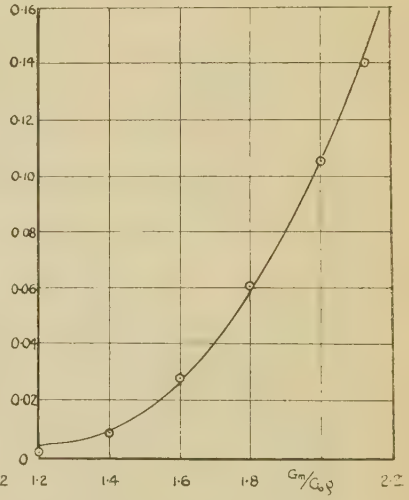

Fig. 1.—Drawn curve calculated from the equation

$$y = (G_m/G_0\rho)^2 - 1 - 2\,G_m/G_0\rho \cdot \log_\epsilon (G_m/G_0\rho).$$

Points calculated from the equation

$$y = (0{\cdot}667\,G_m/G_0\rho - 0{\cdot}843)^2.$$

Fig. 2.—Drawn curve calculated from the equation

$$y = \tfrac{8}{3}\sqrt{G_m/G_0\rho} + \tfrac{1}{3}(G_m/G_0\rho)^2 - 2\,G_m/G_0\rho - 1.$$

Points calculated from the equation

$$y = (0{\cdot}39\,G_m/G_0\rho - 0{\cdot}455)^2.$$

so that the equation (18) finally reduces to

$$0{\cdot}667\frac{G_m}{G_0\rho} = 0{\cdot}843 + \frac{\sqrt{K}\sqrt{\rho}}{\sqrt{r}\,.\,G_0\rho}$$

or $$G_m = 1{\cdot}26\, G_0\rho + 1{\cdot}5\sqrt{K}\sqrt{\frac{\rho}{r}}. \quad . \quad . \quad (19)$$

Case of Sphere-gap Spark Discharge between Equal Spheres.

Similarly, in the case of electrical discharge between equal spheres, assuming field distribution as given in equations (13 *a*), the fundamental relation (16) reduces to

$$K\rho = (G_0\rho)^2 r \left\{ \frac{8}{3}\sqrt{\frac{G_m}{G_0\rho}} + \frac{1}{3}\left(\frac{G_m}{G_0\rho}\right)^2 - 2\frac{G_m}{G_0\rho} - 1 \right\}. \quad (20)$$

The function within the brackets is again best solved graphically as in fig. 2, and reduces to

$$\left\{ 0{\cdot}39\frac{G_m}{G_0\rho} - 0{\cdot}455 \right\}^2,$$

so that the equation (20) takes the form

$$K\rho = (G_0\rho)^2 r. \left\{ 0{\cdot}39\frac{G_m}{G_0\rho} - 0{\cdot}455 \right\}^2$$

or

$$G_m = 1{\cdot}16\, G_0\rho + 2{\cdot}56\sqrt{K}. \sqrt{\frac{\rho}{r}}. \quad . \quad . \quad (21)$$

Case of Uniform Field Spark Discharge.

For spark discharge in uniform fields the field G is independent of the variable x, so that equation (16) becomes

$$(G_{mean} - G_0\rho)^2 S = K\rho,$$

where S is the spacing, or

$$G_{mean} = G_0\rho + \sqrt{K}\sqrt{\frac{\rho}{S}}. \quad . \quad . \quad . \quad (22)$$

If we now assume a value of $K = 57$, the equations for the different types of discharge, (19) (21), (22), become respectively

$$G_m = 1{\cdot}26\, G_0\rho + 11{\cdot}3\ \sqrt{\frac{\rho}{r}},$$

$$G_m = 1{\cdot}16\, G_0\rho + 19{\cdot}3\ \sqrt{\frac{\rho}{r}},$$

$$G_{mean} = G_0\rho + \ 7{\cdot}54\sqrt{\frac{\rho}{S}},$$

which compare with the experimental relations

$$G_m = 1{\cdot}25\, G_0\rho + 12{\cdot}3 \sqrt{\frac{\rho}{r}},$$

$$G_m = 1{\cdot}11\, G_0\rho + 17{\cdot}5 \sqrt{\frac{\rho}{r}},$$

$$G_{\text{mean}} = G_0\rho + 7{\cdot}54\sqrt{\frac{\rho}{r}}.$$

The agreement between the two series of results, experimental and theoretical, is extraordinarily good when one considers the approximations made in the deductions of the theoretical formulæ for corona and sphere-gap spark discharge, and also the order of accuracy entailed in the experimental equations, particularly in the measurement of Z.

The new formula for electrical discharge differs from all previous formulæ or theories in that it gives the constant coefficients X, Y, Z in the equations (1), (2), (3). It will be seen also that the discharge equation satisfies Paschen's law, for the expression considers the actual number of molecules per unit volume of the gas, so that the discharge must be independent of temperature and pressure except in so far as they alter the molecular concentration, *i. e.*, the gas density.

On the Physical Interpretation of Equation (15).

Previous theories of electrical discharge in gases have been based upon the assumption that the ions in the gas, moving in the electric field, can acquire, between collisions with the gas molecules, sufficient energy to produce ionization by collision. The amount of ionization grows until the gas is sufficiently conducting to allow of the passage of a discharge. The least amount of energy which an ion must possess in order to produce ionization by collision is generally termed the "ionization energy or potential" of the molecules or atoms, and experiments have been conducted at low pressures to measure them. The measured values differ considerably from each other for the different gases.

If the above theory of ionization is accepted it follows at once that the "breakdown strength" of a gas should be a function of both the ionization potential and electronic mean-free-path, for discharge at normal pressures in which the electrons are the chief source of ionization.

In fig. 3 the values of the breakdown strengths for the gases investigated by the writer in experiments on corona discharge are plotted graphically against the electronic mean-free-paths of the gases, a graph which does not include the ionization potential of the gas, and which therefore should not be continuous, but rather a random distribution. Actually,

Fig. 3.

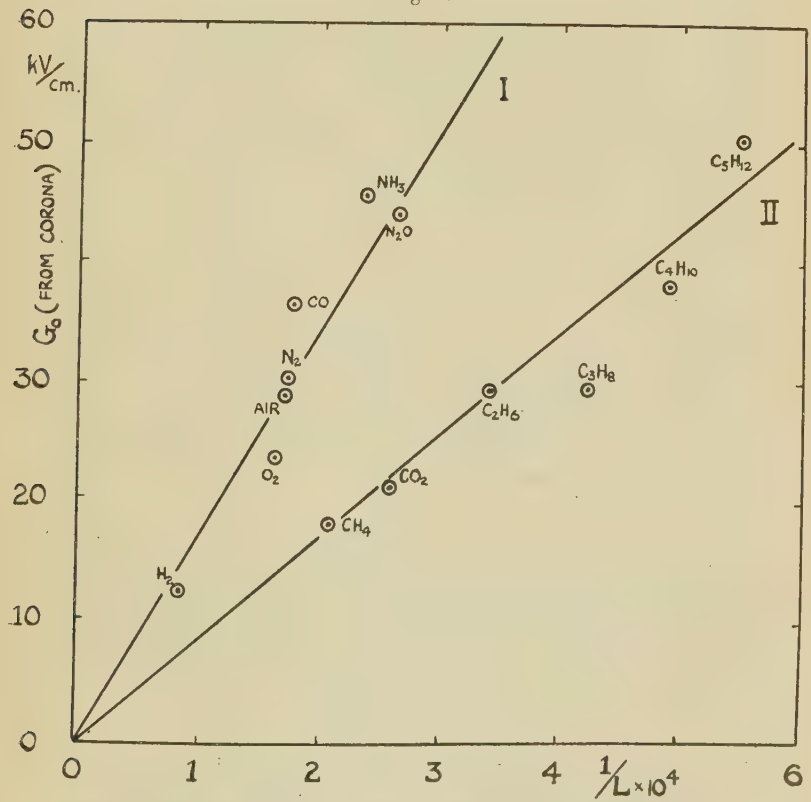

Graph showing the relation between the "breakdown strength" G_0 and the electron mean-free-path L. Drawn curves calculated from the equations

I. G_0 (kv./cm.) $= 17{\cdot}1/(L \times 10^4)$.

II. G_0 (kv./cm.) $= 8{\cdot}55/(L \times 10^4)$.

Temp. 0° C.; pressure 760 mm.

however, it is seen at once that the breakdown strengths are approximately inversely proportional to the mean-free-paths,

with the gases in two separate groups, the constant of proportionality in one case being almost exactly twice the constant in the other. The drawn curves in the two cases are calculated from the equations

$$\left.\begin{aligned} G_0L &= 0{\cdot}855 \text{ volts,} \\ G_0L &= 1{\cdot}71 \text{ volts,} \end{aligned}\right\}, \quad . \quad . \quad . \quad (22a)$$

the former including the paraffins and carbon dioxide and the latter the remainder of the gases investigated.

From linear graphs such as these it follows that the ionization potentials for the gases must be constant, with the gases in two groups, one group having twice the value of the other; this is not in agreement with the experimentally measured values at low pressures.

Can it be that electrical discharge in gases at normal pressures and temperatures is not so much dependent on the ionization potential of gases as has been thought to be the case in the past? Considerable doubt has been thrown on the ionization theory by experiments on spark-lag. Spark-lag is the time interval betwen the application of the breakdown voltage and the passage of a spark or the commencement of discharge, and from considerations of the accepted theory of ionization by collision should be of the order 10^{-5} seconds. Experiments, however, have shown that the actual time is only about 10^{-7} or 10^{-8}, very much smaller than the calculated time [9].

The dependence of the breakdown strength on the mean-free-path of the electrons in a gas appears to be the basis of the correct explanation of the causes of electrical discharge in gases, together with the empirical law of discharge (15), but why the gases should appear in two groups having different constants of proportionality between the mean-free-path and breakdown strength is not yet evident.

Spark Discharge in Mixed Gases.

The formula for sparking potentials in mixed gases,

$$V_{AB} = \frac{V_A p_A + V_B p_B}{p_A + p_B}, \quad . \quad . \quad . \quad . \quad . \quad (23)$$

has been established experimentally by Hayashi [10] for nitrogen-hydrogen mixtures and by Bouty [11] for oxygen-carbon dioxide and carbon dioxide-hydrogen mixtures. In the formula V_A and V_B represent the sparking potentials for the separate constituents A and B, at pressure $p = p_A + p_B$,

and V_{AB} is the sparking potential for a mixture of A and B exerting partial pressures p_A and p_B respectively. The experimental work on sparking in gas mixtures has generally been done with sphere-gaps under conditions giving both uniform and non-uniform fields, in which case the conditions for discharge are different.

It will be shown that the formula above, (23), can be deduced from the fundamental laws of corona and spark discharge in gases.

In considering the theories of electrical discharge in gases at normal pressures it was found that the breakdown strength of a gas was inversely proportional to the electronic mean-free-path, with the gases in two groups having different constants of proportionality. Assuming that the mixture consists of gases in one group, we may write

$$G_0 = \frac{k}{l},$$

where k is independent of the gas. The mean-free-path of the molecules of a gas, and of the electrons also, is proportional to $\frac{1}{N\sigma^2}$, where N is the number of molecules per unit volume and σ the mean molecular radius. If the temperature is constant, therefore,

$$l = \frac{c}{p\sigma^2},$$

where p is the pressure and c is constant for all gases.

For a mixture of two gases, the constituents of which have mean molecular radii σ_A and σ_B, and exert partial pressures p_A and p_B respectively,

$$l_m = \frac{c}{p_A\sigma_A^2 + p_B\sigma_B^2},$$

and for the separate gases

$$l_A = \frac{c}{(p_A + p_B)\sigma_A^2},$$

$$l_B = \frac{c}{(p_A + p_B)\sigma_B^2};$$

$$\therefore \quad \frac{1}{l_m} = \frac{p_A \cdot \frac{1}{l_A} + p_B \frac{1}{l_B}}{p_A + p_B}.$$

Now

$$G_A = \frac{k}{l_A}, \quad G_B = \frac{k}{l_B}, \quad G_m = \frac{k}{l_m};$$

$$\therefore \quad G_m = \frac{p_A G_A + p_B G_B}{p_A + p_B}.$$

Evidence of this mixture law for the breakdown strength is afforded by the results for corona discharge in air and in its constituents nitrogen and oxygen. Thus the calculated value of G_0 in the case of air is 36·1, assuming the values for nitrogen and oxygen to be 38·0 and 29·1, which is very nearly equal to the observed value 35·5.

To prove the sparking law above, (23), we shall consider spark discharge in its two principal forms, namely, sphere-gap spark discharge at values of the spacing radius ratio greater than 0·25 and uniform field spark discharge.

Case of Sphere-gap Spark Discharge.

Consider Russell's theory of sphere-gap spark discharge, and the expression

$$G_{max.} = G_0 \rho \left[1 + \frac{B}{\sqrt{r\rho}}\right],$$

where G_m is the maximum surface gradient for discharge.

Since the results for sparking in gas mixtures are for a fixed spacing, we may write instead of the above

$$V = m G_0 \rho \left[1 + \frac{B}{\sqrt{r\rho}}\right],$$

where V is the breakdown voltage and m is a constant for a given spacing.

Further, we have from the fundamental law of discharge

$$G_0 B = \text{constant } C.$$

The conditions for sparking therefore become

$$V = m\left[G_0 p + C\sqrt{\frac{p}{r}}\right]$$

if the temperature is constant.

For the separate constituents,

$$V_A = m\left[G_A p + C\sqrt{\frac{p}{r}}\right],$$

$$V_B = m\left[G_B p + C\sqrt{\frac{p}{r}}\right],$$

and for the mixture, in which the constituents exert partial pressures p_A and p_B,

$$V_{AB} = m\left[G_{AB}p + C\sqrt{\frac{p}{r}}\right]$$

$$= m\left[\frac{G_A p_A + G_B p_B}{p_A + p_B}.(p_A + p_B) + C\sqrt{\frac{p_A + p_B}{r}}\right];$$

$$\therefore \quad V_{AB} = m\left\{\left[G_A(p_A + p_B) + C\sqrt{\frac{p_A + p_B}{r}}\right]\frac{p_A}{p_A + p_B}\right.$$

$$\left. + \left[G_B(p_A + p_B) + C\sqrt{\frac{p_A + p_B}{r}}\right]\frac{p_B}{p_A + p_B}\right\},$$

i. e.,

$$V_{AB} = \frac{V_A p_A + V_B p_B}{p_A + p_B}.$$

Case of Uniform Field Spark Discharge.

For uniform fields the condition for sparking is

$$V = G_0 \rho S + Z\sqrt{\rho S},$$

where Z is a constant which is approximately independent of the nature of the gas.

If G_A, G_B represent the values of the breakdown strengths of the constituents of a mixture, exerting partial pressures p_A and p_B, then we have for the separate gases, provided the temperature remains constant,

$$V_A = G_A(p_A + p_B)S + Z\sqrt{(p_A + p_B)S},$$

$$V_B = G_B(p_A + p_B)S + Z\sqrt{(p_A + p_B)S},$$

and for the mixture

$$V_{AB} = G_{AB}(p_A + p_B)S + Z\sqrt{(p_A + p_B)S}$$

$$= \left(\frac{G_A p_A + G_B p_B}{p_A + p_B}\right)(p_A + p_B)S + Z\sqrt{(p_A + p_B)S}$$

$$= G_A p_A S.\frac{p_A + p_B}{p_A + p_B} + G_B p_B S.\frac{p_A + p_B}{p_A + p_B} + Z\sqrt{(p_A + p_B)S}$$

$$= \frac{p_A}{p_A + p_B}\left[G_A(p_A + p_B)S + Z\sqrt{(p_A + p_B)S}\right]$$

$$+\frac{p_B}{p_A+p_B}[G_B(p_A+p_B)S+Z\sqrt{(p_A+p_B)S}]$$

$$=\frac{p_A}{p_A+p_B}V_A+\frac{p_B}{p_A+p_B}V_B;$$

$$\therefore \qquad V_{AB}=\frac{p_AV_A+p_BV_B}{p_A+p_B}.$$

It has been suggested by Whitehead [12] that with accurate measurements of discharge potentials in mixtures the gas having the lower ionization potential should have a predominating effect. That this is not generally observed is due to the fact that the so-called ionization potential is approximately the same for all the commoner gases. We might expect, however, such to be the case for a mixture of two gases, one from each of the two groups mentioned above (22 *a*), but experiments by the writer on such mixtures have shown that even in this case the above mixture law (23) is obeyed accurately. It would appear, therefore, that discharge depends less on the actual ionization potentials of the individual molecules of a gas than on the free path of the electrons between the molecules.

In concluding, I wish to express my indebtedness to Professor W. M. Thornton, under whose guidance the work has been carried out, and also to the Department of Scientific and Industrial Research and to Durham County Council for grants which have enabled me to carry out the work.

References.

(1) Stephenson (paper communicated to Physical Society).
(2) Peek, ' Dielectric Phenomena in High Voltage Engineering.'
(3) Kunz, Phys. Rev. viii. p. 22 (1916).
(4) Townsend, " Conduction of Electricity through Gases," ' Electrician,' lxxi. p. 348 (1913).
(5) Keil, *Zeitschr. f. Phys.* x. p. 308 (1922).
(6) Schumann, ' Electrische Durchbruch Feldstarke von Gasen,' p. 170.
(7) Davis, A. I. E. E. xxxiii. p. 589 (1914); Phys. Rev. (1) xxiv. p. 93 (1907).
(8) Sah, A. I. E. E. p. 604 (1927).
(9) Loeb, J. F. I. ccv. p. 305 (1928); ccx. p. 15 (1930); ' Science,' lxix. p. 509 (1929).
(10) Hayashi, A. P. (4) xlv. p. 431 (1914).
(11) Bouty, *C. R.* cxxxvi. p. 669 (1903); cxxxviii. pp. 616, 1691 (1904); cl. pp. 148, 1380, 1643 (1910).
(12) Whitehead, ' Dielectric Phenomena,' p. 58.

XXV. *Investigations on Polarization of Light-Scattering.*—Part II. *By* S. Venkateswaran, *D.Sc.* (*Lond.*) *.

Introduction.

In an earlier paper † the author reported the results of the depolarization of Rayleigh scattering and rotational Raman scattering in some typical liquids. It was shown that the experimental values pointed clearly to the unsatisfactory nature of the classical theories of light-scattering and lent strong support to the theory of the spinning photon. The rotational scattering in liquids appearing in the form of unresolved wings accompanying the Rayleigh lines showed a depolarization of 6/7 in accordance with theory. In the present paper a study of the polarization of the vibrational Raman lines in a number of organic and inorganic liquids is made, and the results are discussed in relation to the molecular structure of the compounds.

Experimental Arrangements.

The liquids are mostly Kahlbaum's and are further purified by distilling in vacuum into the experimental bulbs or tubes which are then sealed off. Light from a mercury arc is focussed on the liquid by means of a glass condenser. The two components of the transverse scattering are focussed successively on to the slit of a Fuess glass spectrograph by means of a suitably oriented large nicol and a lens placed in the path of the scattered beam. The photographs are taken side by side on the same plate under identical conditions. With carbon disulphide the incident light is filtered through a Zeiss filter to allow only the λ 4358 radiation. As methyl iodide shows photochemical decomposition an arrangement is made for continuous distillation during the period of exposure with this liquid.

Sources of Error and the necessary Corrections.

In carrying out polarization measurements by the above method it is necessary to guard against various sources of error.

(a) *Polarization induced by the Spectrograph.*

Owing to oblique refraction at the prism surfaces of the spectrograph, the vertical component loses more than the

* Communicated by Sir C. V. Raman, M.A., D.Sc., F.R.S., &c.

† Phil. Mag. (7) xiv. p. 258 (Aug. 1932).

horizontal, and the depolarization is apparently enhanced. This error is, however, a constant characteristic of the instrument and can be eliminated by careful calibration. Unpolarized light is allowed to fall on the slit of the spectrograph and its state of polarization after passing through the prisms is determined. Two exposures are given side by side on the same plate under the same conditions, in one case the vibration axis of the nicol being vertical and in the other horizontal. The relative times of exposure for the vertical and horizontal components are so adjusted as to *exactly* compensate for the polarization induced by the spectrograph. Under these conditions the degree of blackening of the lines on the photographic plate would be the same as though the instrument transmitted the two polarized components equally well, and the exposures for the two components had been also equal. Independent measurements are also made visually according to Cornu's method, using a double image prism and nicol, and practically identical results are obtained. In order to get the true polarization of the Raman lines the necessary correction is introduced in the times of exposure, the vertical component being exposed for a correspondingly longer time than the horizontal. The actual ratio of the exposures of the two components obtained from the calibration of the spectrograph is 3 : 2.

(b) *Effect of Slit Width.*

Every partially polarized Raman line is accompanied by vibrational rotational scattering. A reasonably narrow slit should be used if the state of polarisation of the pure vibrational scattering is studied. If, however, a very broad slit is used the vibrational rotational scattering is included in the measurements and the value for the aggregate scattering is obtained. As the rotational scattering is depolarized to the extent of 6/7 the results will usually be higher when a broad slit is used than with a narrow one. The broad and narrow slit values will obviously be identical for the vibrational Raman line, which has itself a depolarization of 6/7.

(c) *Correction due to Lack of Transversality in the Incident Beam.*

For entirely eliminating this source of error it is necessary to employ a parallel incident beam and make observations in the transverse direction. For practical purposes, it is found that if a source of light of small angular aperture is focussed

into the liquid, and observation of the scattering is made exactly at the focus, no error is introduced. A point source of light could not, however, be used for illumination in the experiments owing to the feebleness of the scattering. Light from an extended source of mercury arc is therefore condensed into the liquid in long wide tubes with flat ends and photographed end-on, the long image of the mercury arc formed by the condensing lens falling along the axis of the tube. Under these conditions the illumination is found to be intense. A small correction is, therefore, necessary to take into account the divergence of the incident beam. The vertical dimensions of the mercury arc being negligible, the deviations are only in a horizontal plane and the corrections are easily calculated.

Considering a parallel beam of unpolarized light traversing a medium, if ρ is the value of the depolarization factor for transverse observation, and if ρ_θ is the value for observation along a direction making an angle θ with the normal to the track and $\frac{\pi}{2}-\theta$ with the direction of the track, then obviously

$$\rho_\theta = \rho + (1-\rho)\sin^2\theta.$$

In the actual experiment with the mercury lamp if the maximum deviation of the incident beam from the axis is equal to α on either side, the observed value of the depolarization factor in a direction normal to the axis of the incident beam may be obtained by averaging the above expression between the limits $\pm\alpha$ and represented by the equation

$$\rho_{\text{observed}} = \rho + \frac{1-\rho}{2}\left(1-\frac{\sin 2\alpha}{\alpha}\right).$$

Under the conditions of the experiments reported here, α is found to be equal to $\tan^{-1} 3/10$, and substituting this value of α we find

$$\rho_{\text{observed}} = \rho + \frac{1-\rho}{2} \times 0{\cdot}058.$$

It is thus seen that the correction is relatively inappreciable except when ρ is small.

(d) *Background Illumination.*

Care is taken to avoid any stray light and suitable apertures are used for this purpose. The presence of parasitic light leads to serious errors in intensity measurements, and

the suppression of the fainter lines on the photographic plate.

Method of Measurement.

A rigorous experimental evaluation of the states of polarization of the various Raman lines involves the use of the standard method of estimating intensities with the help of the density-log intensities curves, but the widely varying states of polarization and intensities of the numerous Raman lines makes the method somewhat laborious. With a view, however, to carrying out an extensive investigation in a large number of liquids the following method is adopted. The two components of any one line are compared with a series of exposures of varying times (using a constant source of light), all of them being obtained on the same plate, and the ratio of their intensities is taken to be represented approximately by the ratio of the times of the particular exposures with which they match. Such a procedure, although it may not lead to accurate values for the states of polarization, is found to reveal a large number of fundamental features of the polarization phenomena which are likely to be of great help in formulating a quantitative theory of the polarization of the vibrational Raman lines. In the majority of the liquids reported here the evaluation of the ratio of intensities is made as above, using a plate containing graded exposures. The values given for benzene, carbon disulphide, and carbon tetrachloride are of greater accuracy, as the measurements are made with these liquids by adjusting the times of exposure for the two principal components so as to give equality of density on the photographic plate. For this purpose a series of photographs are taken of the vertical and horizontal components side by side, providing a close range of depolarization values. ρ for any particular Raman line can then be determined easily. As the photographic blackening is not strictly proportional to the times of exposure Schwarzschild's correction should be applied for obtaining the true values. ρ, the depolarization of a line, is given by the relation,

$$\rho = I_H/I_V = (T_V/T_H)^{0\cdot86},$$

where I and T represent the intensities and times of exposure respectively of the vertical and horizontal components. This correction is of the same order as that found for lack of transversality in the case of depolarization values and is in the opposite direction.

Results.

The polarization of the Raman lines in 27 liquids has been studied, and the values are tabulated in the accompanying tables. It may be mentioned here that the polarization of a line due to *any given frequency shift* is found to be independent of the frequency of the exciting line. It is also independent of whether the line is of the Stokes type or anti-Stokes type. Hence, in the tables only the different Raman frequencies $\Delta\nu$ of each liquid and their depolarization values are given. The following abbreviations are used :—d = diffuse, s = sharp, b = broad.

Table I.

Liquid.	Raman frequency.	Depolarization.
Hydrogen sulphide (liquid)	2572	0·15
Hydrocyanic acid (liquid).....	2094	0·2
Hydrogen peroxide (perhydrol) ...	875(*s*)	0·15

H_3S and HCN were prepared in the laboratory and liquefied in specially strong glass tubes which were immersed in liquid air and then sealed off.

Table II.

Sulphur trioxide (SO_3).

Raman frequency.	Depolarization.	Raman frequency.	Depolarization.
290	0·8	1068(*s*)	0·3
370(*d*)	0·6	1240(*d*)	0·8
535	0·7	1271(*s*)	0·2
650	0·2	1403(*d*)	0·8
666	0·2	1489(*d*)	0·8
697(*s*)	0·2	1516(*d*)	0·7

The substance is melted in a sealed tube and the Raman spectrum is taken at the room temperature (30° C.). As a certain proportion of the molecules are polymerized at ordinary temperatures, the spectrum shows Raman lines due to both SO_3 and S_2O_6 molecules. The following frequencies are characteristic of the SO_3 molecules :—$\Delta\nu$ 535, 1068, and 1403. The frequencies at 290, 370, 666, 697, 1271, and 1489 are due to S_2O_6 molecules. The line at 1489 shows a structure in that it consists of a relatively sharp central line

with diffuse wings on either side. It may be noted that the depolarization of this line reaches the limiting value 6/7. Three frequencies at 650, 1240, and 1516, not reported before, have been obtained.

TABLE III.

Nitric acid (HNO_3).

Raman frequency.	Depolarization.	Raman frequency.	Depolarization.
462	Less than 0·4	1130	Less than 0·4
638	0·3	1305 (*b*)	0·1
690	0·2	3188, 3420, 3549	Band less than 0·4
951 (*b*)	0·2		
1045 (*s*)	0·1		

A specimen of 65 per cent. strength which had been distilled and sealed in vacuum was used for the investigation. The line at 1045 represents the symmetric oscillation of the nitrate ion, and the one at 1305 is characteristic of the nitric acid molecule. The bands at 3188, 3420, and 3549 are due to water.

TABLE IV.

Phosphorus trichloride (PCl_3).

Raman frequency.	Depolarization.	Raman frequency.	Depolarization.
189 (*s*)	0·9	481 (*d*)	0·7
260 (*s*)	0·2	514 (*d*)	0·2

The line at 189 which is fairly sharp, reaches the limiting depolarization value 6/7. It may be noted that although both the lines at 481 and 514 appear equally very diffuse, the former is almost unpolarized while the latter shows a state of high polarization. This feature persists also in the corresponding lines of arsenic and bismuth trichlorides.

TABLE V.

Carbon disulphide (CS_2).

Raman frequency	400	656 (*s*)	795 (*d*)
Depolarization	0·8	0·2	0·2

TABLE VI.

Methyl alcohol (CH_3OH).

Raman frequency.	Depolarization.	Raman frequency.	Depolarization.
1034	0·5	2835	0·1
1360 (*d*).....	0·7		
1469 (*d*)	0·8	2945	0·3

The Raman frequency at 1034 is due to C–O linkage present in the molecule. The broad diffuse band at 3μ is practically unpolarized ($\rho = 0{\cdot}8$).

TABLE VII.

Formic acid (H.COOH).

Raman frequency.	Depolarization.	Raman frequency.	Depolarization
196 (*b*)	0·9	1223 (*d*)	0·4
690 (*d*)	0·8	1400	0·8
857 (*d*)	0·7	1694	0·3
1052 (*d*)	0·7	2957	0·5

The line due to $\Delta\nu$ 1694 is characteristic of the C=O linkage and shows the best polarization. The line at $\Delta\nu$ 196 is very diffuse and broad, and its origin appears to be due to the presence of associated molecules. This line shows a limiting depolarization value of 6/7. The photographs show little rotational scattering in spite of the high anisotropy of the formic acid molecule ($\rho = {\cdot}55$ sunlight value *). This is evidently due to the high viscosity of the liquid.

TABLE VIII.

Methyl chloride (CH_3Cl).

Raman frequency.	Depolarization.	Raman frequency.	Depolarization.
712 (*d*).....	0·3	2955	0·3
		3030 (*d*)	0·8

This liquid was examined in the original sealed bulb obtained from Messrs. Scherring Kahlbaum. The lines at 712 and 2955 represent the CCl and the CH oscillations respectively.

* K. S. Krishnan, Phil. Mag. l. p. 697 (1925).

Table IX.

Methyl bromide (CH_3Br).

Raman frequency.	Depolarization.	Raman frequency.	Depolarization
594	0·2	2956	0·2

$\Delta\nu$ 594 is characteristic of the C–Br oscillation.

Table X.

Methyl iodide (CH_3I).

Raman frequency.	Depolarization.	Raman frequency.	Depolarization.
522	0·6	2947	0·4

The line at 522 represents the CI oscillation. It may be noted that this line is somewhat diffuse and shows a distinctly higher depolarization value than those characteristic of CCl and CBr oscillations respectively.

Table XI.

Methyl mercaptan (CH_3SH).

Raman frequency.	Depolarization.	Raman frequency.	Depolarization.
704.....	0·3	2573	0·3
805.....	0·4	2871	0·4
1059.....	0·3	2932	0·3
1425(*d*)	0·9	2975(*d*)	0·9

$\Delta\nu$ 2573 and 704 are characteristic of the SH and CS oscillations respectively.

Table XII.

Chloroform ($CHCl_3$).

Raman frequency.	Depolarization.	Raman frequency.	Depolarization.
261.....	0·8	762(*d*)...	0·8
367(*s*)	0·2	1218(*d*).....	0·8
669(*s*)	0·1	3019	0·2

TABLE XIII.

Bromoform ($CHBr_3$).

Raman frequency.	Depolarization.	Raman frequency.	Depolarization.
154	0·8	657	0·7
223	0·2	1146	0·7
540	0·1	3020	0·3

TABLE XIV.

Carbon tetrachloride (CCl_4).

Raman frequency.	Depolarization.	Raman frequency.	Depolarization.
216	0·8	762 (*d*).....	0·8
314	0·8	791 (*d*).....	0·8
459	0·04	1535 (*d*).....	0·3

$\Delta\nu$ 762 shows much higher depolarization than the corresponding line in other chloro compounds.

TABLE XV.

Pentane (C_5H_{12}).

Raman frequency.	Depolarization.	Raman frequency.	Depolarization.
401	Less than 0·2	1461 (*d*).....	0·8
476	,, ,, 0·4	2854 (*d*).....	0·7
766	,, ,, 0·3	2876 (*d*).....	0·2
839	,, ,, 0·2	2906 (*d*).....	0·7
964	,, ,, 0·4	2937 (*d*).....	0·5
1039	,, ,, 0·4	2964 (*d*).....	0·7

TABLE XVI.

Allyl sulphide ($C_6H_{10}S$).

Raman frequency.	Depolarization.	Raman frequency.	Depolarization.
410 (*d*).....	0·4	1405	0·5
581 (*d*).....	0·4	1430 (*d*)	0·5
732 (*s*)	0·2	1491 (*d*)	0·7
753 (*s*)	0·8	1634	0·3
918 (*s*)	0·7	2914	0·3
998 (*d*).....	0·5	2943	0·8
1040	Less than 0·5	2978	0·6
1076	0·4	3009	0·3
1293	0·3	3084	0·9

The Raman frequency at 1634 is due to C=C linkage, and the one at 732 is due to the CS oscillation.

TABLE XVII.

Benzene (C_6H_6).

Raman frequency.	Depolarization.	Raman frequency.	Depolarization.
605	0·8	1605	0·8
849	0·8	3046	0·9
992	0·07	3061	0·4
1584	0·8		

TABLE XVIII.

Nitrobenzene ($C_6H_5NO_2$).

Raman frequency.	Depolarization.	Raman frequency.	Depolarization.
851	Less than 0·4	1347 (*s*)	0·2
1011	0·2	1530 (*d*)	0·6
1116	Less than 0·4	1589	0·8
		3051	0·3

$\Delta\nu$ 1347 is characteristic of all nitro-compounds.

TABLE XIX.

Chlorobenzene (C_6H_5Cl).

Raman frequency.	Depolarization.	Raman frequency.	Depolarization.
195 (*d*)	0·8	1084 (*s*)	0·2
299 (*d*)	0·8		
420 (*s*)	0·4	1160 (*d*)	0·9
615 (*s*)	0·8	1383	0·4
704 (*s*)	0·2	1583 (*d*)	0·8
1004 (*s*)	0·1	3067 (*d*)	0·4
1023 (*s*)	0·2		

The Raman line at 704 is due to C–Cl oscillation. Several of the lines reach the limiting depolarization value 6/7.

TABLE XX.

Bromobenzene (C_6H_5Br).

Raman frequency.	Depolarization.	Raman frequency.	Depolarization.
317	0·3	1079	0·2
673	0·2	1188	0·3
1002	0·1	1590	0·8
1026	0·2	3060	0·4

TABLE XXI.

Mesitylene ($C_6H_3(CH_3)_3$).

Raman frequency.	Depolarization.	Raman frequency.	Depolarization.
233 (*d*).....	0·9	1036	0·3
275 (*d*).....	0·9	1255	0·9
519 (*s*).....	0·9	1301	0·3
578 (*s*).....	0·2	1380 (*d*)	0·6
847 (*d*).....	0·9	1611	0·9
976	0·5	2867 (*b*)	0·3
998 (*s*).....	0·1	2917 (*b*)	0·3
—		3015 (*b*)	0·4

Three new lines at $\Delta\nu$ 847, 976, and 1255 are recorded here.

TABLE XXII.

Salol ($C_6H_4(OH)COOC_6H_5$).

Raman frequency.	Depolarization.	Raman frequency.	Depolarization.
565 (*s*)	0·8	1197 (*d*)	0·6
617	0·8	1250	0·6
674 (*d*).....	0·7	1333	0·6
752 (*d*).....	0·7	1395 (*d*)	0·7
802 (*d*).....	0·6	1467.....	0·6
844 (*s*).....	0·3	1586	0·8
1005 (*s*)	0·2	1617 (*d*).....	0·8
1034 (*s*)	0·2	1693 (*b*).....	0·5
1136	0·6	3076.....	0·5
1163	0·6		

The group of lines between $\Delta\nu$ 1136 and 1333 show the same degree of depolarization.

Table XXIII.

Pyridine (C_5H_5N).

Raman frequency.	Depolarization.	Raman frequency.	Depolarization.
603	0·7	1217	0·6
651	0·8	1576	0·8
988	0·1	3033	0·8
1027	0·2	3056	0·4

Table XXIV.

Thiophene (C_4H_4S).

Raman frequency.	Depolarization.	Raman frequency.	Depolarization.
452 (*d*)	0·7	1035 (*s*)	0·1
607	0·2	1081	0·3
690 (*d*)	0·8	1361 (*s*)	0·1
752 (*d*)	0·9	1409	0·3
835	0·1	3083 (*s*)	0·9
870 (*d*)	0·9	3116	0·3

Table XXV.

Pyrrole (C_4H_4NH).

Raman frequency.	Depolarization.	Raman frequency.	Depolarization.
1003	0·1	1470	0·6
1144	0·2	3100	0·9
1202	0·2	3139	0·4
1384 (*b*)	0·5		

The spectrum shows a broad band extending from λ 4196 to λ 4165 which has a structure. The depolarization value for this band is 0·6. A new frequency at $\Delta\nu$ 3100 is reported.

Discussion of Results.

State of Depolarization and Character of the Lines.

From an examination of the data given in the tables it is not possible to draw any general conclusion regarding the character of the lines such as their sharpness, or diffuseness,

and their corresponding polarization. In a large majority of cases it is found that while sharp lines are well polarized, diffuse lines show high depolarization. It should be recognized, however, that several sharp lines reach the limiting depolarization value 6/7, and that some diffuse lines, such as those at 795 in CS_2 514 in PCl_3, and 1535 in CCl_4, are strongly polarized. In the case of liquids the rotational effect will be present as wings on either side of certain vibrational lines. The latter may therefore be expected to be diffuse, and the aggregate scattering will naturally show high depolarization. We may in this connexion instance the 522 line of methyl iodide, which has a sharp intense core and shows rotational wings on either side.

Inactive Oscillations.

The appearance of inactive frequencies of molecules in Raman spectra in great strength, while they are absent in infra-red absorption, is a matter of considerable theoretical significance. These oscillations are usually of a type involving a high degree of symmetry in the motion of the nuclei, and closely connected with it is the very strong polarization of all inactive lines which is observed. The strong 1045 line in solutions of nitric acid due to the NO_3 ion, and the 991 line of benzene may be referred to in this connexion.

Relation to Molecular Structure.

From an extensive investigation of the Raman spectra of a large number of compounds several attempts have been made to correlate each particular type of chemical bond with a certain characteristic frequency. The oscillation frequencies have also in a number of cases been calculated numerically from the binding force between the constituent vibrating atoms derived from the thermo-chemical data and the effective mass of the vibrating system. But the dynamics of oscillations even in the case of a simple molecule like benzene presents very serious difficulties, and it is therefore premature to attempt to calculate from purely structural considerations the polarization of the Raman lines. We have, therefore, to content ourselves with a general discussion based on the results of various compounds.

From the tables one notices a striking contrast between the polarization of the Raman lines of aliphatic and aromatic compounds. The former class of compounds shows in general more lines which are well polarized than the latter, though it

is true that there are several individual lines also of the aromatics which are strongly polarized and of aliphatics which are almost completely unpolarized. However, the general result bears a strong analogy to the polarization of classical scattering which is greater for the aliphatics than for the aromatics. Apart from the above general relationship between the members of each class of compounds, there are certain interesting features which are to be noted in individual cases. Taking, for example, benzene and its derivatives, they all have several Raman lines in common, though their intensities and precise values of the frequencies differ from compound to compound. These frequencies are presumably due to the benzene nucleus, and the fact that

Table XXVI.

Comparison of the Depolarization of Raman Frequencies of Benzene and its Derivatives.

	Depolarization value.			
Raman frequency.	Benzene.	Chlorobenzene.	Salol.	Mesitylene.
605.....	0·8	0·8	0·8	
992.....	0·07	0·1	0·2	0·1
1021.....	—	0·2	0·2	0·3
1584.....	0·8	0·8	0·8	0·9
3046.....	0·9	—	—	—
3061.....	0·4	0·4	0·5	0·4

they preserve their individuality in a large number of derivatives may be taken to mean that the essential structure of the nucleus is unaltered by mere substitution. Without being able to work out the problem in its details, one by analogy *a priori* can conclude that these lines in the derivatives of benzene must be polarized, at least to a first approximation, in a manner similar to that in benzene. In Table XXVI. are collected together some of these frequencies, and it is evident from a perusal of the table that the polarization of a given frequency is more or less the same in the derivatives.

There is also another interesting fact closely connected with the above, viz., when any frequency splits up into two, due to the complexity of the molecule, both the components show nearly the same polarization characteristic of the

original frequency. We may instance the case of the doublet of frequencies 991 and 1030 in the various benzene derivatives. The observed variations in the relative intensities of these two frequencies resulting from increasing and varying substitutions in the benzene nucleus are discussed in another paper*, and it appears that they are very closely connected with each other. It is probable that they may even have a common origin both arising from the same kind of oscillation.

The analogy between the magnitudes of Raman frequencies in compounds having similar structures also extends to the state of polarization of the corresponding lines. The close agreement between the polarization values of the principal lines of pyridine and those of the corresponding lines in benzene may be cited as an example. The corresponding frequencies in chloroform and bromoform and those due to C—Cl and C—Br oscillations in chloro- and bromobenzenes show respectively the same degree of polarization. A close dependence of the polarization phenomena on the geometrical structure of the molecules is thus seen.

An attempt may be made to extend this result to the case of frequency shifts which are characteristic of the various types of chemical bonds such as C=C, C=O, etc. Here, one meets with some difficulty, since the polarization of the characteristic frequency of any particular group or bond does not appear to be identical in all the derivatives. Qualitatively, however, a great similarity is noticed in the states of polarization of such frequency shifts, the actual differences in the magnitudes of depolarization being presumably due to the influence of the complex nature of the molecules. For instance, the characteristic CS oscillation $\Delta\nu$ 740 in widely different compounds such as carbon disulphide, methyl mercaptan, and allyl sulphide, $\Delta\nu$ 1347, which is characteristic of the nitro group in all nitro compounds, the CCl and CBr lines in halogen compounds, and C=O, SH, and NH oscillations in their corresponding derivatives all show respectively more or less the same degree of polarization.

A comparison of the depolarization values of the 3 μ band characteristic of the CH oscillation brings out in a striking manner the wide range of values shown by the components of this band. This is seen from Table XXVII., where data regarding the states of polarization of these components in some aliphatic and aromatic compounds are collected.

* S. Venkateswaran and S. Bhagavantam, Proc. Roy. Soc. A, cxxviii. p. 252 (1930).

A critical examination of the results brings out clearly an important feature regarding the polarization of the lines at about 1450 in aliphatic and 1600 in aromatic compounds. In earlier papers it was shown that these lines should be associated with the CH transverse oscillation. Irrespective of the nature of the molecule, whether aliphatic, aromatic, or heterocyclic, saturated or unsaturated, the transverse oscillation shows in every case a high degree of depolarization, as is evidenced from Table XXVIII. In all cases the

TABLE XXVII.

Depolarization of Raman lines due to CH oscillations.

Raman frequencies.	2870.	2900.	2940.	2960.	3020.	3040.	3060.	3080.	3100.
Methyl alcohol.....	0·1	—	0·3	—	—	—	—	—	—
Methyl chloride ...	—	—	—	0·3	0·8	—	—	—	—
Methyl bromide ...	—	—	—	0·2	—	—	—	—	—
Methyl iodide	—	—	0·4	—	—	—	—	—	—
Methyl mercaptan .	0·4	—	0·3	0·9	—	—	—	—	—
Chloroform	—	—	—	—	0·2	—	—	—	—
Bromoform	—	—	—	—	0·3	—	—	—	—
Pentane	0·2	0·7	0·5	0·7	—	—	—	—	—
Allyl sulphide	—	0·3	0·8	0·6	0·3	—	—	0·9	—
Benzene	—	—	—	—	—	0·9	0·4	—	—
Chlorobenzene	—	—	—	—	—	—	0·4	—	—
Mesitylene	0·3	0·3	—	—	0·4	—	—	—	—
Salol	—	—	—	—	—	—	—	0·5	—
Pyridine	—	—	—	—	—	0·8	—	0·4	—
Thiophene.....	—	—	—	—	—	—	—	0·9	0·3
Pyrrole.....	—	—	—	—	—	—	—	—	0·9

limiting depolarization value 6/7 is reached. It may be pointed out here that the lines due to these transverse oscillations are invariably somewhat diffuse. The line at $\Delta\nu$ 400 in carbon disulphide which may be attributed to the transverse CS oscillation shows in a similar manner a high depolarization, while the other two lines at 656 and 795 are well polarized. A transverse oscillation of the above type may be associated with an internal rotation in the molecule and as such its high depolarization is explicable.

Of the five frequencies in carbon tetrachloride, $\Delta\nu$ 459 is very well polarized, while the lines at 216, 314, 762, and

791 reach the limiting depolarization value 6/7. The line at $\Delta\nu$ 459 corresponds to a symmetric oscillation of the tetrachloride molecule, and it is not surprising that this oscillation shows a genuine depolarization in view of the fact that the Rayleigh scattering of the carbon tetrachloride molecule shows also a distinct depolarization (5 per cent.). Such a genuine departure of the structure of this molecule from perfect optical symmetry is also evident from the existence of a rotational Raman scattering accompanying the Rayleigh

TABLE XXVIII.

Depolarization of Raman Lines due to transverse Oscillations.

Liquid.	Nature of transverse oscillations.	Raman frequency.	Depolarization value.
Carbon disulphide	CS	400	0·8
Formic acid	CH	1400	0·8
Methyl alcohol	,,	1469	0·8
Methyl mercaptan	,,	1425	0·9
Pentane	,,	1461	0·6
Allyl sulphide	,,	1491	0·8
Benzene	,,	1584	0·8
Nitrobenzene	,,	1589	0·5
Chlorobenzene	,,	1583	0·8
Mesitylene	,,	1611	0·9
Salol	,,	1586	0·8
Pyridine	,,	1576	0·8
Pyrrole	,,	1470	0·6

lines which can be seen in the photographs. Further, as has already been reported by the author *, the depolarization of the classical scattering in this liquid, measured with a narrow slit of the spectrograph, shows a definite decrease from the wide slit value. It is thus evident that the wing is of a genuine rotational origin, and, as may be expected, it is practically unpolarized.

Recently, Cabannes has reported, however, that the small depolarization shown by the symmetric oscillation may be attributed to the isotopes of chlorine and not to a genuine

* *Loc. cit.*

imperfection in the symmetry of the molecule. It may be pointed out that the view regarding the non-symmetrical nature of the tetrahedral molecule is not by itself inherently improbable. We may, for instance, refer to the simplest case of methane in this connexion. Careful experiments on the Rayleigh scattering have shown that this gas shows a definite and appreciable depolarization, and Bhagavantam * finds that the Raman line arising from the oscillation corresponding to a symmetric expansion of this molecule also shows a depolarization of about 8 per cent.

Of the inorganic compounds the spectrum of hydrogen-peroxide is important owing to the simplicity of the structure of its molecule. The liquid gives Raman lines corresponding to $\Delta\nu$ 400, 875, and 903, in addition to the water-bands †. Of these, the line at 875 is the most prominent and sharp.

TABLE XXIX.

Substance.	Formula.	Raman frequencies.		
Ethane	H_3C-CH_3	999	—	—
Cyanogen	$N\equiv C-C\equiv N$	860	—	2334
Hydrogen peroxide	HO—OH	875	—	—
Oxygen	O=O	—	1552	—
Ethylene	$H_2C=CH_2$	—	1342	—
Acetylene	$HC\equiv CH$	—	—	1979

Various formulæ have been suggested, such as HO−OH, where the oxygen atom is bivalent; HO≡OH, where both the oxygen atoms are tetravalent; $H_2O=O$, where one of the oxygen atoms is bivalent and the other tetravalent. Each of these formulæ appears to be supported by evidence from chemical reactions of hydrogen-peroxide or the analogous peroxides. A consideration of the Raman spectrum of this compound enables us to determine uniquely its constitution. In this connexion we may compare it with the Raman spectra of compounds having similar structures. In Table XXIX. are given the values of the most prominent frequencies of a few of such compounds.

For all practical purposes all the above molecules may be treated in a manner similar to those of the diatomic molecules of the type X_2, and hence we may expect one prominent

* 'Nature,' cxxix. p. 830 (1932).

† S. Venkateswaran, 'Nature,' cxxvii. p. 406 (1931).

frequency in all of them. The value of this frequency depends, however, on various circumstances, such as the mass of the two groups, the strength of their binding, etc., and from the chemical point of view three distinct cases, namely, binding through a single bond, a double bond, and a triple bond may be recognized. The frequencies in the three cases fall in wholly different regions, viz., about 900, 1500, and 2000 respectively. A glance at the above table shows immediately that hydrogen peroxide falls in the first group and should be represented by the formula HO—OH. In spite of the differences in chemical binding, all these principal frequencies may be expected to show similar states of polarization and also a general correspondence in this respect with other cases of diatomic molecules such as H_2, O_2, N_2. The following table shows the depolarization values of the principal Raman lines of a few diatomic molecules.

TABLE XXX.

Substance.	Raman frequency.	Depolarization value.
*Hydrogen H—H	4156	0·16
*Oxygen O=O.....	1557	Less than 0·3
*Acetylene (HC=CH)	1974	Less than 0·2
Hydrogen peroxide (HO—OH) ...	875	0·15

It is seen that in all cases the principal line is very well polarized.

The existence of a weak Raman line at $\Delta\nu$ 400 in carbon disulphide may be identified with the transverse oscillation of the carbon atom in the symmetry plane of the molecule. The oscillation is a degenerate one and is equivalent to an internal rotation of the carbon atom in that plane, and its high depolarization has evidently to be ascribed to these characters of the oscillation †. It has been shown previously ‡ that the two frequencies at 656 and 795 appear in all compounds having the CS linkage and should both be attributed to this oscillation. The same degree of polarization exhibited by the Raman lines due to these two frequencies affords further support to this view.

* Values obtained by Bhagavantam.
† 'Nature,' cxxix. p. 167 (1932).
‡ S. Venkateswaran, Ind. Jour. Phys. vi. p. 51 (1931).

Summary.

Polarization measurements of the vibrational Raman lines in 27 liquids are reported, and the results are discussed in relation to the molecular structure of these compounds. A close dependence of the polarization phenomenon on the geometrical structure of the molecule is observed. The lines characteristic of the oscillation of the benzene nucleus are polarized respectively more or less to the same extent in the derivatives. The components of the CH band assume a wide range of depolarization values. Raman lines arising from transverse oscillations are invariably highly depolarized, all of them showing the limiting depolarization value 6/7.

From a consideration of the Raman spectrum of hydrogen peroxide it is shown that the two oxygen atoms in the molecule are probably attached with a single bond, and that the compound should be represented by the formula HO—OH.

The author desires to thank Prof. Sir C. V. Raman, D.Sc., F.R.S., N.L., for his kind interest in the work.

Indian Association for the
Cultivation of Science,
210 Bow Bazar Street,
Calcutta.

XXVI. *Ionization by Positive Ions.* *By* J. S. Townsend, *M.A., Wykeham Professor of Physics, Oxford, and* F. Llewellyn Jones, *M.A., D.Phil., Senior Demy, Magdalen College, Oxford* *.

THE theory of disruptive discharges in gases which was deduced from experiments made many years ago at the Electrical Laboratory, Oxford, involves the hypothesis that molecules or atoms of the gas are ionized by the collisions of positive ions. It was well known from the experiments of Villard that the positive ions also set free electrons from the negative electrode.

These properties of positive ions are discussed in the treatise on Electricity in Gases †, where it is shown that the relative importance of the two effects in contributing

* Communicated by the Authors.

† See Sections 230, 238, 290, and 299.

to the conductivity of the gas depends on various circumstances. Thus in discharges from positively charged points it is necessary to assume that the ionization of the gas is the predominating effect. In discharges between parallel plates there were no conclusive experiments to show the relative values of the two effects, but from general considerations of the sparking potentials obtained with electrodes of ordinary metals, it was concluded that at pressures greater than that corresponding to the minimum sparkling potential the number of electrons set free from the negative electrode was small compared with the number generated by the collisions of positive ions with molecules of the gas.

The number set free from the electrode depends on the metal of which it is made, the emission from alkali metals being much greater than the emission from ordinary metals.

2. Recently we have made experiments to determine separately the two effects of the positive ions in currents between parallel plates when the gas pressure is of the order of that corresponding to the minimum sparkling potential *. The arrangement of the apparatus is shown by the diagram (fig. 1). The electrodes comprised four circular disks A, B, E, and F, of thin copper 6 cm. in diameter, with cylindrical rings round the edges which fitted into a quartz cylinder, also two semicircular plates C and D, 5·6 cm. in diameter, of copper ·5 mm. thick.

The distance between the disks A and B was 2 cm., between B and E 2·1 cm., and between E and F 3 cm. The electrodes C and D were 1 millimetre from the disk E. The planes of the electrodes were perpendicular to the axis P, Q of the cylinder. All the electrodes were insulated by quartz rods (not shown in the figure).

The disk B had a slit S, 1·5 cm. long and 4 mm. wide, with its centre at the centre of the disk. A shutter W of thin copper rested on the disk, and was connected to a magnet M in a side tube T, so that it could be placed over the slit, or withdrawn to the side to leave the slit open. When the shutter was over the slit it formed part

* A brief account of the results has already been given in a communication to 'Nature,' 6th September, 1932.

of the electrode B, and in order to ensure good contact they were connected by a flexible wire in the tube T.

The disk E had a slit S_1 at the centre 1·5 cm. long and 2 mm. wide, and the disk F a slit S_2 1·5 cm. long and 3 mm. wide with the centre of the slit 6 mm. from the centre of the disk.

The straight edges of the semicircular electrodes C and D were 4 mm. apart, and were placed symmetrically

Fig. 1.

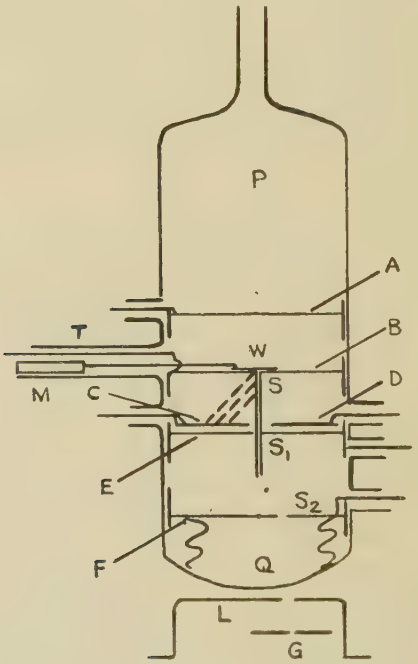

on either side of the disk E with the slit in E midway between them. The edges of the slits were parallel to the straight edges of the electrodes C and D. When a stream of positive ions passed through the slits and moved under an electric force to the disk B, none of the ions were intercepted by the electrodes C and D, since the width of the slit in E was only 2 mm.

The apparatus was heated for several hours to expel gases from the electrodes and the surface of the quartz.

The experiments were made with hydrogen which was prepared by the electrolysis of barium hydrate, and admitted to the quartz cylinder through a palladium tube.

3. The positive ions which passed through the slits were generated in the gas between the electrodes E and F by the collisions of electrons with molecules of the gas.

The electrons were set free from the lower surface of the disk E by ultra-violet light from the spark gap G in a condenser discharge. The light was limited to a narrow beam by a slit in the screen L, so that no direct light from the spark-gap entered the apparatus except through the slit S_2 in the disk F. The beam fell on a narrow area of the disk E opposite the slit S_2, so that no direct light should pass through the slit S_1 and fall on the electrode B.

A uniform magnetic force was maintained in the whole space between the electrodes (from A to F) by two large coils on either side of the quartz cylinder. The electrons set free from the disk E were thus deflected towards the centre of the cylinder, where positive ions were generated and moved under the electric force towards the slit S_1.

Since the rate of ionization in the space between the electrodes E and F depends on the electric force, a current of positive ions of any required intensity was obtained through the slit S_1 by adjusting the potential difference between the disks E and F.

4. The electrodes C, D, and E were at the same potential, which was the earth potential, and B was at a negative potential V, so that the positive ions that pass through the slit S_1 move towards the disk B under the force $Z = V/2$, the distance of B from the electrodes C and D being 2 cm.

The principal stream of positive ions is shown in the figure by the narrow lines through the slit S_1.

When the slit S is closed the positive ions impinge on the electrode B, a large proportion falling on the shutter W.

When the force Z is sufficiently large, electrons are set free by the collisions of the positive ions with molecules of the gas, and also from the electrode. These electrons are also deflected by the magnetic force, as shown by the dotted lines in the figure, and the force was adjusted

to give a deflexion which brought all the electrons generated by the positive ions to the electrode C (the deflexion of the positive ions was very small and may be left out of consideration). Under these conditions there is no current to the electrode D, and this electrode was therefore connected to E, which was maintained at zero potential.

The negative charge received by the electrode C was measured by an electrostatic balance arranged so that the electrode remained at zero potential while the current was flowing.

5. In order to estimate the effect of the positive ions, it is necessary to correct the observations by deducting from the charges received by the electrodes B and C the small charge received when the force between the disks E and F is very small, and no positive ions pass through the slit S_1. These small charges are due to the action of diffused light that passes through the slit S_1 and sets free electrons from the electrode B. The electrode B thus acquires a small positive charge and C a small negative charge.

Having determined these corrections the force between the plates E and F was adjusted so that the current of positive ions that passed through the slit S_1 was large compared with the current between the electrodes B and C due to the diffused light. It was usually found that a sufficiently large current of positive ions was obtained when the electrode F was at a potential of about 180 volts, the current due to diffused light being then about 2 per cent. of the current of positive ions received by the electrode B.

The currents of positive ions passing through the slit S_1 were of the order 10^{-11} amp.

It is undesirable to have larger currents, as the charge in the gas would disturb the field of force in the space between the electrodes.

The currents obtained under these conditions were sufficiently large to be measured accurately by observing the charges received by the electrodes A, B, and C, when the ultra-violet light acted for ten seconds on the electrode E. The charges were measured by an electrostatic balance comprising a sensitive electrometer connected to small air condensers and a potentiometer.

It was arranged so that the potential of the insulated electrode did not change while it acquired a charge. It is unnecessary to give details of the connexions of the condensers to the electrodes, as similar methods of measuring small currents have been described in previous papers. When the current to one of the electrodes was being measured, the other electrodes were maintained at constant potentials by a battery of small accumulators.

6. The action of the positive ions that move under a force Z from the slit S_1 to the electrode B is indicated directly by the negative charge c, received by the electrode C in a given time t. If the electrode B with the slit S closed receives the positive charge b in the same time the current passing through the slit S_1 is $(b-c)/t$.

The action of the positive ions depends on the intensity of the force Z and the pressure p of the gas. This was observed by the experiments made with hydrogen at pressures from 1 millimetre to ·2 mm.

The effect of changing the force when the pressure is constant is shown by the experiments with the gas at ·45 mm. pressure. In this case the charge c was about 1 per cent. of the charge b when the force Z was 60 volts per centimetre, about 10 per cent. when the force was 84 volts per centimetre, and 24 per cent. when the force was 103 volts per centimetre. This does not mean that the number of electrons generated by a given number of positive ions moving under a force of 103 volts per centimetre is about 24 times as great as the number generated under a force of 60 volts per centimetre. The electrons generated by the positive ions ionize molecules of the gas, and this effect increases with the force. Thus the large increase in the ratio c/b obtained by increasing the force must be attributed to two factors, the increase in the activity of the positive ions, and the increase in the activity of the electrons generated by the positive ions.

The force required to obtain appreciable ionization with positive ions increases with the pressure. In hydrogen at a pressure ·25 mm. the charge c was about 15 per cent. of b when the force was 70 volts per centimetre, but with the same force and the gas at a pressure of 1 millimetre the charge c was less than 1 per cent. of b.

7. When the slit S is open and the electrode A is at a lower potential than B, some of the positive ions pass

through the slit and are received by the electrode A. In this case if a_1 and b_1 be the positive charges received by the electrodes A and B and c_1 the negative charge received by the electrode C in a time t, the current of positive ions passing through the slit S_1 is $(a_1+b_1-c_1)/t$. This is the same as the current $(b-c)/t$ obtained with the slit S closed, since the current through S_1 is not affected by opening or closing the slit S.

The potential difference between the electrodes A and B was about 40 volts at the lower pressures and 80 volts at the high pressures, and the experiments show that with these potentials the positive ions do not ionize the gas in the space between the electrodes A and B to an appreciable extent or set free electrons from the electrode A.

The current a_1/t is therefore the current of positive ions through the slit S.

TABLE I.

p.	Z.	c.	b.	c_1.	b_1.	a_1.
·72	111	19·6	119	17·0	58	59
·72	132	81	181	76	120	56
·45	84	9·0	109	8·0	54	54
·45	103	31·3	131	27·8	71	56·5
·45	125	90	190	80	123	57
·25	69	16·5	116	13·6	64	49
·25	103	42·5	142	36	79	57

8. The results of experiments with hydrogen at the pressures ·25, ·45, and ·72 millimetres are given in Table I.

The electric force Z in the space between the electrodes B and C is given in volts per centimetre. The negative charge c received by the electrode C and the positive charge received by the electrode B with the slit S closed are given in arbitrary units. The charges $(b-c)$ carried by the principal stream of positive ions is taken as 100 in each case. The negative charge c_1 received by the electrode C and the positive charges a_1 and b_1 received by the electrodes A and B with the slit S open are in the same units as c and b $[(b-c) = (a_1+b_1-c_1)]$. These are the corrected values of the charges after allowing for the small current between the electrodes due to diffused light. (The correction was about 2 per cent. of the observed value of the charge $(b-c)$.)

With a given force Z and pressure p the ratio c/b depends on the intensity of the magnetic force.

In the experiments with the gas at ·45 mm. pressure the magnetic force was adjusted to the value H, which gave a maximum value of the ratio c/b when the electric force was 125 volts per cm. At that point the rate of change of the ratio c/b with the intensity of the magnetic force was very small. In the experiments with the gas at ·25 mm. pressure the magnetic force was $25 \times H/45$ and at ·72 mm pressure the magnetic force was $72 \times H/45$.

This ensured that all the electrons generated in the space between B and C were collected on C.

9. A large proportion of the ions in the principal stream impinge on the shutter W when the slit S is closed, and when the slit is open they pass through and convey the charge a_1 to the electrode A. Thus when the slit is opened the number of ions in the principal stream that impinge on the electrode B is diminished, the reduction in the number of impacts being in the ratio $a_1/(b-c)$. There is also a reduction in the charge received by the electrode C from c to c_1, but the ratio of this reduction to the original charge $(c-c_1)/c$ is much less than the ratio $a_1/(b-c)$. The average value of $(c-c_1)/c$ as shown by the figures in Table I. is ·114, whereas the average value of $a_1/(b-c)$ is ·56.

Under these conditions it is necessary to attribute the greater part of the charge c to the ionization of the gas by the primary stream of positive ions, which is unchanged by opening the slit S.

10. In order to estimate what proportion of the charge c may be attributed to these different actions of the positive ions, let βn be the number of molecules ionized by the number n of positive ions in moving 1 centimetre through the gas. Since the electrodes B and C were 2 centimetres apart the number of electrons generated in the gas by the primary stream of positive ions is $2\beta n$. These electrons move towards the electrode C and ionize the gas so that the number that arrive at the electrode is amplified. Let $2x\beta n$ be the total number conveyed to the electrode C by this process. The positive ions generated in the gas by the electrons fall on the part of the electrode B which is opposite C, and do not pass through

to the electrode A when the slit S is opened. Similarly, let γn be the number of electrons set free from the electrode B by the impacts of the number n of positive ions, and $y\gamma n$ the number that arrive at the electrode C. The factor y is greater than x, since the electrons set free from B traverse the whole distance between C and B (which is twice the mean distance traversed by the electrons generated in the gas). The charge C is therefore made up of two parts, one proportional to β and the other proportional to γ, and may be expressed in the form:

$$c = 2x\beta(b-c)+y\gamma(b-c). \quad . \quad . \quad . \quad . \quad (1)$$

When the slit S is opened there is no change in the action of the positive ions on the molecules of the gas, but the

Table II.

p.	Z.	Z/p.	$2x\beta$.	$y\gamma$.	β/p.	γ.
·72	111	154	·152	·043	·0135	·0017
·72	132	186	·72	·09	·033	·0018
·45	84	186	·13	·023	·035	·0023
·45	103	230	·25	·062	·052	·004
·45	125	276	·74	·16	·090	·007
·25	69	276	·127	·044	·095	·0085
·25	103	412	·305	·12	·16	·015

number of positive ions in the primary stream that impinge on the electrode B is reduced in the proportion of $(b-c)$ to $(b-c-a_1)$. The charge c_1 received by the electrode C thus becomes

$$c_1 = 2x\beta(b-c)+y\gamma(b-c-a_1). \quad . \quad . \quad . \quad . \quad (2)$$

The following formulæ are thus obtained:

$$2x\beta = c/(b-c)-(c-c_1)/a_1 \quad . \quad . \quad . \quad . \quad . \quad (3)$$

and

$$y\gamma = (c-c_1)/a_1 \quad . \quad . \quad . \quad . \quad . \quad . \quad . \quad (4)$$

The values of $2x\beta$ and $y\gamma$ in the different experiments are given in Table II. The numbers give the proportions in which the two effects of the principal stream of positive ions contribute to the charge C. The figures show that about three quarters of the charge is to be attributed to the ionization of molecules of the gas by the stream

of positive ions, and one quarter to electrons set free from the electrode.

The experimental error in the determination of the charges c and c_1 is about 2 or 3 per cent., so that the probable error in the values of $(c-c_1)$ is about 20 or 30 per cent., since the difference $(c-c_1)$ is about 10 per cent. of c. There is the same probable error in the calculation of the quantity $y\gamma$.

11. The factors x and y depend principally on the ionization by the collisions of electrons with molecules of the gas, and to a lesser degree on the action of the positive ions. Since the motion of the electrons in these experiments is affected by the magnetic force, the coefficient of ionization is not exactly the same as the coefficient α determined by the early experiments where there was no magnetic force.

It is sufficient, however, for approximate calculations of x and y to take those values of α as being the coefficients of ionization in these experiments.

In the early experiments it was found that the photoelectric currents between parallel plates were given approximately by the formula $n = n_0 e^{\alpha d}$, when the potentials between the plates were less than one-half or two-thirds of the sparking potential. For a first approximation, therefore, the values of x and y in the experiments with the smaller forces at the three different pressures, given in Table I. may be calculated by the formulæ, $x = (e^{\alpha d}-1)/\alpha d$ and $y = e^{\alpha d}$. (In the experiments the values of Z/p are 276, 186, and 154, and the corresponding values of α/p are 3·1, 2·5, and 2·15.) The results thus obtained show that γ is small compared with β, and in order to calculate these coefficients from the results of the experiments with the larger forces it is necessary to take into consideration the ionization of the gas by positive ions, and to express x and y in terms of α and β. The formula for y thus becomes

$$y = (\alpha-\beta)e^{(\alpha-\beta)d}/(\alpha-\beta e^{(\alpha-\beta)d}), \quad . \quad . \quad . \quad (5)$$

as in the expression for the photoelectric currents between parallel plates.

The corresponding formula for x may be obtained from the expression for the current through a gas uniformly ionized by Röntgen rays. In this case if $n_0 d$ be the

saturation current, the currents N obtained with large forces are given by the formula

$$(N\alpha+n_0)e^{\beta d}=(N\beta+n_0)e^{\alpha d} \quad , \quad . \quad . \quad . \quad (6)$$

The factor x is the ratio $N/n_0 d$.

The expressions for x and y may be expanded in series of ascending powers of β, and for these calculations it is only necessary to consider the two principal terms of the expansions. The simplified formulæ are

$$x=(e^{\alpha d}-1)(1+\beta e^{\alpha d}/\alpha)/\alpha d \quad . \quad . \quad . \quad . \quad . \quad . \quad (7)$$

and

$$y=e^{\alpha d}(1+\beta e^{\alpha d}/\alpha). \quad . \quad . \quad . \quad . \quad . \quad . \quad . \quad (8)$$

The values of β/p and γ obtained by taking these formulæ for x and y are given in the last two columns of Table II. It is convenient to give β/p instead of β, since β/p is a function of Z/p.

The figures show that there are large increases in β/p and γ when Z/p is increased from 154 to 412.

12. It is of interest to compare the results of these experiments with the original estimates of the coefficient β which were deduced from measurements of the amplification of photoelectric currents between parallel plates by the process of ionization by collision. In most of those determinations the range of values of Z/p was the same as in disruptive discharges, where the pressure of the gas is greater than that corresponding to the minimum sparkling potential. Under these conditions the effect of ionization of the gas by positive ions was considered to be more important than the effect of the emission from the negative electrode, and in order to simplify the calculations a formula for the currents was adopted which involved the coefficients α and β.

The first values of β thus obtained have been given by curves where the ordinates are β/p and the abscissæ Z/p. In order to deduce the correct values of the coefficient of ionization of the gas by positive ions it is necessary to estimate the effect of the electrons set free from the negative electrode by the impacts of positive ions. The correction for this effect is easily determined when the coefficient γ is small of the order shown by the numbers in Table II. The increase in photoelectric currents between parallel plates due to the ionization of molecules of the gas by the collisions of electrons, and the emission

of electrons from the negative electrode by the impacts of positive ions, is given by a formula involving α and γ, which may be expressed in a series of ascending powers of γ. The terms in γ become important when $e^{\alpha d}$ is a large number, d being the distance between the plates. For a considerable range of distances it is sufficient to consider the first two terms of the series, and to take the following formula for the current

$$n = n_0 e^{\alpha d}(1+\gamma e^{\alpha d}). \quad . \quad . \quad . \quad . \quad . \quad (9)$$

The formula for the increase in the photoelectric currents between parallel plates due to the ionization of the molecules of gas by the collisions of electrons and positive ions, may be expressed in a similar manner in a series of ascending powers of β, as in equation (8).

In this case the formula for n is

$$n = n_0 e^{\alpha d}(1+\beta e^{\alpha d}/\alpha). \quad . \quad . \quad . \quad . \quad . \quad (10$$

This formula, as has already been shown more generally, is obtained from (9) by substituting β/α for γ. The formulæ show that the effect of the emission from the negative electrode is the same as if β were increased by the amount $\gamma\alpha$.

The original * values of β/p obtained for hydrogen are

·22, ·05, and ·03,

corresponding to the values of Z/p

276, 186, and 154.

These results may be compared with the values of $\beta/p+\gamma\alpha/p$ obtained from Table II., which are

·12, ·038, and ·017.

In the earlier experiments the electrodes were of zinc, and in the recent experiments they were of copper, so that the differences between the results of the two investigations are probably due to differences in the emission of electrons from the negative electrode. This may be seen from the results of various other investigations.

Thus in Warburg's † early experiments on the cathode fall of potential in hydrogen he found that with a copper electrode the cathode fall of potential was 280 volts,

* 'Electricity in Gases,' p. 331. J. S. Townsend, Phil. Mag. vol. vi. p. 607 (1903).

† E. Warburg, Wied. *Ann.* xl. p. 1 (1890).

but with a zinc electrode the cathode fall of potential was 218 volts. Also large differences were observed by Aston in the potential required to maintain currents in hydrogen between electrodes of different metals. With a negative electrode of copper a potential of 660 volts was required to maintain a current of 3·2 milliamperes per square cm. of the electrode, and with a zinc electrode a potential of 503 volts was required to maintain the same current, the pressure of the hydrogen being very nearly the same (·27 mm.) in each case *.

These experiments show that the emission of electrons from a zinc electrode caused by the impacts of hydrogen ions is greater than the emission from a copper surface caused by hydrogen ions moving with the same velocity, which may explain the difference between the values of $(\beta/p+\gamma\alpha/p)$ found in this investigation and the values of β/p found from the first investigations of the ionization of gas by positive ions.

XXVII. *Electrodeless Discharges in Uniform Fields.*

By G. D. Yarnold, *B.A., Merton College, Oxford* †.

THE theory of the uniform positive column in a direct current discharge, which was given by Townsend many years ago, and which has since been found to apply to the uniform luminous columns in electrodeless discharges in cylindrical tubes, when the electric force is parallel to the axis, has recently been applied to the case of electrodeless discharges in spherical bulbs. It is supposed that the discharge is excited by placing the bulb midway between two large parallel plates, connected to the ends of a solenoid in which continuous oscillations are induced. The theory is also extended to the case of a discharge in a cylindrical tube placed midway between the plates with its axis perpendicular to the direction of the electric force ‡.

The electrons and positive ions in the discharge move in opposite directions, their directions of motion being reversed at intervals equal to half the periodic time of the

* F. W. Aston, Proc. Roy. Soc. A, lxxxvii. p. 437 (1912).
† Communicated by Prof. J. S. Townsend, F.R.S.
‡ J. S. Townsend, Phil. Mag. xiii. p. 745 (April 1932).

oscillations of the solenoid. The effect of the displacement of the charges is to give rise to an electric force F throughout most of the space inside the bulb. This force is opposite in direction to the mean force V/d, where V is the potential difference between the plates and d is their distance apart. The electric force throughout the greater part of the gas is therefore reduced to a value Z equal to $(V/d - F)$. According to the theory, the force Z is a constant, independent of the current in the gas, provided the current is small. The force F depends on the current, however, and hence the potential V between the plates depends on the current.

The following relation has been obtained between the quantities Z and V/d,

$$Z(1+T^2I^2)^{\frac{1}{2}} = V/d,$$

which is sufficiently accurate provided the distance d between the plates is greater than three times the radius of the bulb or tube. In this equation T is a constant, and I is a quantity which is proportional to the number of electrons per cubic centimetre of the gas. The product TI is therefore proportional to the current in the gas. This formula applies to the case of a discharge in either a spherical bulb or a cylindrical tube placed midway between the plates.

It is possible to test the validity of the theory by measuring the intensity of the light emitted from the space where the force Z is constant. The intensity of the light emitted by the discharge is proportional to the number of electrons per cubic centimetre in the gas, and hence I can be measured in arbitrary units by means of a photoelectric cell.

Two series of experiments have been made. In one, observations were made on discharges in a spherical bulb containing neon at various pressures. In the other series, observations were made on discharges in cylindrical tubes which had been filled with pure helium at different pressures and sealed off for use in connexion with other work.

The usual method was adopted for the purification of the neon. After a preliminary purification by means of charcoal cooled in liquid air, the gas was left in contact with palladium black to remove hydrogen. It was then passed into the reservoir containing charcoal cooled in

liquid air, where it was kept for at least twenty-four hours before being used. The neon probably contained a small percentage of helium.

The bulb was of pyrex 9 cm. in diameter. In order to remove impurities from the walls a small quantity of pure neon was admitted, and the bulb was maintained for three or four hours at a temperature of 400° C. by means of an electric furnace. After this it was evacuated and the process repeated several times. Fresh gas was used for the experiments at each different pressure.

The cylindrical tubes containing helium were of quartz 4 cm. in diameter.

Fig. 1.

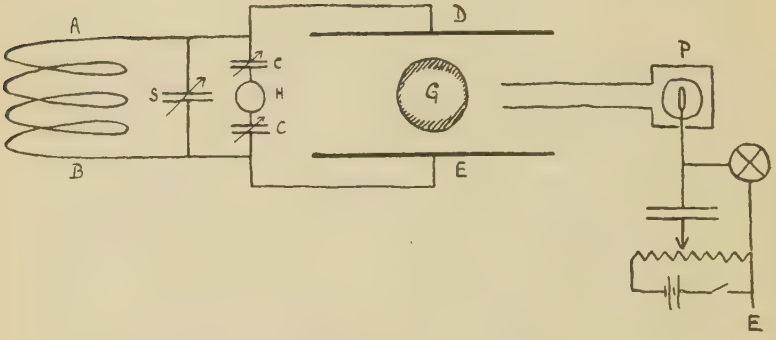

The electrical arrangements are shown in fig. 1. The coil AB was loosely coupled with a continuous-wave generator, and tuned by means of the condenser S. Its ends were connected to the two parallel plates D and E, the potential difference between them being measured, as usual, by a thermoammeter H in series with two condensers of equal capacity C. The potential was adjusted to any desired value by means of the filament rheostat of the generator and by the condenser S. The wavelength of the oscillations was 100 metres.

The parallel plates were each 30 cm. square. In the experiments on discharges in the bulb they were 15 cm. apart, and in those on discharges in the tubes 8 cm. apart.

With small currents the discharge is uniform throughout the bulb, but as the current increases the discharge becomes brighter at the edges of the bulb than in the centre, as shown by the shading in the figure. According

to the theory, the force Z is constant in the part which is uniform and is independent of the current, provided the brighter parts of the discharge do not extend far from the surface of the bulb. It is therefore necessary to exclude light from the brighter parts of the discharge from the photoelectric cell.

The photoelectric cell P was contained in an ebonite case, and the light entering it was limited by an ebonite tube which projected into the space between the plates. The photoelectric current was measured by an electrostatic balance by the usual method.

Fig. 2.

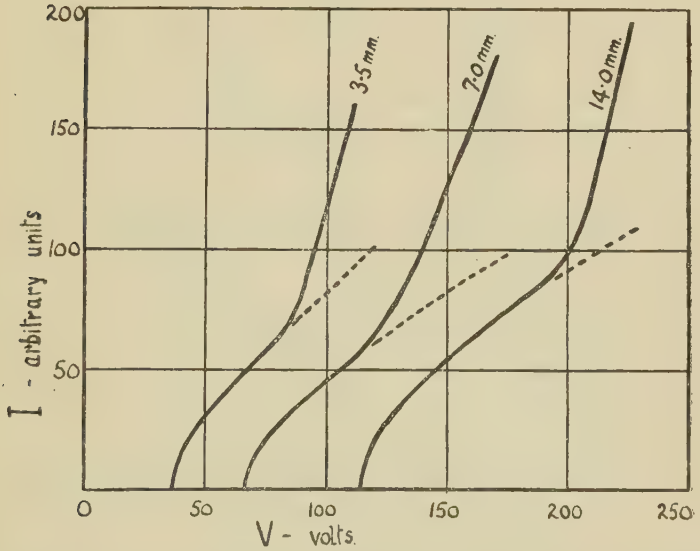

The values obtained for I in arbitrary units corresponding to different potentials V are shown in Table I. for the experiments on neon discharges in the bulb, and in Table II. for the experiments on helium discharges in the tubes. The values of V are root mean square values expressed in volts.

The results are shown graphically in figs. 2 and 3, where the ordinates are proportional to I and the abscissæ to V. Fig. 2 relates to the results in Table I. and fig. 3 to those in Table II. The curves corresponding to two of the pressures in neon are omitted to avoid confusing

the figure. The continuous curves represent the results of the experiments. The dotted curves represent the relation between I and V given by the formula

$$Z(1+T^2I^2)^{\frac{1}{2}}=V/d,$$

when the force Z and the constant T^2 have the values given in the tables.

The dotted curves coincide with the continuous curves for the lower values of V. Thus the experiments are in good agreement with the theory for the smaller currents.

Fig. 3.

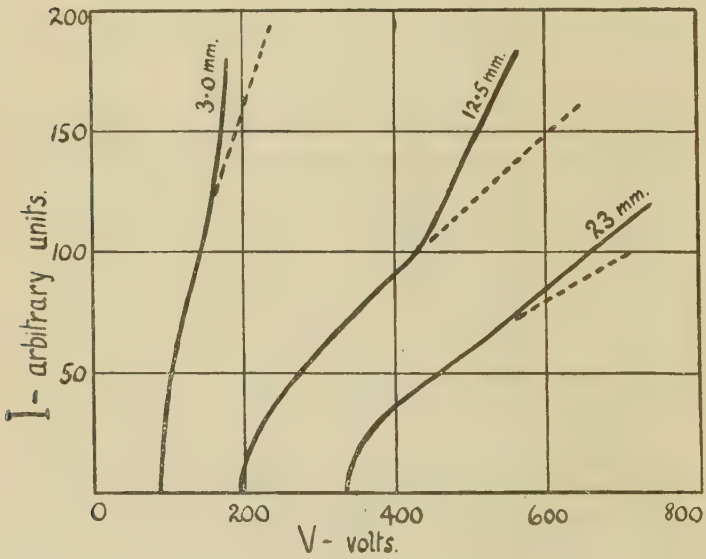

When the current becomes large, however, I increases more rapidly with the potential V than the theory indicates.

With large values of V the space where the force is not uniform extends towards the centre of the bulb, and it is impossible to exclude light from these parts from the photoelectric cell. It is probable that the large values found for I when the potential V is great are partly due to the fact that the photoelectric cell receives light from the brighter parts of the discharge.

It will be observed that the ratio Z/p diminishes as the pressure increases. Thus with the pressure of 20·5 mm. of neon the value of Z/p is 0·51, and with the pressure

of 3 mm. the value of Z/p is 0·69. Since the rate at which electrons are generated increases rapidly with Z/p, the experiments show that at the higher pressures the supply of electrons by the ionization of the gas is less than at the lower pressures. This is in accordance with the theory, since the loss of electrons by diffusion to the sides, which is less at the higher pressures, must be balanced by the ionization of the gas.

TABLE I.

Neon Discharges in Bulb.

1·13 mm.		3·5 mm.		7·0 mm.		14·0 mm.		20·5 mm.	
$Z=1·53$. $T^2=3·33\times10^{-3}$.		$Z=2·4$. $T^2=9·61\times10^{-4}$.		$Z=4·4$. $T^2=6·17\times10^{-4}$.		$Z=7·6$. $T^2=2·48\times10^{-4}$.		$Z=10·4$. $T^2=1·28\times10^{-4}$.	
V.	I.	V.	I.	V.	I.	V.	I.	V.	I.
23	0	36	0	66	0	114	0	156	0
32	17	41	18	73	19	120	22	162	26
43	28	46	27	82	30	141	47	171	42
53	36	54	35	90	37	153	56	180	56
64	48	65	48	100	47	165	65	195	68
75	62	76	59	114	58	183	78	213	80
85	81	89	80	124	72	195	90	228	96
93	98	99	116	138	100	210	122	240	120
98	118	108	150	148	120	225	164	249	148
107	156	114	196	166	168	237	198	264	188

The same result also appears in the experiments with helium, since the value of Z/p is 1·8 when the pressure is 23 mm., and 3·6 when the pressure is 3 mm.

Similar results have also been obtained in the experiments in which the electric force is parallel to the axis of the tube, both for the positive columns of direct current discharges and for the uniform columns of high frequency discharges *.

* J. S. Townsend and W. Nethercot, Phil. Mag. vii. p. 600 (March 1929); P. Johnson, Phil. Mag. x. p. 921 (Nov. 1930); F. Llewellyn Jones, Phil. Mag. xi. p. 163 (Jan. 1931).

The force Z in the helium discharges in the tubes is greater in each case than the force in a discharge excited with sleeves in the same tube. This result is in agreement with the experiments of Gill and Donaldson, which showed that the potential necessary to maintain a discharge

TABLE II.

Helium Discharges in Tubes.

3·0 mm.		12·5 mm.		23·0 mm.	
$Z=10{\cdot}8$. $T^2=1{\cdot}73\times10^{-4}$.		$Z=24{\cdot}4$. $T^2=3{\cdot}87\times10^{-4}$.		$Z=41{\cdot}0$. $T^2=3{\cdot}59\times10^{-4}$.	
V.	I.	V.	I.	V.	I.
86	0	195	0	330	0
96	38	213	23	348	16
114	59	252	39	366	25
132	91	294	58	390	33
147	108	336	70	420	41
165	139	360	81	450	48
186	175	408	94	516	64
		450	108	582	80
		486	136	660	100
		558	180	747	122

in a tube depends on the inclination of the axis of the tube to the direction of the electric force *.

In conclusion, I should like to thank Professor Townsend for his advice and criticism throughout this work.

* E. W. B. Gill and R. H. Donaldson, Phil. Mag. xii. p. 719 (Sept. 1931).

XXVIII. *The Thermal Conductivity of Air. By* H. S. Gregory, *Ph.D., A.R.C.S., D.I.C., Assistant Professor of Physics, and* C. T. Archer, *M.Sc., A.R.C.S., D.I.C., Lecturer in Physics* *.

THE recent determinations of the thermal conductivities of the rare gases—helium, argon, neon, krypton, and zenon—which have been carried out by Curie and Lepape, and an account of which has been published in the *Journal de Physique* [1], are specially related to the previous work of the authors of the present paper on the "Thermal Conductivity of Air" published in 1926 [2].

The cooling thermometer method was adopted by Curie and Lepape, but was modified so that the final values of the conductivities were dependent on a predetermined value of the conductivity of air. For this purpose they chose the value obtained by the authors as mentioned above, viz., 583×10^{-7} cal. cm.$^{-1}$ sec.$^{-1}$ deg.$^{-1}$ at 0° C.

In view of this the authors feel that it is necessary to give further evidence in support of their original work, and at the same time to reply to the criticism of their work by Hercus and Laby [3].

Since the publication of their original paper much work has been done at the Imperial College of Science and Technology by the authors and by others using similar methods. In every case the results obtained have tended to confirm the authors' original findings in respect to air. It is of interest to note also that Weber [4] repeated his determinations, with the result that he obtained the value 574×10^{-7} at 0° C., as compared with the value 568×10^{-7} found in his original work [5]. This later work was carried out by Weber after Schneider [6] had obtained the value 590×10^{-7}, using Weber's methods.

The cooling thermometer method used recently by Curie and Lepape [1] is more susceptible of application to comparative observations than to absolute determinations, but nevertheless a high standard of accuracy was attained in its use in the investigations of Müller [7] whose work, in the authors' opinion, compares very

* Communicated by the Authors.

favourably in accuracy with the more recent investigations of Weber [5], Schneider [6], and others. It seems limited as compared with modern experiment in that mercurial thermometry was employed, but the conditions of pressure and dimensions were varied to an elaborate extent, and the method can be commended from the point of view of the excellent manner in which the convective losses, radiation, and thermometer stem losses were allowed for. The procedure in Müller's work was in some respects parallel with the original procedure of the authors using the hot-wire method. The method has yielded surprisingly consistent results amongst the various observers, the average results being in very close agreement with those obtained by the hot-wire method. It is of interest to note that Smoluchowski [8] made use of this method in his early experiments on the temperature drop correction.

The most important sources of error inherent in the hot-wire method are the complicated effects of convection and temperature drop, the latter of which is closely bound up with the effect of accommodation. With regard to the former no theoretical basis for the calculation of the effects of convection has yet been put forward, though it is generally accepted that with suitable design of apparatus in conjunction with observations at low pressures the effect is negligibly small. At the same time the temperature drop effect increases as the pressure is decreased, and for this reason it becomes difficult to decide at what pressure the two effects can be separated. If it is accepted that convection is minimized at low pressures, it remains only to settle the temperature drop correction.

During the past two years Dr. Gregory has been engaged in developing a modification of the authors' original procedure in an investigation of the effect of temperature on the thermal conductivity of hydrogen over a wide range of temperatures. In this work it has been found possible to eliminate the two effects of convection and temperature drop from the heat conduction. A brief treatment of the method is given here :—

Kundt and Warburg [9], who made the first theoretical and practical investigation of the slip effect in the viscous flow of gases, predicted a corresponding effect at the surface of a heated solid in contact with a gas. They

defined the discontinuity of temperature in such a case by the relation

$$\Delta\theta = -\gamma \frac{d\theta}{dn},$$

in which n represents the normal to the surface of the solid and θ the temperature of the surface. They established experimentally that γ was directly proportional to the mean free path of the gas.

Smoluchowski [8] verified their predictions experimentally, using the cooling thermometer method, and made determinations of the temperature drop. For air and hydrogen he obtained values of γ equal to $6{\cdot}96\,\lambda$ and $1{\cdot}70\,\lambda$ respectively, λ being the mean free path.

Smoluchowski [10] also investigated the effect of temperature drop from a theoretical aspect, basing his calculations on the kinetic theory of gases as developed by Clausius, and deduced a formula, afterwards modified by Weber [5], to include the accommodation constant a as defined by Knudsen [12],

$$\gamma = \lambda\left\{0{\cdot}70 + \frac{4(1-a)}{3a}\right\}.$$

In a more recent calculation of γ, Smoluchowski [11] made use of Maxwell's hypothesis that molecules may be regarded as centres of forces of repulsion, the forces varying inversely as the fifth power of the distance. This leads to the relation

$$\gamma = \lambda\left\{\frac{15}{2\pi} \cdot \frac{2-a}{2a}\right\}.$$

Hence

$$\Delta\theta = -\lambda\left\{\frac{15}{2\pi} \cdot \frac{2-a}{2a} \cdot \frac{d\theta}{dn}\right\}.$$

Applying this relation to the cylindrical distribution of temperature as used in the authors' experiments, we have for the Fourier's equation modified by such considerations

$$Q = \frac{2\pi K l \theta}{\log_e \frac{r_2}{r_1} + \frac{\beta}{P}\left(\frac{1}{r_1} + \frac{1}{r_2}\right)}, \quad . \quad . \quad . \quad (1)$$

where P represents the pressure of the gas, r_1 and r_2 the radii of the wire and inner surface of the glass tube respectively, and β a constant given by

$$\beta = \lambda_0 \left\{ \frac{15}{2\pi} \cdot \frac{2-a}{2a} \right\}, \quad \text{where} \quad \lambda = \frac{\lambda_0}{P}.$$

Equation (1) can be written in the form

$$\frac{1}{Q} = \frac{\log_e \frac{r_2}{r_1}}{2\pi K l \theta} + \frac{\beta \left(\frac{1}{r_1} + \frac{1}{r_2} \right)}{P \cdot 2\pi K l \theta}$$

$$= \frac{1}{Q_0} + \frac{\beta}{P \cdot 2\pi K l \theta} \left(\frac{1}{r_2} + \frac{1}{r_1} \right). \quad . \quad . \quad (2)$$

Hence, if θ is kept constant and P is varied, a linear relation exists between $\frac{1}{Q}$ and $\frac{1}{P}$. The intercept of the line gives the quantity $\frac{\log_e \frac{r_2}{r_1}}{2\pi K l \theta}$, from which K, the thermal conductivity is known, and the slope is a measure of the quantity β, from which the accommodation constant a can be calculated.

During the past two years also Mr. Archer has been engaged in a precise investigation of the convection losses associated with the hot-wire method and their dependence on the conditions of pressure, temperature, and dimensions of apparatus. The results of this work have been expressed as a series of characteristic isothermals for various gases, and show that with tubes of large dimensions the temperature drop effect and the convection effect overlap to a marked extent. The results show definitely that the choice of a suitable dimension of tube is a very important factor in the use of the hot-wire method for the measurement of the thermal conductivities of gases.

One of the most important modifications imposed on the hot-wire method by the authors is related to the ease with which the temperature of the wire can be adjusted to constancy of value while the pressure of the surrounding gas is varied through a range of values. It must be emphasized that such an adjustment is even more sus-

ceptible of accuracy than the calculation of the temperature of the wire corresponding to each pressure, which was necessary in the work of other observers using this method. The calculated value of the temperature of the wire in the authors' work has an accuracy of about 0·01° C., while the accuracy to which its constancy can be adjusted is in the neighbourhood of 0·0001° C. The variation with pressure of the heat transmission at constant temperature can be followed and examined with great ease and precision, since such variation is expressed in terms of the varying current only. With respect to the radiation correction, the hot-wire method is distinctly better than other methods, since the small dimensions of the wire make such losses almost negligible in comparison with the total heat loss.

Apart from the earlier experiments of Stafford [13], it would seem that the hot-wire method is the most consistent, not only amongst the various investigators who have used the method, but also from the fact that for any particular conditions a result can be repeated to an accuracy of one part in 2000.

The plate method, which was first used by Todd [14] and later modified very considerably by Hercus and Laby [15], gave values for air at 0° C. of 494×10^{-7} and 540×10^{-7} respectively, a discrepancy of about 9 per cent., and the authors consider that much more research and modification is necessary before such a method can be considered as giving results acceptable as standard. The plate method has nothing to commend it in comparison with the hot-wire method as regards accuracy of temperature determination. The convective losses can be regarded as non-existent, and the temperature drop effect as well, but the method is less accurate with respect to the correction for radiation, while the correct procedure of varying the pressure at constant temperature would involve many serious complications.

Equation (2) above has been applied to a re-examination of the authors' original results [2], along with results which have been obtained with other systems of tubes of different dimensions.

The accompanying figure indicates the graphs drawn by adopting this procedure in the case of the original work. N and W refer to narrow and wide systems respectively.

From these, and from similar graphs obtained by using the results of later experimental work, the values of the accommodation coefficient for platinum-air have been calculated. The mean value of this coefficient thus obtained is found to be 0·80, which is in good agreement with the values obtained by other observers, especially

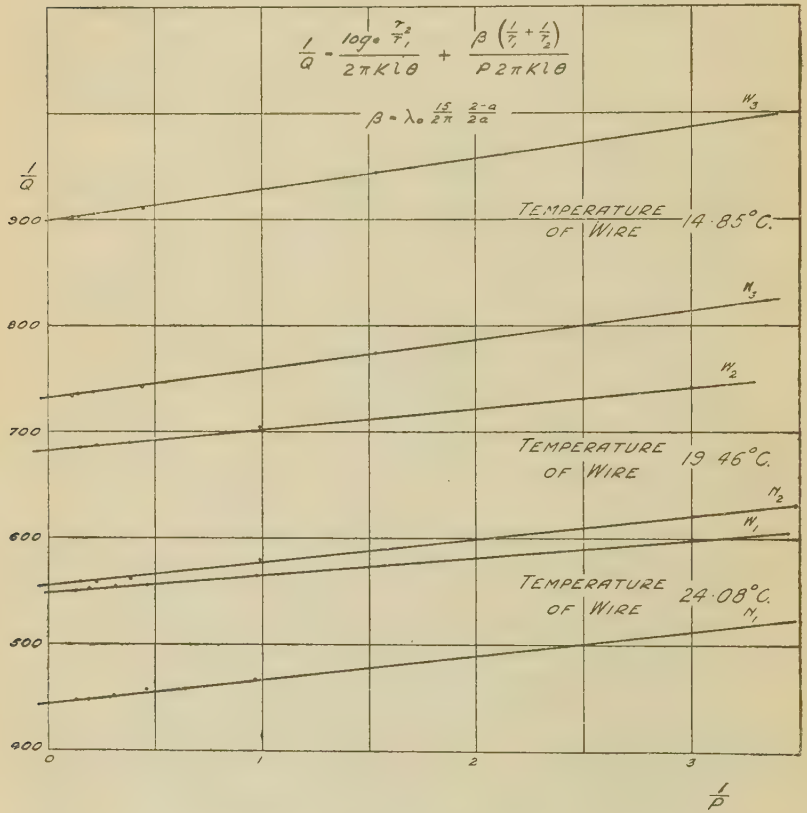

in view of the fact that in the case of the original apparatus the temperature drop effect was small on account of the larger radius of the emitting wire, viz., 0·007696 cm., as compared with 0·00506 cm. in the other apparatus. Also, the values of the thermal conductivity of air have been redetermined from these graphs, and the average of the values from the three sets of tubes has been found to be 585×10^{-7} at 0° C.

The dimensions of the apparatus are shown in the following table :—

	1.	2.	3.	
Radius of platinum wire ..	0·007696	0·0050655	0·0050596	cm.
Internal radius, narrow tube.	0·4592	0·5831	0·5874	„
External „ „ „	0·5215	0·6346	0·6439	„
Internal radius, wide tube .	1·1714	1·4033	1·4020	„
External „ „ „	1·2360	1·4925	1·4560	„

Column 1 refers to the apparatus used by the authors in their original work, while columns 2 and 3 refer to apparatus used by the authors and others in a continuation of the work on thermal conduction in gases.

The paper of Hercus and Laby [3] referred to above criticized the authors' investigation very pointedly on the question of their failure to apply a correction for the temperature drop and accommodation effect. The authors would like to point out that at the time of publication of their work they were unwilling to consider the application of a correction based on the theoretical considerations of the kinetic theory of gases to purely experimental results, because such corrections in the case of the apparatus they employed—the emitting wire being of comparatively large diameter—would have been of the order of 0·33 per cent., which was the limit of accuracy of their determinations. In the present paper the method of allowing for the temperature drop and accommodation correction is purely an experimental one, the effects being eliminated experimentally from the heat conduction.

The paper states also that the authors' value of the thermal conductivity of air at 0° C. requires explanation on the grounds that it is too high. It might be pointed out that many investigators using the hot-wire method and the cooling thermometer method have obtained similar high values, and, indeed, such high values seem to be the case rather than otherwise.

The value quoted by Professor Laby and Miss Nelson in the International Critical Tables is 533×10^{-7}, this being given as the " weighted " mean of nineteen observations. In obtaining this mean the greatest weight is

given to the values obtained by the plate method, although they differ amongst themselves by about 9 per cent., and these are weighted ten times as heavily as corresponding results of the same order obtained by the cooling thermometer method. In the authors' opinion many of these nineteen observations should not be included in the calculation of an average if due regard is to be paid to modern experimental accuracy. A more satisfactory method of arriving at a standard value would appear to be to consider only observations made during the last twenty years. If this is done, and equal weight is given to each result, a mean value of 571×10^{-7} is obtained. At the same time the hot-wire method, especially in recent years, has certainly given the most consistent results, which range from 568×10^{-7} to 590×10^{-7}, and give an average value of 579×10^{-7}.

In the paper referred to above, Curie and Lepape [1], using the best available data for the viscosity and the specific heat at constant volume, have determined the value of the ratio $\frac{K_0}{\eta_0 C_v}$ for each of the monatomic gases helium, argon, neon, krypton, and zenon in terms of the authors' value of K at 0° C., viz., 583×10^{-7}. The average value of this ratio thus obtained was 2·52. If, however, the mean value of K_0 quoted in the International Critical Tables is used in the same manner the average value of the ratio obtained is 2·31, which is not in accordance with the predictions of the kinetic theory of gases. In view of this, together with the re-examination of the original findings with respect to air at 0° C., the more recent work eliminating the temperature drop and the convection effects, and giving an average value of 585×10^{-7} — within 0·33 per cent. of the original value,—the authors consider that their original procedure for the elimination of convection losses has been amply substantiated.

References.

(1) Curie and Lepape, *Journ. de Phys.* 2 (7), xii. p. 392 (1931).
(2) Gregory and Archer, Proc. Roy. Soc. A, cx. p. 91 (1926).
(3) Hercus and Laby, Phil. Mag. (7) iii. p. 1061 (1927).
(4) Weber, S., *Ann. d. Phys.* iv. 82, p. 479 (1927).
(5) Weber, S., *Ann. d. Phys.* liv. 21, p. 325 (1917).
(6) Schneider, *Ann. d. Phys.* lxxix. p. 177 (1926).
(7) Müller, Wied. *Ann.* lx. p. 82 (1897).

(8) Smoluchowski, Phil. Mag. xlvi. p. 192 (1898).
(9) Kundt and Warburg, Pogg. *Ann.* clvi. p. 177 (1875).
(10) Smoluchowski, *Akad. Wiss. Wien*, cvii. p. 306 (1898).
(11) Smoluchowski, *Akad. Wiss. Wien.* cviii. p. 5 (1899).
12) Knudsen, *Ann. d. Phys.* xi. p. 102 (1900).
(13) Stafford, *Zeit. Phys. Chem.* lxxvii. p. 66 (1911).
(14) Todd, Proc. Roy. Soc. A, lxxxiii. p. 19 (1909).
(15) Hercus and Laby, Proc. Roy. Soc. A, xcv. p. 190 (1919).

Royal College of Science,
South Kensington,
London, S.W. 7.

XXIX. *Transmission of Sound Through Partitions.* By A. H. Davis, *D.Sc., Physics Department, National Physical Laboratory, Teddington, Middlesex* *.

THIS paper considers a number of experimental results for the transmission of sound through simple solid panels (ranging from a sheet of paper to a brick wall) and indicates the extent to which it is possible to calculate the order of the transmission to be expected, and the general manner of its variation with the frequency of the test note, and with the weight of the panel.

The experimental figures used in the work are those given in fig. 1. They were obtained at the National Physical Laboratory † in tests in which panels of various materials covered an aperture about 5 ft. × 4 ft. in size between two soundproof rooms. In one of the rooms sound was directed towards the test partition, and in the other room measurements were made of the fraction transmitted. From the results it should be noted that high frequency notes are easier to exclude than low, but some cause—possibly resonance, modifies results at particular frequencies. When the results are averaged for sounds of different pitch, it is found that the average reduction factor for a given panel is determined largely by the weight of the panel (fig. 2).

Transmission of Sound through a Rigid Homogeneous Panel.

In connexion with the theory of the transmission of sound through homogeneous panels, it is to be noted

* Communicated by the Author.
† A. H. Davis and T. S. Littler, Phil. Mag. vol. vii. p. 1050 (1929).

Fig. 1.

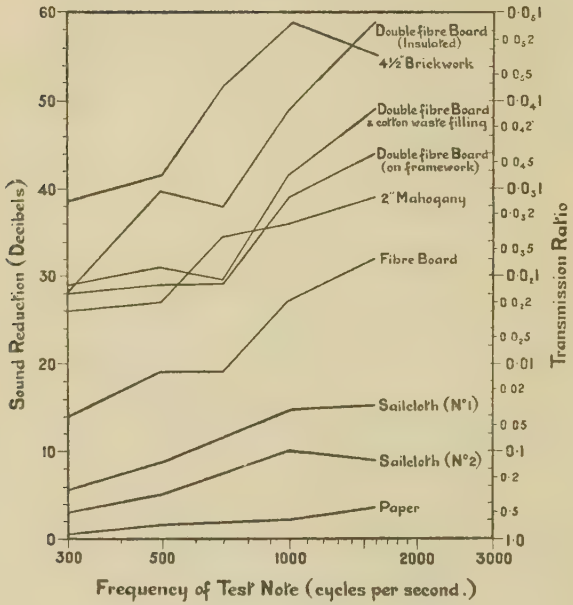

Sound transmission through partitions.

Fig. 2.

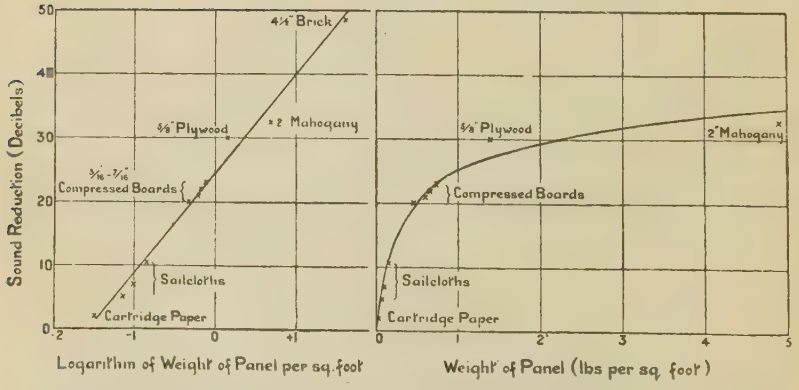

Transmission of sound through single partitions. Relation between reduction of sound (averaged over a series of frequencies) and weight of panel.

that Rayleigh calculated the reflexion of plane waves from an infinite thin plate separating two media. His formula ('Theory of Sound,' 2nd edit. vol. ii. p. 88, 1896) shows that the fraction of incident sound energy reflected in air from a rigid non-absorbent material is given by

$$\left(\frac{R_1}{R_2}-\frac{R_2}{R_1}\right)^2 \Big/ \left\{ 4\cot^2\left(\frac{2\pi l}{\lambda}\right)+\left(\frac{R_1}{R_2}+\frac{R_2}{R_1}\right)^2 \right\},$$

where l is the thickness of the plate, λ the wave-length of sound in the plate, and R_1 and R_2 are respectively the radiation resistances ($\rho_1 V_1$ and $\rho_2 V_2$) of the air and of the material of the plate. Assuming that there is no absorption of sound in the plate the remainder is transmitted and may be shown to be

$$\frac{4+4\cot^2\left(\frac{2\pi l}{\lambda}\right)}{\left(\frac{R_1}{R_2}+\frac{R_2}{R_1}\right)^2+4\cot^2\left(\frac{2\pi l}{\lambda}\right)}.$$

The reciprocal of this is the sound reduction factor for the plate and may be written

$$1+\frac{1}{4}\left(\frac{R_1}{R_2}-\frac{R_2}{R_1}\right)^2 \sin^2\left(\frac{2\pi l}{\lambda}\right).$$

When $2\pi l/\lambda$ is small we may write $4\pi^2 l^2/\lambda^2$ for $\sin^2\left(\frac{2\pi l}{\lambda}\right)$. If, further, R_2 is large compared with R_1, as it is when R_2 relates to a solid and R_1 to air, we have

$$\text{Reduction factor} = 1+\frac{\pi^2 l^2 . {R_2}^2}{\lambda^2 {R_1}^2} \text{ approx.},$$

which yields when rewritten,

$$1+\frac{\omega^2 m^2}{4{R_1}^2},$$

when $m(=\rho_2 l)$ is the mass per unit area of the plate.

On this basis calculation has been made of the transmission of sound through thin panels having weights per unit area * corresponding to those of the paper, sailcloth No. 2, fibre board, 2 in. mahogany, and a $4\frac{1}{2}$ in.

* It is convenient to note that a weight of 2·05 lbs. per sq. ft. = 1 gm. per sq. cm.

brick panel. Owing to the enormous range of reduction factors involved it has been desirable to express results logarithmically, and the reduction is given in decibels, having been calculated from the relation :

$$\text{Reduction in decibels} = 10 \log_{10} (\text{reduction factor}).$$

TABLE I.

Transmission of Sound through Homogeneous Panels. (Comparison of experimental results with calculated values.) N.B.—R_1 (air) = 41 $\therefore 4 R_1^2 = 6700$.

Panel.		Pulsatance of sound.	Calculated reduction factor,	Reduction factor in decibels.	
Type.	Weight,	ω.	$1+(\omega^2 m^2/6700)$.	Calculated.	Observed.
	gm./cm.²				
Paper	0·015	1880	1·1	0·8	0·5
		6280	2·3	4	2
		10000	4·4	6	4
Sailcloth	0·044	1880	2·0	3	3
		6280	12	11	10
		10000	30	15	9
Fibre board	0·32	1880	54	17	14
		6280	600	28	27
		10000	1500	32	32
Mahogany 2 in. ..	2·4	1880	3000	35	26
		6280	34000	45	36
		10000	86000	49	39
Brick wall	20	1880	210000	53	38
		6280	2400000	64	59
		10000	6000000	68	55

Results are given in Table I., together with experimental values obtained by Davis and Littler for oblique transmission through panels of finite size—5 ft. × 4 ft.

Clearly the order of the result of calculation is in agreement with experiment for the lighter partitions of paper, sailcloth, and $\frac{1}{2}$ in. fibre board, not only as regards the general trend of the variation of the reduction factor with frequency, but in absolute magnitude as well. On the other hand, however, the heavier mahogany board and brick panels transmit some ten times as much sound as the above considerations would suggest, the

observed reduction being some 10 decibels less than the calculated.

It is possibly to be inferred that the latter panels are resonant in the manner of a drum membrane and that, through this resonance, they transmit more sound than otherwise would be the case. It remains therefore to modify the formulæ to take account of any drumlike resonance.

Transmission of Sound by a Thin Massive Partition, under Elastic Restraint.

In the transmission of sound through rigid partitions the mechanism is presumably as follows :—The sound falls upon the first face of the partition and is there partly reflected and partly transmitted in accordance with the laws of refraction of sound at a surface of separation between two media. The transmitted sound then proceeds to the second face, where further refraction takes place. When the wall is thin compared with the wave-length of the sound the actual wave-transmission of sound through the wall is not of great importance, and it is possible to regard the partition as an infinitely thin massive membrane. Indeed, in the approximate formulæ given above for the case of a thin panel, it is seen to be the total mass that is important, for the density, thickness, and acoustical resistance have disappeared from the equation.

This applies to the case of plane waves falling upon an infinite non-resonant partition. In practice, however, the partition is clamped at the edges, and may vibrate as a whole in the manner of the diaphragm of a drum, and may have a series of natural frequencies. In deriving equations to cover the transmission of sound through panels of this type it is assumed below that the panel is an infinite one, but that it can vibrate as a whole under the action of elastic restraints.

Let an infinite diaphragm of mass m per unit area, be located in the plane $x = 0$. Let a sound wave $\dot{\xi}_1 = \dot{\xi}_{01} e^{i\omega\left(t + \frac{x}{c_1}\right)}$ be incident normally upon the diaphragm from the medium to the left of the origin, where ξ_1 represents particle displacement at a time t in the plane $x = x$, c_1 being the velocity of sound in the

medium. Under the action of this sound the plate will be displaced and will move in a manner represented by $\dot{\xi}_2 = \dot{\xi}_{02}\, e^{i\omega t}$. There will also be a transmitted wave sent out into the air from the other side of the diaphragm, and a reflected wave * sent back towards the sending region.

The following equations therefore represent the conditions.

In the first medium

$$\dot{\xi}_1 = \dot{\xi}_{01}\, e^{i\omega\left(t-\frac{x}{c_1}\right)} + \dot{\xi}_{01}'\, e^{i\omega\left(t+\frac{x}{c_1}\right)},$$

the second term representing the reflected wave,

For the partition

$$\xi_2 = \dot{\xi}_{02}\, e^{i\omega t}.$$

For the wave transmitted on the other side of the partition

$$\dot{\xi}_3 = \dot{\xi}_{03}\, e^{i\omega\left(t-\frac{x}{c}\right)}.$$

At the boundary between the first medium and the panel, velocity must be continuous, and we have

$$\dot{\xi}_{01} + \dot{\xi}_{01}' = \dot{\xi}_{02};$$

similarly, considering the second medium,

$$\dot{\xi}_{03} = \dot{\xi}_{02}.$$

The pressure variations causing the motion of the panel, arise from the sum of the effects of the pressure variations associated with the incident, reflected and transmitted waves. The total force on unit area of the plate may be written

$$\delta p_{01} + \delta p_{01}' - \delta p_{03},\ i.e.,\ \rho c(\dot{\xi}_{01} - \dot{\xi}_{01}' - \dot{\xi}_{03})\, e^{i\omega t},$$

since $\delta p = \pm c\rho\dot{\xi}$. Particular attention has been paid to the sign of c, which depends upon the direction of propagation. It is convenient to write R for $c\rho$, and we thus arrive at the following equation to represent the motion of the panel

$$m\ddot{\xi}_2 + r\dot{\xi}_2 + S\xi_2 = R\,(\dot{\xi}_{01} - \dot{\xi}_{01}' - \dot{\xi}_{03})\, e^{i\omega t},$$

where S defines the elastic restraint of the panel and r the dissipative resistance.

* This arises from the fact that the solutions of the equation $\frac{\delta^2\theta}{\delta t^2} = C\,\frac{\delta^2\theta}{\delta x^2}$ must be of the type $\theta = A.f(ct-x) + B.F(ct+x)$.

This may be rewritten, when the relations between $\dot{\xi}_{01}$, $\dot{\xi}_{01}'$, and $\dot{\xi}_{03}$ are considered,

$$m\ddot{\xi}_2+(r+2\mathrm{R})\,\dot{\xi}_2+\mathrm{S}\xi_2=2\mathrm{R}\dot{\xi}_{01}\,e^{i\omega t}.$$

Solving this gives

$$\dot{\xi}_2=\frac{2\mathrm{R}\dot{\xi}_{01}\,e^{i\omega t}}{\mathrm{Z}}=\xi_{02}\,e^{i\omega t},$$

where

$$\mathrm{Z}=(r+2\mathrm{R})+i\left(m\omega-\frac{s}{\omega}\right)$$

i. e.,

$$\mathrm{Z}^2=(r+2\mathrm{R})^2+\left(m-\frac{s}{\omega}\right)^2.$$

The energy transmission coefficient for the panel is given by $\left(\frac{\dot{\xi}_{03}}{\dot{\xi}_{01}}\right)^2$, and its reciprocal, the reduction factor as ordinarily defined, becomes

$$\left(\frac{\dot{\xi}_{01}}{\dot{\xi}_{03}}\right)^2=\left(\frac{\dot{\xi}_{01}}{\dot{\xi}_{02}}\right)^2=\frac{\mathrm{Z}^2}{4\mathrm{R}^2}$$

$$=\frac{(r+2\mathrm{R})^2+\left(m\omega-\frac{s}{\omega}\right)^2}{4\mathrm{R}^2}.$$

The expression for the reduction factor may be put in another form by writing ω_0 for the natural pulsatance $\sqrt{\frac{s}{m}}$ of the panel, and becomes

$$\frac{(r+2\mathrm{R})^2+m^2\omega^2(1-\omega^2{}_0/\omega^2)^2}{4\mathrm{R}^2}.$$

When there is no appreciable dissipation in the panel itself r may be neglected and the reduction factor becomes

$$1+\frac{(m\omega-s/\omega)^2}{4\mathrm{R}^2}=1+\frac{m^2\omega^2(1-\omega_0{}^2/\omega^2)^2}{4\mathrm{R}^2}.$$

This reduces to the form given earlier for a thin unconstrained panel when s is put equal to 0, or when ω_0 is small compared with ω. Also it should be noted that the effect of a resonance at frequency determined

by ω_0 is to reduce the reduction factor below what it would be if resonance did not occur. The new formulæ are thus consistent with the observed fact that the sound reduction factors of a brick wall or of a mahogany board fall below those calculable by Rayleigh's formula. When, however, calculation is made of the values to be attributed to ω_0 to account for the observed reduction factors for these partitions at various frequencies, it is necessary to assign some value to the damping r. Assuming it to be negligible in comparison with $m\omega$—a reasonable assumption,—it appears that a single resonance will not suffice to reconcile theory with experiment at all test frequencies. The inference is that each partition as tested has several resonant frequencies, a conclusion which is consistent with the well-known fact that a clamped elastic plate has several modes of vibration, and with observations of the resonance of actual panels (Davis and Littler, *loc. cit.* p. 1052).

Summary.

It would appear that Rayleigh's formula is generally applicable to the transmission of sound through light thin panels such as paper, sailcloth, or fibre board. The preponderating effect of mass is evident from the equation, together with a tendency for the reduction factor to vary as the square of the frequency of the incident sound. With materials as light as paper a term due to air damping is important, and less variation with frequency occurs. For heavy panels such as 2 in. boards or brick walls, the reduction factor falls short of that calculable from Rayleigh's formula. A new equation has been derived to allow for resonance of panels, and it indicates that resonances can account for reduced insulating value. When the equation is applied to actual panels, however, it appears that no single resonance will reconcile theory with experiment. It is necessary to consider that each panel may have several modes of resonance—a fact consistent with the general theory of the vibration of plates, and with experiment (see Davis and Littler, *loc. cit.* p. 1052).

XXX. *The Vibrations of a Chladni Plate.* *By* Robert Cameron Colwell, *Ph.D., Professor of Physics, West Virginia University* *.

[Plate VIII.]

THE differential equation of motion of a square plate with free edges is given by Rayleigh † in the form

$$(\nabla^4 - k^4)w = 0 \quad . \quad . \quad . \quad . \quad . \quad . \quad (1)$$

This may be written

$$\left\{\frac{\partial^2 w}{\partial x^2} + \frac{\partial^2 w}{\partial y^2} - k^2 w\right\}\left\{\frac{\partial^2 w}{\partial x^2} + \frac{\partial^2 w}{\partial y^2} + k^2 w\right\} = 0. \quad . \quad (2)$$

The boundary conditions are

$$\frac{\partial^2 w}{\partial x^2} + \mu \frac{\partial^2 w}{\partial y^2} = 0, \quad . \quad . \quad . \quad (3)$$

$$\frac{\partial}{\partial x}\left\{\frac{\partial^2 w}{\partial x^2} + (2-\mu)\frac{\partial^2 w}{\partial y^2}\right\} = 0, \quad . \quad . \quad . \quad (4)$$

for the edges parallel to the y axis with two others for the edges parallel to the x axis obtained from (3) and (4) by the interchange of x and y. At the corners of the square

$$\frac{\partial^2 w}{\partial x\, \partial y} = 0 \ddagger.$$

No general solution of these equations has ever been given, but Ritz § has shown that the figures of a square plate found by experiment will be satisfied to within one or two per cent. by a series in the form

$$w = \Sigma \alpha_{mn} u'_m(x) v'_n(y), \quad . \quad . \quad . \quad . \quad . \quad (5)$$

in which $u'_m(x)$ and $v'_n(y)$ are the normal functions of the vibration of a bar with free ends. The differential equation of such a bar is

$$\frac{d^4 u}{dx^4} = k^4(u), \quad . \quad . \quad . \quad . \quad . \quad . \quad (6)$$

* Communicated by the Author.
† Rayleigh, 'Sound,' i. pp. 359 and 371.
‡ Lamb, Lond. Math. Proc. xxi. p. 70 (1890).
§ Ritz, *Ann. der Phys.* xxviii. p. 737 (1909).

with the boundary conditions at each end

$$\left(\frac{d^2u}{dx^2}\right)_{\substack{x=o\\x=a}}=0, \qquad \left(\frac{d^3u}{dx^3}\right)_{\substack{x=o\\x=a}}=0, \quad . \quad . \quad . \quad (7)$$

in which a is the length of the rod

Ritz finds the coefficient α_{mn} in equation (5) by assuming that the wave form set up in the rod can be determined by the principle of least action. This would be entirely true if the plate were vibrating freely. In this paper it is assumed that the vibrations set up in a plate by a valve oscillator are not strictly speaking free, but are to some extent controlled by the device which excites them. Thus if the vacuum tube oscillator gives out a pure note, it is reasonable to suppose that the plate vibrates in unison with this single pure tone. A further justification for this assumption is found in the paper by Ritz *, in which he takes only two terms of equation (5) for all the higher vibrations. Equation (5) is thus reduced from a polynomial to the binomial

$$w=\mathrm{A}u'_m(x)v'_n(y)+\mathrm{B}u'_n(x)v'_m(y). \quad . \quad . \quad . \quad (8)$$

The plate may vibrate with more than one note, but the overtones are not discussed in this paper.

The solution for the rod found from equation (6) is

$$u'_m(x)=\mathrm{A}\cos k_m x+\mathrm{B}\sin k_m x+\mathrm{C}e^{k_m x}+\mathrm{D}e^{-k_m x}. \quad . \quad (9)$$

The simplest case occurs when the motion is strictly periodic with respect to x, C and D vanishing †. All the functions are trigonometric and the differential equation $d^4u/dx^4=k^4u$ reduces to a second degree equation. The vibrating rod is then comparable to a wire with free ends and its differential equation becomes $d^2u/dx^2+k^2u=0$. The possibility of eliminating the hyperbolic functions from the rod and also from the plate must be decided by experiment. It is found that in the interior of the plate trigonometric functions are sufficient to determine the nodal lines in certain cases, but this type of function can never satisfy the boundary conditions; hence, this simple form of vibration cannot exist at the free ends of a rod nor at the edges of a plate except as an approximation. If the hyperbolic functions

* Ritz, *loc. cit.*

† Rayleigh, 'Sound,' i. p. 261.

are eliminated from the equation of a plate (equation 2) the remaining factor will be

$$\frac{\partial^2 w}{\partial x^2}+\frac{\partial^2 w}{\partial y^2}+k^2 w=0. \quad . \quad . \quad . \quad . \quad . \quad (10)$$

This is the equation for a vibrating membrane.

It is clear, therefore, that the general equation (2) can represent a plate which vibrates like a membrane in the interior but not at the boundaries. This vibration gives a series of figures which will now be discussed. These figures are characterized by the fact that if two nodal lines cut at a point inside the plate, they always cut at right angles—a nodal series typical of a vibrating membrane. Near the edges a correction must be made using both hyperbolic and trigonometric terms.

Ritz* has shown that a vibration of this kind is possible. He takes the function in the form

$$w=ax^2+2bxy+cy^2+dx^3+\ldots. \quad . \quad . \quad . \quad (11)$$

When two nodal lines cut one another in $x=0$, $y=0$, w will also equal zero as well as $\partial w/\partial x$ and $\partial w/\partial y$. In the case of membranes, the equation $\partial^2 w/\partial x^2+\partial^2 w/y^2+k^2 w=0$ must be satisfied identically. All these conditions are fulfilled provided $a+c=0$, but the latter is also the condition that the two straight lines defined by $ax^2+2bxy+c^2=0$ should cut one another at right angles. The differential equation of vibration for a plate is of the fourth order (not the second), so no definite conclusion can be drawn regarding the nodal lines of a plate, they may cut at any angle. If, however, they cut at right angles, we can take only sine and cosine functions inside the plate using the hyperbolic functions at the boundaries. The appropriate expression for such vibrations in the interior of a square plate with free edges will be

$$w=\mathrm{A}\cos\frac{m\pi x}{a}\cos\frac{n\pi y}{a}+\mathrm{B}\cos\frac{n\pi x}{a}\cos\frac{m\pi y}{a}=0, \quad . \quad (12)$$

in which a is the length of one side of the plate.

For brevity, we shall write equation (12) in the form

$$w=\mathrm{A}u_m v_n+\mathrm{B}u_n v_m, \quad . \quad . \quad . \quad . \quad . \quad (13)$$

in which $u_m=\cos m\pi x/a$, $v_n=\cos n\pi y/a$. Then $u'_m(x)$, $v'_n(y)$ contain both trigonometric and hyperbolic terms, while the unprimed terms u_m, v_n contain trigonometric expressions only.

* Ritz, *Ann. der Phys.* xxviii. p. 758 (1909).

The nodal lines of the restricted cases discussed here may now be developed from equation (13) by equating it to zero and giving suitable values to A, B, m and n. A few of these will be found mathematically and compared with the actual sand nodes. The boundary correction will be neglected temporarily.

The equation for the small square AOBC in fig. 1 *a* is

$$w = u_2 v_3 + u_3 v_2 . \quad . \quad . \quad . \quad . \quad . \quad . \quad (14)$$

For the large square, which is (14) repeated four times,

$$w = u_4 v_6 + u_6 v_4 . \quad . \quad . \quad . \quad . \quad . \quad . \quad (15)$$

In fig. 1 *b* the nodal lines of A′O′B′C′ are simple mirror images of (14) ; their equation is

$$w = u_2 v_3 - u_3 v_2 . \quad . \quad . \quad . \quad . \quad . \quad . \quad (16)$$

Fig. 1 *a*.

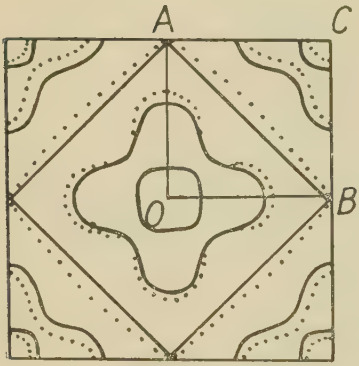

Fig. 1 *b*.

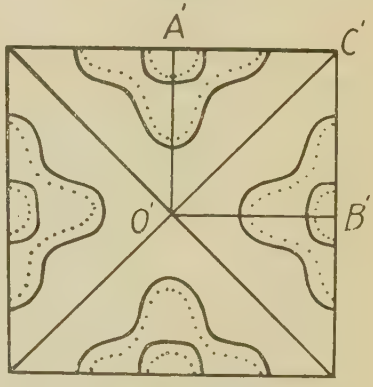

The heavy lines are plotted from equation (24); the dotted lines from equation (27).

The nodal lines of the complete square are given by

$$w = u_4 v_6 - u_6 v_4 . \quad . \quad . \quad . \quad . \quad . \quad . \quad (17)$$

The equations for figs. 2 *a* and 2 *b* are developed in exactly the same way. The nodal lines in the square ABCD were found by trial to be

$$w = 2u_2 v_1 - u_1 v_2 . \quad . \quad . \quad . \quad . \quad . \quad . \quad (18)$$

The nodal lines of EOFD, fig. 2 *a*, are therefore

$$w = 2u_4 v_2 - u_2 v_4 . \quad . \quad . \quad . \quad . \quad . \quad . \quad (19)$$

Those of the large square fig. 2 *a*

$$w = 2u_8 v_4 - u_4 v_8 . \quad . \quad . \quad . \quad . \quad . \quad . \quad (20)$$

The equations for A′B′C′D′, E′O′F′D′ and the complete square in fig. 2 *b* are in order

$$w = 2u_1v_2 + u_2v_1. \quad . \quad . \quad . \quad . \quad . \quad . \quad (21)$$

$$w = 2u_2v_4 + u_4v_2. \quad . \quad . \quad . \quad . \quad . \quad . \quad (22)$$

$$w = 2u_4v_8 + u_8v_4. \quad . \quad . \quad . \quad . \quad . \quad . \quad (23)$$

From these equations we see the possibility of building up extremely complicated nodal figures from comparatively simple ones. The method is restricted, however, to those cases in which the plate behaves like a membrane in any region not too close to the edges. Within these regions the function w is expressible in sine and cosine functions.

Fig. 2 *a*.

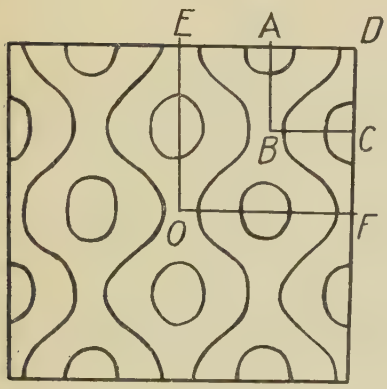

Fig. 2 *b*.

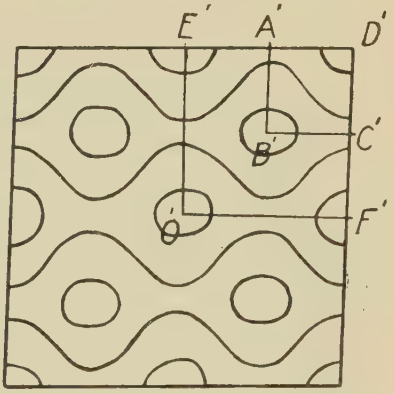

When high accuracy is desired at the boundaries, hyperbolic functions must be used in addition to the trigonometric.

Equations (15) and (17) come directly from (14) and (16), because at these vibrations the plate breaks into four equal squares, each of which vibrates exactly like the part AOBC and A′O′B′C′. This may be seen at once by dividing figs. 1 *a* and 1 *b* into four equal parts and comparing each with the figures plotted from (14) and (16). It is also proved by plotting equations (15) and (17) and comparing with the figures. This method of building up complicated figures from simple ones may be generalized as follows. The equation for a vibrating plate with the hyperbolic terms suppressed takes the form

$$\mathrm{A}\cos\frac{qm\pi x}{a}\cos\frac{qn\pi y}{a} + \mathrm{B}\cos\frac{qn\pi x}{a}\cos\frac{qm\pi y}{a} = 0.$$

Then $q=1$ will give a certain vibration of the plate. For $q=2$ the plate will divide into four squares, each of which vibrates exactly as the whole plate does for $q=1$. When $q=3$ the plate breaks up into nine equal squares and so forth. It is still necessary to make a correction along the boundaries; the method of doing this will now be discussed.

When the hyperbolic functions are not suppressed the general solution of equation (6) is

$$u'(x) = C_1 \sin kx + C_2 \cos kx + C_3 \sinh kx + C_4 \cosh kx. \quad . \quad (25)$$

With the neglect of a multiplying factor which has no significance so far as the nodal points of the rod are concerned, the boundary equations require that

$$u'_m(x) = (\sin k_m a + \sinh k_m a)(\sin k_m x + \sinh k_m x) + (\cos k_m a - \cosh k_m a)(\cos k_m x + \cosh k_m x). \quad . \quad . \quad (25)$$

The necessary condition that $\cos k_m a \cosh k_m a = 1$, is also the frequency equation which determines the possible vibrations of the rod. For high frequencies $k^m a$ is approximately $m\pi - \pi/2$. The values of $u'_m(x)$, $u'_n(x)$, $v'_m(y)$, and $v'_n(y)$ found from (25) are substituted in equation (8), which is then equated to zero for the nodal lines. The resultant expression is an equation in x and y which can be plotted. This is done only near the edges, since the simpler expressions $u_m(a)$, $u_n(x)$, $v_m(y)$, $v_n(y)$ suffice inside the plate.

For large value of m, let us say $m > 5$, the hyperbolic functions are much larger than the trigonometric, and (25) may be written

$$u'_m(x) = \sinh k_m a(\sin k_m x + \sinh k_m x) - \cosh k_m a(\cos k_m x + \cosh k_m x). \quad . \quad . \quad (26)$$

Since for large values of m, $\sinh k_m a$ and $\cosh k_m a$ are practically equal, equation (26) may be further simplified into

$$u'_m(x) = \sinh k_m a\{\sin k_m x - \cos k_m x - e^{-k_m x}\}. \quad . \quad (27)$$

Thus the bracketed factor in equation (27) which determines the nodal points tends to have only trigonometric terms as x changes from 0 to $a/2$.

The tendency of a rod with free ends to have the same nodal system as a free wire is shown by the fact that near the middle of the bar the nodes are uniformly spaced *.

* Rayleigh, 'Sound,' i. pp. 284–285.

The analogous tendency of a plate to have nodal lines like a membrane is also indicated by the experimental fact that near the centre of the plate two intersecting nodal lines meet at right angles. The reason for this is that the value of $u'_m(x)$ determined from equation (26) has in it the difference between two trigonometric terms and the difference between two hyperbolic terms. As we pass from the edge of the plate to the centre the hyperbolic terms approach one another in value, so that they disappear from the equation, leaving only the trigonometric terms which are characteristic of a membrane. For very high notes (i. e., m and n large) the hyperbolic terms disappear very rapidly so that the corrections for the figures developed from trigonometric functions (equation 24) need be applied near the edges only. In figs. 1 *a* and 1 *b* the dotted lines have been calculated

Fig. 3 *a*.

Fig. 3 *b*.

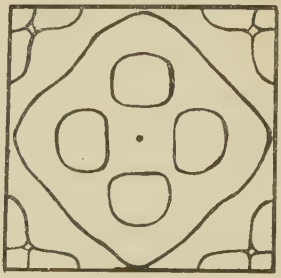

from equation (27) ; even for the comparatively small values of m and n used, the region near the centre of the plate behaves like a membrane. It is almost needless to state that this resemblance between membranes and plates refers to the nodal lines only and does not apply to the amplitude of the vibrations nor the sequence of tones : these are entirely different for the two cases.

All the sand figures shown above were formed with the electric oscillator *, the plate resting upon rubber mats, or upon four points on the nodal lines. The two figures above (figs. 3*a*, 3*b*) were chosen from a large number of curves which were found by a new method in which the plate was balanced upon a small metal cone attached to the centre of the oscillating diaphragm. The ordinary telephone receiver or an electro-dynamic loud speaker may be used.

* Colwell, Phil. Mag. xii. p. 320 (Suppl., Aug. 1931).

A Chladni plate has a small circular hole in the centre which fits down over the metal cone. The plate must be exactly level at all times. It is then as free as possible from outside constraints. The point of support is also the point at which the vibration is applied.

Appendix.

The first four photographic reproductions on Pl. VIII., which show the Chladni figures produced by the electric vibrator, should be compared with figs. 1 *a*, 1 *b* and 2 *a*, 2 *b*.

XXXI. *Notices respecting New Books.*

Intermediate Physics. By C. J. Smith. [Pp. viii+650.] (London: Edward Arnold & Co. Price 14*s*.)

Of the making of books on Elementary Physics there is no end. Yet the teacher still looks in vain for the Introductory treatment which he can recommend without reserve. Although Dr. Smith's attempt to provide a textbook for undergraduates in their first year and for the advanced classes of schools is admirable in many ways, it can hardly be regarded as a well-balanced introduction. The earlier chapters on Measurement, Properties of Matter, and Heat are excellent—and throughout the book adequate descriptions are given of laboratory experiments which the student may perform for himself—many of these appearing in a textbook for the first time.

Yet, in spite of the author's somewhat needless apology for numerous references to Applied Sciences, many applications, especially of recent developments, that might well find a place in an up-to-date textbook will be sought for in vain. Indeed, the treatment of Modern Physics is altogether too sketchy. Transformers are dismissed in one short paragraph, Alternating Currents in another, while the whole of Discharge-tube phenomena, X-rays, and Radioactivity are given in a chapter of some ten pages.

The printing and general arrangement of the book leave nothing to be desired, and the author's brother is to be congratulated on the excellence of the diagrams.

Electrons and Waves. By H. Stanley Allen. [Pp. vii+336.] (Macmillan & C., London, 1932. Price 8*s*. 6*d*.)

Professor Allen has given a very interesting and, needless to say, a very scholarly account of the main principles and conclusions of the most recent advances in atomic and quantum physics. In

writing it he has attempted to steer a middle course between the "popular" exposition and the serious technical treatise and has succeeded in his difficult task better than might have been expected. The book is not entirely homogeneous in character. One would imagine, for instance, that a reader who could profit by Professor Allen's lucid but by no means facile account of the Principles of Relativity would hardly require, though he might certainly enjoy, the elementary account of the rise of the atomic theory contained in the earlier pages. Such concessions to weakness, however, are not very numerous, and it is a little difficult to judge how much illumination readers who have not some knowledge of physics will carry away from a perusal of this book. On the other hand, physicists, engineers, mathematicians, and chemists (and they must now form a large majority), who for obvious reasons have not been able to follow closely the latest advances in the subject, should welcome with avidity this well-balanced and orderly survey of the new territories so recently opened up; a survey which, while never losing itself in technicalities or trivialities, shirks none of the difficulties involved in the subject.

Philosophie. By Dr. Karl Jaspers. (Berlin: Julius Springer, 1932. Three volumes, pp. 340, 440, 237.)

It is impossible, within the limits of a short review, to give an adequate account of this monumental work, in which Dr. Jaspers expounds at length and with a truly Kantian array of technical terms his view of the nature and scope of philosophy. In the first volume, entitled 'Philosophische Weltorientierung,' he develops, in the spirit of Kant, the doctrine that knowledge, in the strict sense of scientific knowledge, is confined to phenomenal existence and hence is essentially relative, since every phenomenon is necessarily related both to other phenomena and, as object, to a knowing subject. The philosopher seeks to penetrate beyond this relativity. How can he do so? The answer to this question is found in the second volume, entitled 'Existenzerhellung.' I have to realise that in my immediate experience of myself as feeling, willing, and acting I overcome the duality of the subject-object relation; here freedom and self-determination reveal themselves; here is the fixed point round which all relativity revolves. This kind of being Dr. Jasper terms "Existenz," and his system is accordingly an "Existenzphilosophie." But I am not alone in the world; there are other "existences" who disclose their being to me through what the author calls "Kommunikation," that power of common feeling and common action upon which the continuity of human society rests. Moreover, there is the world in which men live, a phenomenal world pointing to a "Transzendenz" upon which it depends and which can only reveal itself to us through

phenomena. The third volume, 'Metaphysik,' deals with our efforts to determine the nature of this ultimate being. The author insists, with Kant, that we cannot *know* this transcendent being, though we are so constituted that we must seek for it. The book of nature is written in cipher; art, mythology, science, philosophy are all in their several ways attempts to read the cipher, for which there is no key; for there is no objective criterion of truth. Philosophy has often gone astray and sought to construct an Ontology; every such effort must fail, because no rational system can transcend the duality of subject and object. In the last resort philosophy is a personal affair: it must be present in one man and in the space of one life. It is futile to criticise philosophical doctrines in isolation from the complete systems of which they form part: the work of the great thinkers—a Kant, a Hegel, a Plotinus—must be read as each expressing the experience of specially gifted individuals.

The book shares fully in the merits and demerits of modern German bookmaking: the printing is quite delightful, but there is no index.

Elements of the Theory of Resonance illustrated by the Motion of a Pendulum. By E. W. Brown, Sc.D., F.R.S. [Pp. iv+60.] (Cambridge: At the University Press, 1932. Price 3*s.* 6*d.*)

In this booklet, based on a course of lectures at the Rice Institute, certain generally neglected aspects of the theory of resonance are discussed. For some mechanical systems a reasonably close approximation to the motion may be obtained by introducing a damping term into the usual simple equations; for others, however, this method fails. The defect lies in the fact that, in general, the forces in a vibrating system are not strictly proportional to the displacements. This means that the phenomena cannot be investigated by linear differential equations alone. As long as the amplitudes are small, the usual method can be applied; but at or near resonance non-linear equations must be used. A related point stressed is that resonance is not a single case of motion but a group of cases, for which the solutions of the equations are not continuous with those for the non-resonance cases.

Equations of various degrees of generality are considered, and solutions obtained in convenient form for the different cases which arise. The results are illustrated by reference to the simple pendulum, the pendulum with an oscillating support, and systems of coupled pendulums. The presentation is admirably lucid and concise. The author hints at the possibility of important applications of the results in gravitational

problems. Independently of this, the booklet, in providing a significant addendum to, and commentary on, the usual treatment of the protean phenomenon of resonance, should be of wide interest.

Philosophical Aspects of Modern Science. By C. E. M. Joad. [Pp. 334.] (London: George Allen and Unwin Ltd., 1932. Price 10*s.* 6*d.* net.)

As long as it was possible to correlate phenomena in terms of the time honoured scientific concepts deriving from Newton, it seemed that philosophical criticism and speculation were irrelevant to science. These concepts were almost treated as being given directly in the world of sense experience, which it was the business of science to explore. During recent years, however, the fundamental concepts of science have become more and more remote from this familiar world, and the philosophical problem of the status of the world pictures of science, of the status of "scientific objects," has forced itself on the attention even of scientists. Some, intoxicated by a new excitement, have plunged lightly into the primrose path of metaphysical speculation—as to the nature, implied by science, of the universe as a whole. Their brilliant descriptions of their journeyings have aroused a widespread interest in a realm worthy to be explored. It is, however, legitimate for the philosopher to point out that the paths they have traversed are not entirely unknown; that they have gone little, if any, further than previous travellers; and that much of their time has been spent in going in circles.

In this book Mr. Joad supplies a corrective to the more speculative parts of the writings of Eddington, Jeans, and Russell. Their views are expounded fairly and sympathetically—and with a lucidity which is fatal to them. The weak points are not mercilessly exposed. They become apparent. This is not to say that the views are shown to be valueless. Rather, as a result of criticism, what is of value is revealed, and the way is opened for sounder construction. In the second part of the book a very clear discussion is given of the status of sense data, physical objects and scientific objects, and of the relations between them. Finally, the conclusions of modern science are considered in the light of Mr. Joad's own theory of value. Here is introduced the interpretation of the universe as containing a plurality of realms of being, and it is one which, with its apotheosis of the mystic, is hardly likely to carry conviction to the scientific mind. Mr. Joad's book will, however, be appreciated for its reasoned criticism of the philosopical views of particular scientists, and for the admirable general

discussion of the relation between the worlds of sense and science, by all who are alive to the philosophical problems of modern science.

Les Principes de la Mécanique Quantique. By P. A. M. Dirac. Translated by Al. Proca and J. Ullmo. (Vol. xxi. of the 'Conférences-Rapports sur la Physique.') (Les Presses Universitaires de France. Price 95 frs.)

The lapse of time since the work of Dirac first appeared has served to show increasingly its great and fundamental importance. On the one hand, there is the great range of the problems he has attacked and the brilliant mathematical methods developed for their solution. On the other, there is the philosophical attitude implied in his treatment of these problems: the conclusion that electrons and photons are unknowable entities, and the warning that in picturing them as "waves" or "particles" we may be mistakenly ascribing to them properties that belong only to their mathematical representations. The present translation of the book gives a close and accurate rendering of the English text. An appendix, written by M. Proca, has also been added, which gives a short account of Poisson and Lagrange brackets in classical mechanics. Special reference is made to the expression of the Hamiltonian equations of motion and of the condition for a contact transformation of a dynamical system in terms of these brackets. This appendix will undoubtedly add to the value of the book by indicating the type of result in classical mechanics that may be expected to reappear in quantum mechanics.

The Distribution of Prime Numbers. By A. E. Ingham. (Cambridge Tracts in Mathematics and Mathematical Physics, No. 30, 1932. Price 7*s.* 6*d.* net.)

This tract makes very attractive reading. Its subject is the theory of the distribution of the prime numbers in the series of natural numbers. Based upon the manuscript of Littlewood and Harald Bohr, it gives a detailed account of prime number theory, the major part of the book being devoted to the analytical theory founded on the Zeta function of Riemann. The work is designed to be of interest not only to the high-brow specialist in prime number theory, but also to the general (mathematical) reader. Though it is complete in itself, the tract has been planned in conjunction with the tract 'The Zeta Function of Riemann' recently written by Titchmarsh.

[*The Editors do not hold themselves responsible for the views expressed by their correspondents.*]

FIG. 1.

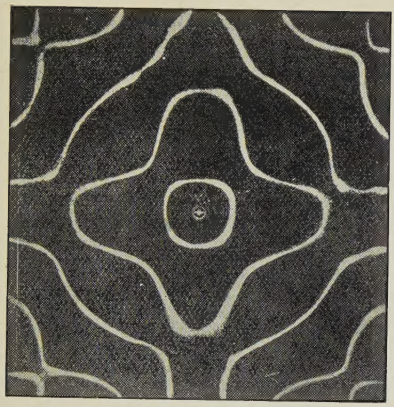

FIG. 2.

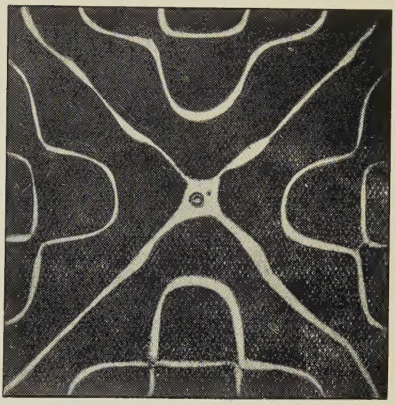

FIG. 3.

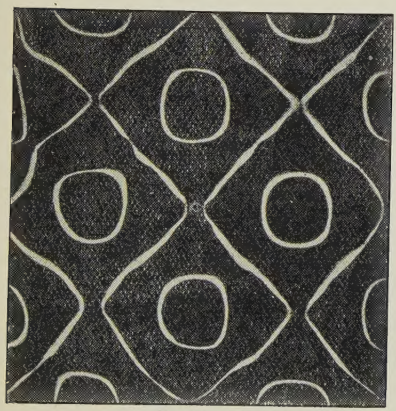

FIG. 4.

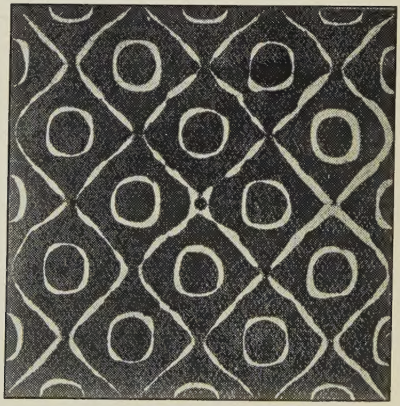

FIG. 5.

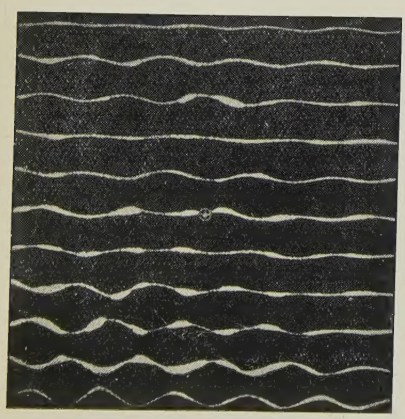

FIG. 6.